1-D and 2-D Digital Filters Design Using Model Reduction and Optimization Methods for Broadband Beamforming and Interference Rejection

by

Abdussalam Omar
B.Sc., Higher Institute of Electronics , Baniwalid- Libya, 1997
M.Sc., Academy of Graduate Studies, Tripoli- Libya, 2007

A DISSERTATION SUBMITTED IN PARTIAL FULFILLMENT
OF THE REQUIREMENTS FOR THE DEGREE OF
DOCTOR OF PHILOSOPHY
in the Department of
Electrical and Computer Engineering

We acknowledge and respect the Lək^{w}əŋən (Songhees and Esquimalt) Peoples on whose territory the university stands, and the Lək^{w}əŋən and W̱SÁNEĆ Peoples whose historical relationships with the land continue to this day.

1-D and 2-D Digital Filters Design Using Model Reduction and Optimization Methods for Broadband Beamforming and Interference Rejection

by

Abdussalam Omar
B.Sc., Higher Institute of Electronics , Baniwalid- Libya, 1997
M.Sc., Academy of Graduate Studies, Tripoli- Libya, 2007

Supervisory Committee

Prof. Panajotis Agathoklis, Supervisor
(Department of Electrical and Computer Engineering)

Prof. Dale Shpak, Co-supervisor
(Department of Electrical and Computer Engineering)

Prof. Jens Bornemann, Departmental Member
(Department of Electrical and Computer Engineering)

Prof. Yang Shi, Outside Member
(Department of Mechanical Engineering)

ABSTRACT

This thesis presents several design algorithms for nearly linear-phase one-dimensional (1-D) and two-dimensional (2-D) infinite impulse response (IIR) digital filters. Optimization techniques as well as model order reduction (MOR) filter design methods are considered in this study.

For 1-D, finite impulse response (FIR) filters can achieve perfectly linear phase which makes them important in applications such as the field of audio signal processing where a flat delay characteristic may be desired. However, in most applications a perfectly linear phase response is not required and filters that have nearly linear phase response are quite acceptable. In such cases, IIR filters are more attractive than FIR filters. The design of IIR filters is more challenging than that of FIR filters because it results in a highly nonlinear objective function that requires sophisticated optimization methods. The 1-D optimization method proposed here solves the problem of approximating specified magnitude and linear-phase responses simultaneously. Since IIR filters can be designed to have nearly linear phase response in the passband, their passband group delay is usually considerably smaller than the delay of linear-phase FIR filters with equivalent magnitude responses. Meeting a required minimum stopband attenuation or a minimum deviation from the desired magnitude and phase responses in the passbands are common design constraints that can be handled by the proposed optimization method for 1-D IIR filter. Also, an important constraint in the design of IIR filters is the prescription of a maximum pole radius, which allows to guarantee the stability margin and low coefficient selectivity for the obtained filter for finite-precision implementations. These design specifications are consistent with the constraints which often arise in practical filter design problems. In this research work, an optimization method for solving this constrained 1-D IIR design problem is presented.

The above optimization method used for designing 1-D IIR filters is extended to 2-D separable-denominator IIR digital filters with nearly linear phase in the passband. During the development of the proposed design techniques for 2-D digital filters, a special emphasis has been placed on their computational efficiency and a method for the design of 2-D IIR digital filters based on a balanced realization (BR) model order reduction technique is proposed. In this method, the initial design is a linear phase 2-D FIR filter realized in a 2-D state space model, which leads to a stable 2-D separable-denominator IIR filter with nearly linear phase in the passband. The model

reduction method is based on structured controllability P_s and structured observability Q_s gramians. These gramians are block-diagonal positive-definite matrices satisfying 2-D Lyapunov inequalities. An efficient general algorithm is developed to compute these matrices by minimizing the trace of P_s and the trace of Q_s under Linear Matrix Inequalities (LMI) constraints. The use of these gramians ensures that the resulting 2-D IIR filter is a 2-D stable filter. Furthermore, the obtained nearly linear-phase 2-D IIR filter is more economical and computationally more efficient than the original 2-D FIR filter.

Numerical examples using MATLAB show that the proposed method provides a good compromise between the filter selectivity and computational complexity when compared to existing techniques, making the results of this dissertation directly applicable to many practical applications. For example, in the field of array signal processing, 2-D digital filters having a fan-shaped filter in the passband emerge as powerful tools, particularly when employed as beamformers in scenarios where the Direction of Arrivals (DOAs) of the desired broadband Plane Waves (PWs) are known. In such cases, the designed 2-D FIR and IIR filters having a fan-shaped filter passband in the 2-D frequency domains are used as beamformers. Benefiting from the knowledge of DOAs of the desired broadband PWs, these filters are used to extract the signal of interest (SOI), suppress the interference, and reduce the noise corrupting the SOI. The successful implementation of 2-D FIR and IIR fan filters as beamformers not only enhances the rejection of the interference but also demonstrates its capability to reduce the effect of AWGN. This dual functionality holds significant implications for practical applications in digital signal processing, in which robustness against interference and noise is important. Simulation results demonstrate a good performance of the proposed beamformers and confirmed that the filters obtained using the proposed methods are capable of extracting and enhancing the desired 2-D broadband signals according to their directions of arrival under severe interference and noise.

Contents

List of Tables

List of Figures

List of Acronyms

1-D	One-dimensional
2-D	Two-dimensional
AWGN	Additive white Gaussian noise
avg	average
atten	attenuation
BIBO	Bounded input bounded out stable
BMT	Balanced model truncation
CD	Continuous domain
DSP	Digital Signal Processing
DOA	Direction of Arrivals
dB	Decibel
diag	diagonal
Freq	Frequency
FIR	Finite-duration impulse response
FM	Fornasini and Marchesini
FM1	First Fornasini and Marchesini model
FM2	Second Fornasini and Marchesini model
GA	Genetic algorithm
IIR	Infinite-duration impulse response
Int	Interference
IP	Interior point
iff	If and only if
MOR	Model order reduction
MD	Multi-Dimensional
Mag	Magnitude
min	Minimum
max	Maximum
PWs	Plane Waves
Qf	Quality factor
ROS	Region of support
SOS	Second order section
s.t	Subject to
svd	Singular Value Decomposition
SOI	Signal of interest
SDP	semi-definite problem
SNIR	Signal-to-Noise-plus-Interference Ratio
SNR	Signal-to-Noise Ratio
tr	trace

ACKNOWLEDGEMENTS

I want to start by giving thanks to Allah Almighty, who has given me the strength to finish my research work.

I wish to express my gratitude to a great number of people! My family, friends, coworkers, teachers, and those people who have helped me, whether directly or indirectly.

First and foremost, I would like to thank my direct supervisor, Prof. Panajohts Agathoklis for giving me this opportunity to work under his supervision, for his guidance, new research ideas, financial support, patience and ever helping attitude and broadening my thinking canvas. Also, I would like to thank my co-supervisor Prof. Dale Shpak for his necessary support, advice, suggestions, ideas and useful discussions. I really admire their commitment and dedication to the field of multidimensional signal processing.

I would also like to thank my committee members, Prof. Jens Bornemann, Prof. Yang Shi at the University of Victoria for their comments and advice. Special thanks to Dr. Belaid Moa for being very supportive to me and providing useful discussions. Very special thanks to Mrs. Lori Hunter for encouragement and support during this long journey.

My mother and my parents-in-law for their encouragement and kindness they bestowed on me which gave my family and I a very pleasant relief from sadness of being away from home country. My wife Muna for her devotion and patience. Thanks to my children, Ali, Kawter, Abdullah, Sarah, and Mohamed for their unconditional love and providing me a quiet time to work sometimes. Their continuous encouragement and motivation during numerous hard times had a very important impact towards successful completion of this work. God bless all of you!

I am very grateful to UVic staff Mrs. Ashleigh Carlsen, Mrs. Amy Issel, Mrs. Jessica Fox, Mr. Kevin Jones, and Mr. Dan Mai for their kind assistance, and willingness to help at anytime.

To those who are not listed here, I say profound thanks for bringing pleasant moments in my life.

Thanks to my home country Libya, Collage of Electronic Technology, Bani Walid, and Ministry of Higher Education, for having trust in me and for sending me abroad for higher education.

At last, Canada, the great land with nice people and splendid natural beauty. Where I could see different colors of life which enriched my experiences of life, making my

journey here much more than an academic endeavor only. Thank you very much, Canada!

Dedicated to my beloved home country

LIBYA

Chapter 1

Introduction

1.1 Overview

Digital filters are integral parts of many digital signal processing systems, including control systems, systems for audio and video processing, communication systems, and systems for medical applications. Due to the increasing number of applications involving digital signal processing and digital filtering, the variety of requirements that have to be met by digital filters has increased as well. Consequently, there is a need for flexible techniques that can design digital filters satisfying sophisticated specifications.

This thesis presents different methods for the design of 1-D and 2-D digital filters. The proposed methods allow for specification on the magnitude and phase of the filter's frequency response. The design problem is a complex approximation problem where a complex desired frequency response prescribing the desired magnitude and phase responses is approximated by the actual frequency response of the digital filter. We are mainly interested in the design of nearly linear-phase 1-D and 2-D IIR digital filters but FIR filters are considered as well. Optimization and model order reduction techniques are the two methods that can be used to design IIR filters. We also present a design method that can take into account specifications on magnitude and linear-phase responses simultaneously. In terms of the applications of these filters, consideration is given to the beamforming and filtering of distinct PWs, where each originates from a different direction and they exhibit varying magnitudes and time-varying frequencies.

1.2 Motivation and Problem Statement

Digital filters are one of the most common building blocks in electrical and electronic engineering and have an important role, whether in 1-D or 2-D digital signal processing [5–7]. Linear filters are defined as a system that used to modify, reshape, or manipulate the frequency spectrum of a signal according to some predefined amplitude or frequency response specifications [6–8]. Digital filters are of two types: finite impulse response (FIR) filters or non-recursive filters and infinite impulse response (IIR) filters or recursive filters [6–8]. In this work, the design of digital filters, in general, involves three major steps [6–8]. The first step is an approximation. This step involves determination of the order and the coefficients of the filter to satisfy the design specifications. Stability is the main required property in this step where the designed filter should represent a stable digital filter [9–11]. The next step is converting the designed filter transfer function into a signal-flow graph, network, or a state-space representation and this step known as a filter realization. The last step of the filter design process is the implementation [6–8].

2-D digital filters are similar to their 1-D counterparts. They are discrete systems that can be linear or nonlinear, shift-invariant or shift-dependent, causal or noncausal, and stable or unstable [6, 7]. They can be characterized in terms of difference equations, transfer functions, or state-space equations in two independent variables. They benefit from analogous properties of 1-D filters. For example, 2-D IIR filters typically use a smaller number of coefficients to meet the filter specifications than 2-D FIR filters. Stability is a very important issue for the IIR filters, while it is not for the FIR filters [6, 7].

Several methods for the analysis, design, and realization of 1-D and 2-D digital filters exist today [12, 13]. These methods include the window method, the McClellan transformation, singular value decomposition, impulse response gramian, and several optimization techniques [4, 14–19]. For instance, the Impulse Response Gramians (IRG) model reduction method proposed by Sreeram and Agathoklis [19] involves designing an FIR filter which satisfies the desired frequency response followed by obtaining a lower order IIR filter which approximates the frequency response of the FIR filter. Among these methods, the design of linear-phase digital filters, in particular, has attracted considerable attention as they allow distortion-free filtering of the wave forms [19]. Although this property can easily be achieved by using FIR digital filters, they have the drawback of requiring higher order than IIR filters [19] and,

although causal IIR filters can approximate linear phase, they cannot achieve exactly linear phase. Additionally, in many filter design problems it is required to satisfy the linear-phase characteristics in the passband with the lowest order possible [19, 20]. Hence, there is always a need for the design of filters with optimal properties such as low order, linear-phase, etc. This research work aims at improving the methods for achieving such properties. The general question that we are interested in answering is stated as follows:

> *Given an initial filter, design, analyze and realize a lower-order filter with specific requirements such as stability, phase linearity, and magnitude constraints for each band.*

The above statement can be treated in two different ways. The first is a constrained optimization problem, and the second way is a model order reduction problem.

1.2.1 Constrained Optimization for 1-D and 2-D Digital Filters

The design problem of the nearly linear-phase digital filter is formulated as a constrained optimization problem. The group delay deviation of the filter is minimized under a set of constraints in terms of the passband ripple, transition band, stopband attenuation, and stability of the filter. One motivation for using this method is mainly to satisfy simultaneous specifications on magnitude and phase or group delay characteristics. IIR filters are of interest if high selectivity as well as approximation of a phase response are required at the same time since FIR filters with equivalent frequency responses are usually of a higher order, need more memory, and generally have more computational complexity for their implementation.

1.2.2 Model Order Reduction for 2-D Digital Filters

Model order reduction method for separable denominator 2-D recursive digital filters with approximately linear phase in the passband is proposed. The method is based on the balanced realization model reduction using structured controllability and structured observability Gramians. A computationally-efficient method for computing the controllability and observability Gramians of 2-D digital filters is developed. This computation algorithm for Gramians is based on solving Lyapunov equations by minimizing the traces of the controllability and observability matrices under linear matrix

inequalities (LMI) constraints. The Gramian matrices P and Q are block diagonal and positive definite matrices. By finding these Gramians, if they exist, one can say the system is minimal and stable, and then the next step is the model reduction design.

1.3 Literature Review

Many signal processing applications, including image processing, beam filters, TV transmission, satellite image processing, video signal filtering, X-ray, and medicinal imaging, have made use of two-dimensional digital filters [12, 17, 21–23]. Numerous approaches have been proposed for their design; see for example [4, 15, 24–38]. In particular, the design of nearly linear-phase IIR digital filters has significant interest in the field of digital signal processing. These filters are crucial in applications requiring low complexity and precise control over both magnitude and phase responses. Designing IIR filters for practical applications often involves adhering to several constraints. These constraints ensure that the filters meet real-world performance requirements, such as minimum stopband attenuation, maximum deviation from desired responses, low group delay in the passband and stability. The challenge lies in developing design techniques that can address the inherent trade-offs between achieving desired frequency characteristics and maintaining computational efficiency.

Optimization techniques are central to the design of nearly linear-phase IIR filters. The primary goal of these techniques is to approximate specified magnitude and phase responses simultaneously. Various methods have been proposed to address this problem, including convex optimization, iterative reweighted least squares, and evolutionary algorithms. Convex optimization has been widely applied due to its robustness and the availability of efficient solvers. Techniques such as semidefinite programming (SDP) allow for the formulation of filter design problems as convex optimization tasks, ensuring global optimality under certain conditions [39]. Some research demonstrated the application of linear programming and SDP in the design of IIR filters with prescribed magnitude and phase specifications, highlighting its effectiveness in handling complex design constraints [40, 41]. For some design methods such as iteratively re-weighted least squares methods, they iteratively adjust the weighting of errors in the magnitude and phase responses, aiming to minimize the overall approximation error. These approaches have been shown to be particularly useful in achieving a balance between magnitude and phase accuracy [42–44]. By iter-

atively refining the filter coefficients, these methods can produce filters with superior performance in different applications.

Usually the designed filters are having a high order which leads to additional memory requirements and enormous computations. Sometimes, the designed filters are too large to store due to limited computer memory. To circumvent these complexities, reducing the size of the 2-D filter is necessary. The method to reduce a filter with a high order to a lower one is called model order reduction (MOR). The fundamental aim of MOR is to replace the high order filter by substantially lower order one while the response of the original filter is approximated to the highest possible extent. In certain cases, some important features such as stability, passivity, definiteness, symmetry and so forth of the original filter must be preserved in the reduced filter. The incentive for obtaining a reduced model for a 2-D digital filter arises when one is confronted with a complex high order filter for real-time processing and implementation. Since a model is a mathematical representation of a filter or the characterization of a given discrete filter from the input-output data information, the simplification of this model is highly desirable in various synthesis and analysis problem. However, the reduced model should represent the original filter model with sufficient fidelity such that performance objectives can be met using the reduced model instead of the original one.

In the opinion of many investigators of model reduction, two developments have dramatically changed the status of the model reduction theory. These are the theories of Moor's balanced realization and Optimal Hankel-Norm approximation [21]. A wide variety of model methods for the model reduction have been proposed over the last decades for 2-D digital filters. Reduction by finding an approximate transfer function of lower degree was proposed by P. Paraskevopoulos et al. [45]. This method transforms a 2-D transfer function model reduction problem into an overdetermined linear algebraic system of equations by using orthogonal series. A system of equations is considered overdetermined if there are more equations than unknowns. The issue for this method is that it has no solution when constructed with random coefficients. However, an overdetermined system will have solutions in some cases, for example if some equation occurs several times in the system, or if some equations are linear combination of the others. The degree of the obtained result 2-D transfer function is obviously smaller than the degree of the original one. Another method, developed by T. Guo et al. [38], is also based on a transfer function reduction. This method uses bilinear Routh approximations instead of orthogonal series and it is only applicable

to separable-denominator systems. These systems can be thought of as the result of a cascade interconnection between two 1-D systems, so they are much easier to treat as, for example, the 2-D state-space realizations of Roesser's model, which have the property that either A_{12} or A_{21} is a zero matrix.

Other design approaches generalize the idea of the 1-D Hankel matrix approximation for 2-D systems. H. Luo et al. [46] presented a method in which the problem of model order reduction is formulated as an unconstrained optimization problem, whose objective function includes a term that depends on the sum of the discarded 2-D Hankel singular values. M. Diab et al. [47] used the singular value decomposition of the horizontal and vertical Hankel matrices of the system to obtain diagonal gramians which are used to derive a reduced order model. Some other methods consider the Fornasini-Marchesini [48] and the Roesser's model [49]. The majority of these algorithms use the Roesser state-space model and try to generalize the notion of a balanced realization for 2-D systems. C. Xiao and P. Agathoklis [4] proposed a new method for designing separable denominator 2-D IIR digital filters with nearly linear phase in the passband. This method is based on the extension of the impulse response gramians from 1-D case to 2-D separable denominator filters. See also [19,35,36]. It is found that the biggest computation effort required by most of these algorithms is the solution of Lyapunov equations, especially for high-order filters. Also, in some methods, the stability of the obtained reduced order model is guaranteed if the original system is also stable. Otherwise, the stability property of the reduced-order model is still a major concern.

1.4 Thesis Contribution

In this work, we propose a new and computationally efficient technique for designing nearly linear phase 2-D IIR digital filters. The main contribution of this thesis are design techniques that can be used to produce low order (1-D, 2-D separable denominator) recursive digital filters with nearly linear phase in the passband that have low complexity having similar response characteristics to FIR filters. In addition, we have the following:

1) Improving design methods for 1-D IIR filters with nearly linear-phase in the passband using a constrained optimization method.

2) Reducing the computation complexity associated with 2-D modern signal processing systems by designing separable denominator 2-D IIR digital filters with nearly linear-phase in the passband using 2-D balanced realization model reduction.

3) A constrained optimization technique for the design of separable denominator 2-D IIR digital filters with nearly linear phase in the passband is proposed. The design problem is developed and formulated as a constrained optimization problem where the group delay deviation in the passband is minimized subject to a set of linear constraints.

4) Beamforming and plane wave (PW) filtering using 2-D FIR and IIR digital fan filters are presented. The filters obtained by the proposed methods are used to pass the Signal of Interest (SOI) received from a specified direction, reduce the noise, and reject interference signals coming from different directions. The 2-D FIR and IIR fan filters are designed to have passbands that enclose the region of support (ROS) of the desired plane wave and reject other unwanted signals as interference.

1.5 Thesis Organization

The structure of this thesis is meticulously designed to systematically address the problem statement and objectives outlined. Each chapter builds on the preceding one, ensuring a coherent flow of ideas and findings. Below is a detailed organization of the thesis:

Chapter 1: Introduction

Chapter 1 lays the foundation for the thesis by presenting a short overview for digital filters as an integral part of many digital signal processing systems. In addition, the motivation, the problem statement and how they can be treated, the literature review, and the thesis contributions are included in this chapter.

Chapter 2: Preliminary Definitions and Background Materials

In Chapter 2, a brief overview is provided, including definitions and essential background materials necessary for the thesis. This chapter functions as an introductory primer, ensuring that readers are thoroughly equipped with the requisite knowledge to comprehend subsequent discussions. Essential mathematical representations for

1-D and 2-D digital filters and notations that form the basis of the analyses in the thesis are presented.

This chapter explores the stability of both 1-D and 2-D discrete systems. It covers various definitions of stability, including BIBO stability, Lyapunov stability, and some other definitions of stability. These concepts are crucial for analyzing the behavior of digital filters.

Detailed definitions and discussions on the controllability and observability of 1-D and 2-D discrete systems are provided. The chapter explains the significance of these properties in the context of system design and analysis. It also introduces the controllability and observability gramians for 2-D systems, clarifying their role in determining the system's ability to be controlled and observed.

This chapter also addresses the concepts of minimal realization and balanced realization in the context of system theory. Minimal realization ensures that the system representation is as simple as possible without losing any essential dynamics. Thise concept is crucial for efficient system design and implementation.

By covering these topics, Chapter 2 lays a robust groundwork for the thesis, ensuring that readers have a comprehensive understanding of the essential concepts and theories needed to appreciate and engage with the advanced discussions in the subsequent chapters.

Chapter 3: Improved Design Method for Nearly Linear-Phase 1-D IIR Filter Using Constrained Optimization

Chapter 3 introduces an improved constrained optimization technique aimed at designing 1-D recursive digital filters with nearly linear-phase characteristics in the passband. The chapter details the methodology for improving filter performance through constrained optimization, discussing both the magnitude response and the linearity of the group delay of the filter in the passband. Key results and performance analyses of the designed filters are presented and compared with other methods, demonstrating the effectiveness of the proposed technique.

Chapter 4: LMI-based Design of Nearly Linear-Phase 2-D Recursive Digital Filters Using Balanced Realization Model Reduction

In Chapter 4, the focus shifts to model reduction for 2-D recursive digital filters using the concept of balanced realization. The chapter addresses the challenges associated with reducing the order of digital filter models while maintaining their performance characteristics. Techniques for achieving model order reduction, based on the controllability and observability gramians, are explored. A computationally-efficient method

for solving these gramians under Linear Matrix Inequalities (LMI) is developed. Furthermore, this chapter proposes a balanced realization technique specifically for separable denominator 2-D recursive digital filters.

Chapter 5: A Nonlinear Optimization Design Algorithm for Nearly Linear-Phase 2-D IIR Digital Filters

Chapter 5 presents a new nonlinear optimization design algorithm to obtain separable denominator 2-D IIR digital filters with nearly linear-phase in the passband. This chapter delves into the algorithm's development, optimization criteria, and practical applications. Detailed performance evaluations and comparisons with existing methods are provided, showing the advantages of the proposed approach in achieving desired filter characteristics.

Chapter 6: Broadband Beamforming and Interference Rejection of Plane Waves using 2-D FIR and IIR Digital Filters

Chapter 6 explores the practical applications of 2-D FIR and IIR digital filters in the field of array signal processing. The chapter primarily focuses on beamforming and the filtering of plane waves using 2-D FIR and IIR fan filters. Detailed case studies and application scenarios are presented, highlighting the efficacy of the filters in real-world signal processing tasks, focusing mainly on the efficiency and resources management of the reduced order 2-D IIR filter. For the reduced-order 2-D IIR filter, it not only reduces the number of coefficients but also offers significant advantages in resource management. With fewer coefficients, the memory requirements for storing filter parameters are significantly lowered, which is especially beneficial for embedded systems or devices with limited memory capacity. Additionally, the reduction in coefficients decreases the number of arithmetic operations, resulting in faster processing times and enhanced real-time performance. This reduced computational demand also translates to improved energy efficiency, making such filters well-suited for low-power applications. However, despite these advantages, IIR filters may be susceptible to round-off errors and coefficient quantization issues when implemented using fixed-point arithmetic. These errors, stemming from the filter's finite poles and zeros, can limit its practical effectiveness compared to FIR filters, depending on the implementation.

Chapter 7: Conclusion and Future Work

This chapter concludes with a discussion of the potential for future research and developments in this area.

Chapter 2

A Brief Overview

2.1 Preliminaries Background

A discrete-time 1-D state-space model can be represented by:

$$x(n+1) = Ax(n) + bu(n) \tag{2.1}$$

$$y(n) = cx(n) + du(n) \tag{2.2}$$

where $x(n) \in \mathbb{R}^n$ is the state vector, $u(n) \in \mathbb{R}^p$ is the input vector, $y(n) \in \mathbb{R}^m$ is the output vector, and $A \in \mathbb{R}^{n \times n}$, $b \in \mathbb{R}^{n \times p}$, $c \in \mathbb{R}^{m \times n}$, and $d \in \mathbb{R}^{m \times p}$. The dimension or order of the model $\Sigma = (A, b, c, d)$ is defined by the number of state components, i.e., it corresponds to the value of n. The transfer function of the above 1-D model (2.1)-(2.2) is given by:

$$H(z) = \mathbf{c}\left[I(z) - A\right]^{-1}\mathbf{b} + \mathbf{d} \tag{2.3}$$

It is well known that an IIR digital filter as a discrete-time system can be represented by (2.1) and (2.2) or described by the following transfer function:

$$H(z) = \frac{\Sigma_{i=0}^{M} a_i z^{-i}}{1 + \Sigma_{i=1}^{N} b_i z^{-i}} \tag{2.4}$$

In the following, we recall some definitions and properties of 1-D systems that will be useful in this study.

2.2 Stability

2.2.1 Definition

Definition 2.1: An IIR digital filter is said to be stable if every bounded input produces a bounded output [50]. A necessary and sufficient condition on the impulse response for stability is given in the following theorem.

Theorem 2.1: [50] A necessary and sufficient condition for an IIR digital filter to be stable is that its impulse response $h(n)$ is absolutely summable, namely,

$$\Sigma_{n=-\infty}^{\infty}|h(n)| < \infty \tag{2.5}$$

2.2.2 Stability in Terms of Poles

For a causal IIR digital filter whose transfer function is a rational function of the form

$$H(z) = \frac{\Sigma_{i=0}^{M} a_i z^{-i}}{1 + \Sigma_{i=1}^{N} b_i z^{-i}} \tag{2.6}$$

its stability can be characterized in terms of its poles, which are defined as the roots $\{p_i | i = 1, 2, 3, ...N\}$ of the equation $1 + \Sigma_{i=1}^{N} b_i z^{-i}$ in the z-plane [50].

Theorem 2.2: [50] The IIR filter in (2.6) is stable if and only if all its poles, p_i, are located strictly inside the unit circle of the z-plane [50], namely,

$$|p_i| < 1 \quad for\ i = 1, 2, 3, ...N \tag{2.7}$$

2.2.3 Jury-Marden Criterion

An efficient and easy-to-use stability criterion was developed by Jury using a result of Marden [50]. In this criterion, an array of numbers known as the Jury-Marden array is constructed as follows: The first two rows of the array are just the coefficients of polynomial $B(z) = \Sigma_{i=0}^{N} b_i z^{N-i}$ in ascending and descending orders [50], respectively. The elements of the third and fourth rows are calculated as:

$$c_i = \det \begin{bmatrix} b_0 & b_{N-i} \\ b_N & b_i \end{bmatrix} \quad \text{for i=0, 1, 2, ..., N-1} \tag{2.8}$$

and those of the fifth and sixth rows as:

$$d_i = \det \begin{bmatrix} c_0 & c_{N-1-i} \\ c_{N-1} & c_i \end{bmatrix} \quad \text{for i=0, 1, 2, ..., N-2} \tag{2.9}$$

and so on until a total of $2N-3$ rows are computed. There will be three components in the last row, which are denoted as r_0, r_1, and r_2. The stability criterion of Jury-Marden can now be stated as in the following theorem [50].

Theorem 2.3: [50] All zeros of a polynomial $B(z)$ are strictly inside the unit circle of the z-plane if and only if the following conditions are satisfied:

(i) $B(1) > 0$

(ii) $(-1)^N B(-1) > 0$

(iii) $b_0 > |b_N|$

$|c_0| > |c_N - 1|$

$|d_0| > |d_N - 2|$

.....

.....

$|r_0| > |r_2|$

2.2.4 Stability Triangle of Second-Order Polynomials

By applying the Jury-Marden criterion to a second-order polynomial of the form:

$$B(z) = z^2 + b_1 z + b_2 \tag{2.10}$$

one can conclude that $B(z)$ is stable if and only if the coefficients $\{b_1, b_2\}$ satisfy [50]

$$b_2 < 1, -b_1 - b_2 < 1, and \;\; b_1 - b_2 < 1 \tag{2.11}$$

The region defined by the three linear constraints in (2.11) is depicted in Figure 2.1, which is often referred to as the stability triangle [50].

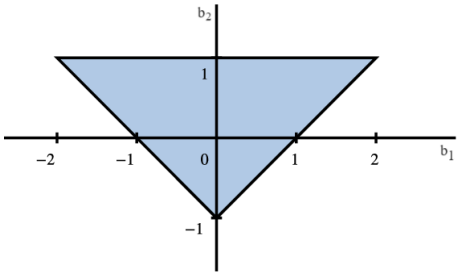

Figure 2.1: Stability triangle

2.2.5 Lyapunov Criterion

An IIR digital filter characterized in state-space (2.1) and (2.2) is stable if and only if the magnitudes of the eigenvalues of system matrix A are strictly less than unity [50].
Theorem 2.4: [50] **Lyapunov**
The state-space digital filter in (2.1) and (2.2) is stable if and only if for a positive definite matrix Q there exists a unique positive definite matrix P that satisfies the Lyapunov equation

$$A^T P A - P = -Q \tag{2.12}$$

The Lyapunov criterion is suitable for IIR filters that are modeled in state-space.

2.3 Controllability and Observability

Definition 2.2: The system (2.1) or the pair (A,b) is said to be controllable if, for any initial state x_0 and any final state x_f, there exists a finite sequence of input samples, $u(0), u(1), \cdots, u(n_f - 1)$, that transfers the system from x_0 to x_f, i.e., such that $x(0)$=x_0 and $x(n_f)$=x_f. Otherwise, the system is said to be uncontrollable.
The controllability matrix $\mathcal{C}$ for a stable state-space realization (A, b, c, d) is defined as:

$$\mathcal{C} = [b \;\; Ab \;\; A^2 b \;\; .....A^{n-1} b] \tag{2.13}$$

Definition 2.3: The system (2.2) or the pair (A, c) is said to be observable if, for zero inputs, any unknown initial state x_0 can be determined from a finite sequence of observations of the output, $y(0)$, $y(1), \cdots, y(n_f - 1)$. Otherwise, the system is said to be unobservable.
The observability matrix $\mathcal{O}$ for a stable state-space realization (A, b, c, d) is defined

as:

$$\mathcal{O} = [c \;\; cA \;\; cA^2 \;\; .....cA^{n-1}]^T \tag{2.14}$$

Controllability and observability of a system can be checked through the following theorems.

Theorem 2.5: [51] The following condition is necessary and sufficient for a model $\Sigma = (A, b, c, d)$ to be controllable:

1. $\text{rank}(\mathcal{C}) = n$.

where n is the order of the system.

Moreover, if all eigenvalues of A have modulus less than one, then $\Sigma = (A, b, c, d)$ is controllable if and only if the unique solution P of the Lyapunov equation

$$P - APA^T = bb^T \tag{2.15}$$

is positive definite. Such solution is called the controllability gramian of the model.

Theorem 2.6: [51] The following condition is necessary and sufficient for a model $\Sigma = (A, b, c, d)$ to be observable:

1. $\text{rank}(\mathcal{O}) = n$.

Moreover, if all eigenvalues of A have modulus less than one, then $\Sigma = (A, b, c, d)$ is observable if and only if the unique solution Q of the Lyapunov equation

$$Q - A^TQA = c^Tc \tag{2.16}$$

is positive definite. Such solution is called the observability gramian of the model.

2.4 Minimality and Balanced Realization

We start this section by the following definitions.

Definition 2.4: [51] Given a linear stable system $\Sigma = (A, b, c, d)$, the singular values of the system, $\sigma_1 \geq \sigma_2 \geq \cdots \geq \sigma_n > 0$, are the square roots of the eigenvalues of the product of the controllability and observability gramians.

Definition 2.5: [51] The stable state-space system (2.1) and (2.2) is called minimal if and only if the pairs (A, b) is controllable and (A, c) is observable.

Definition 2.6: [51] The minimal state-space representation given by (2.1) and (2.2) is called balanced if the controllability and observability gramians P and Q are equal and diagonal, i.e.,

$$P = Q = diag(\sigma_1, \sigma_2, \sigma_3, \cdots, \sigma_n), \sigma_1 \geq \sigma_2 \geq \cdots \geq \sigma_n > 0 \tag{2.17}$$

where σ_i, $i = 1, 2, \cdots, n$, are known as Hankel singular values of the system.
For a balanced realization system, its Hankel singular values are arranged in a decreasing order where the size of the values reflect the controllability and observability energy of the states. The magnitude of σ_i in (2.17) reflects the controllability and observability energy of the states. In other words, the state associated with the bigger singular value has a higher controllability and observability energy and has more influence on input/output responses. Based on this concept, it is possible to truncate the states corresponding to the small singular values without significantly affecting the main input/output dynamic properties of the original system [52]. In addition, the system is assumed to be stable, which implies that the controllability matrix P and the observability matrix Q are positive-definite matrices. Therefore, if the system is minimal and stable then these gramians P and Q are the unique algebraic solutions to the Lyapunov equations (2.15) and (2.16).

2.4.1 Balanced State-Space Realization of a FIR Transfer Function

Consider the N^{th}-order FIR digital filter transfer function given by

$$H(z) = \Sigma_{n=0}^{N} h_n z^{-n} \tag{2.18}$$

The digital filter can be expressed by the following N-dimensional state space form:

$$x(n+1) = Ax(n) + bu(n) \tag{2.19}$$

$$y(n) = cx(n) + du(n) \tag{2.20}$$

where $x(n)$ is the N^{th}-order state vector, $u(n)$ is the scalar input sequence, $y(n)$ is the scalar output sequence, and A, b, c and d are the $N \times N, N \times 1, 1 \times N$ and 1×1 real coefficient matrices, respectively. Assuming that the system meets the conditions of controllability, observability, and stability. The transfer function H(z) of this system

can be described as

$$H(z) = c(zI - A)^{-1}b + d \tag{2.21}$$

It can be verified that the following (A, b, c, d) offers a valid state-space realization of the transfer function H(z).

$A = \begin{bmatrix} 0 & I_{N-1} \\ 0 & 0 \end{bmatrix}$, $b = \begin{bmatrix} h_1 \\ . \\ . \\ h_N \end{bmatrix}$, c= [1 0 0 ... 0], d=$h_0$

Once a state-space realization is found, it can be verified by definition that

$$A' = T^{-1}AT \tag{2.22}$$

$$b' = T^{-1}b \tag{2.23}$$

$$c' = cT \tag{2.24}$$

$$d' = d \tag{2.25}$$

is also a realization of H(z) for an arbitrary nonsingular matrix T that transforms the generalized system into balanced system, when gramian controllability matrix P and gramian observability matrix Q are positive definite. The most interesting realization of H(z) among the numerous realizations is a balanced realization

$$x(n+1) = Ax(n) + bu(n) \tag{2.26}$$

$$y(n) = cx(n) + du(n) \tag{2.27}$$

This approximation is not only satisfying $H(z) = c(zI - A)^{-1}b + d$, but more importantly, has diagonal and equal controllability and observability gramians, where the controllability gramian P for a stable state-space realization A,b,c,d is defined as

$$P = \Sigma_{i=0}^{\infty} A^i b b^T A^{(i)^T} \tag{2.28}$$

and the observability gramian Q for a stable realization A,b,c,d is defined as

$$Q = \Sigma_{i=0}^{\infty} A^{(i)^T} c^T c A^i \tag{2.29}$$

These gramians are positive definite matrices and have a desirable property where they satisfy the following Lyapunov equations

$$P - APA^T = bb^T \tag{2.30}$$

$$Q - A^TQA = c^Tc \tag{2.31}$$

If the above matrix P is equal to matrix Q, and is diagonal, namely

$$P = Q = diag(\sigma_1, \sigma_2, ...\sigma_n) \tag{2.32}$$

then the system is called balanced system, where $\sigma_1 \geqslant \sigma_2 \geqslant ..... \geqslant \sigma_n \geqslant 0$; σ_i is Hankel singular value.

Now, considering that the original system is stable and minimal, the steps of model reduction in brief can be summarized as follows [50]:

Step 1: Determine controllability and observability gramians by solving Lyapunov equations in (2.30) and (2.31).

Step 2: Compute the coordinate transformation matrix T as follows:

i) Since P is positive definite, one can find an orthogonal matrix U such that $U^TPU = diag(\zeta_1, \zeta_2, ...\zeta_N)$ where $\zeta_1 \geqslant \zeta_2 \geqslant, ... \geqslant \zeta_N \geqslant 0$ are the eigenvalues the of controllability gramian P.

ii) Perform $\zeta_i = \sigma_i^2$ for $i = 1, 2, ..., N$, and construct the following matrix $V = diag(\sqrt{\sigma_1}, \sqrt{\sigma_2}, ...\sqrt{\sigma_N})$

iii) Compute $T = UV$.

Step 3: Obtain the balanced realization minimal model $(A_b, b_b, c_b, d) = (T^{-1}AT, T^{-1}b, cT, d)$.

At the end, the balanced realization based design method can be implemented by following the next steps:-

1) For digital filters, design a good-quality FIR filter $H(z)$ that approximates the desired frequency response $H_d(z)$.

2) Find a balanced realization (A_b, b_b, c_b, d) for $H(z)$.

3) For a stable IIR filter of order r (with $r < N$) that approximates the same desired frequency response $H_d(z)$, the transfer function of the required IIR filter , say $H_r(z)$, can be constructed by partitioning the balanced realization obtained in step 2 as

$$A_b = \begin{bmatrix} A_r & * \\ * & * \end{bmatrix} \tag{2.33}$$

$$b_b = \begin{bmatrix} b_r \\ * \end{bmatrix} \tag{2.34}$$

$$c_b = \begin{bmatrix} c_r & * \end{bmatrix} \tag{2.35}$$

Where $A_r \in R^{r\times r}, b_r \in R^{r\times 1}, c_r \in R^{1\times r}$, and has a transfer function as

$$H_r(z) = c_r(zI - A_r)^{-1}b_r + d \tag{2.36}$$

2.5 State-Space Models of 2-D Digital Filters

Roesser's model is a fundamental framework for representing 2-D discrete systems in state space [49, 53]. This model was proposed by R.P. Roesser in 1975, and is extensively used due to its generality and relative simplicity and as it directly represents many practical 2-D problems [49]. This model helps in analyzing the stability, controllability, and observability of 2-D systems, extending the capabilities of traditional 1-D systems theory to 2-D systems.
The Roesser's model is defined as follows:

$$\begin{bmatrix} x^h(m+1,n) \\ \\ x^v(m,n+1) \end{bmatrix} = \begin{bmatrix} A_{11} & A_{12} \\ \\ A_{21} & A_{22} \end{bmatrix} \begin{bmatrix} x^h(m,n) \\ \\ x^v(m,n) \end{bmatrix} + \begin{bmatrix} b_1 \\ \\ b_2 \end{bmatrix} u(m,n) \tag{2.37}$$

$$\equiv \mathbf{A}x(m,n) + \mathbf{b}u(m,n) \tag{2.38}$$

$$y(m,n) = \begin{bmatrix} c_1 & c_2 \end{bmatrix} x(m,n) + d\ u(m,n) \equiv \mathbf{c}x(m,n) + \mathbf{d}u(m,n) \tag{2.39}$$

The matrices $\mathbf{A}, \mathbf{b}, \mathbf{c}$ can be decomposed as follows:

$$\mathbf{A} = \begin{bmatrix} A_{11} & A_{12} \\ A_{21} & A_{22} \end{bmatrix}, \mathbf{b} = \begin{bmatrix} b_1 \\ b_2 \end{bmatrix}, \mathbf{c} = \begin{bmatrix} c_1 & c_2 \end{bmatrix}, \tag{2.40}$$

Throughout this discussion, m, n, are respectively integer-valued horizontal and vertical coordinates, $x^h(m,n) \in \mathbb{R}^{m\times 1}$ is the horizontal state vector, $x^v(m,n) \in \mathbb{R}^{n\times 1}$ is

the vertical state vector, $u(m,n) \in \mathbb{R}$ is the input, and $y(m,n) \in \mathbb{R}$ is the output. $A_{11}, A_{12}, A_{21}, A_{22}, b_1, b_2, c_1, c_2$, and d are real matrices with appropriate dimensions. The transfer function matrix of the 2-D system (2.37) and (2.39) is given by

$$H(z_1, z_2) = \mathbf{c}\left[I(z_1, z_2) - A\right]^{-1}\mathbf{b} + \mathbf{d} \tag{2.41}$$

where $I(z_1, z_2) = diag\{z_1 I_m, z_2 I_n\}$.

Mathematically, the transfer function of 2-D IIR digital filter can be expressed as:

$$H(z_1, z_2) = \frac{A(z_1, z_2)}{B(z_1, z_2)} = \frac{\sum_{n=0}^{N_2}\sum_{m=0}^{N_1} a_{mn} z_1^{-m} z_2^{-n}}{\sum_{n=0}^{N_2}\sum_{m=0}^{N_1} b_{mn} z_1^{-m} z_2^{-n}}, \quad b_{00} = 1 \tag{2.42}$$

Here, the transfer function of a 2-D IIR filter is represented as a ratio of two polynomials in the z_1 and z_2 variables, where z_1 and z_2 correspond to the spatial dimensions of the input signal.

Other models proposed by Fornasini and Marchesini (FM), the FM models are extensively applied in signal processing [54] and control [55]. The first FM model, often abbreviated as FM1, describes a 2-D system using state-space representation. This model is defined by the following equations [56]:

$$x(m+1, n+1) = A_0 x(m,n) + A_1 x(m, n+1) + A_2 x(m+1, n) + b_0 u(m,n) \tag{2.43}$$

$$y(m,n) = cx(m,n) \tag{2.44}$$

Here, $x(m,n)$ represents the state vector at coordinates (m,n), $u(m,n)$ is the input vector, and $y(m,n)$ is the output vector. The matrices A_0, A_1, A_2, b_0 and c are system matrices that define the dynamics of the 2-D system.

The second FM model, or FM2, is another state-space representation for 2-D systems. It is described by the following equations [48]:

$$x(m+1, n+1) = A_1 x(m, n+1) + A_2 x(m+1, n) + b_1 u(m, n+1) + b_2 u(m+1, n) \tag{2.45}$$

$$y(m,n) = cx(m,n) \tag{2.46}$$

In this model, $x(m,n), u(m,n)$, and $y(m,n)$ retain their meanings as state, input,

and output vectors, respectively.

2.6 Stability of 2-D IIR Filters

2.6.1 BIBO Stability

Over the past decades, there has emerged a considerable interest in stability analysis of 2-D discrete systems, and different methods and mathematical concepts have been developed, see for example, for Roesser model [9, 57–63], and for FM model [64–78] and references therein. This thesis does not aim to get into a detailed discussion of 2-D system stability. However, just like in the 1-D case, stability of a practical 2-D system is a necessary property. To investigate the stability of 2-D discrete linear system, it is required to introduce some essential concepts that will be useful for this review.

Consider a 2-D digital filter characterized by the transfer function:

$$H(z_1, z_2) = \frac{A(z_1, z_2)}{B(z_1, z_2)} = c \begin{bmatrix} z_1 I_m - A_{11} & -A_{12} \\ -A_{21} & z_2 I_n - A_{22} \end{bmatrix}^{-1} b + d \tag{2.47}$$

Here $A(z_1, z_2)$ and $B(z_1, z_2)$ are polynomials in z_1 and z_2, representing the numerator and denominator coefficients, respectively. If two polynomials $A(z_1, z_2)$ and $B(z_1, z_2)$ have no common factors, they are said to be factor coprime. On the other hand, if there are no points (z_1, z_2) at which the two polynomials assume the value of zero, the two polynomials are said to be zero coprime. Two polynomials in *one* variable are factor coprime if and only if they are zero coprime. Nevertheless, two polynomials in *two* variables can be zero coprime without being factor coprime. It is commonly known that two-variable polynomials and rational functions cannot be factored into first-order polynomials. Instead, it can be factored into irreducible factors, which are two-variable polynomials in and of themselves but are not factorable into any other factors [1]. Two polynomials which have no irreducible factors in common are said to be mutually prime [1].

Through out this discussion and as in [1], we will assume $B(0,0) \neq 0$ so that $B(z_1, z_2) \neq 0$ in some neighborhood ${U_\epsilon}^2 \triangleq \{(z_1, z_2) : |z_1| < \epsilon, |z_2| < \epsilon\}$ of (0,0), hence in ${U_\epsilon}^2$ the

function $H(z_1, z_2)$ is analytic and has power series expansion

$$H(z_1, z_2) = \sum_{m,n=0}^{\infty} h_{mn} z_1^m z_2^n \tag{2.48}$$

where h_{mn} is defined to be the impulse response of $H(z_1, z_2)$. Here, a particular notion of stability is considered: a 2-D system is said to be bounded-input- bounded-output (BIBO) stable if an amplitude bounded input always originates an amplitude bounded output. The strict definition of BIBO stability for 2-D systems is as follows:
Definition 2.7: [21] A 2-D system with input $u(m, n)$ and output $y(m, n)$ is said to be BIBO stable if, for all $M < \infty$ such that $\|u(m, n)\| < M$, there exists an $N < \infty$ such that $\|y(m, n)\| < N$.
It is well known that the 2-D digital filter represented by $H(z_1, z_2)$ is BIBO stable iff $\{h_{mn}\} \in l_1$, i.e., $\sum_{m,n=0}^{\infty} |h_{mn}| < \infty$ [1]. To continue the discussion about 2-D stability, the impulse response is called square summable if $\{h_{mn}\} \in l_2$, i.e., $\sum_{m,n=0}^{\infty} |h_{mn}|^2 < \infty$, and the impulse response is bounded if for some finite M we have $|h_{mn}| < M \ \forall m, n$ [1]. We define $U^2 \triangleq \{(z_1, z_2) : |z_1| < 1, |z_2| < 1\}$ to be the open unit bidisc, $\bar{U}^2 \triangleq \{(z_1, z_2) : |z_1| \leq 1, |z_2| \leq 1\}$ to be the closed unit bidisc and T^2=$\{(z_1, z_2) : |z_1| = 1, |z_2| = 1\}$ to be the distinguished boundary of the unit bidisc. Given the impulse response of the system, the following theorem states a criterion for checking its stability. This criterion is analogous to a result that stands for 1-D systems.
Theorem 2.7: [1] A 2-D system with impulse response $h(m, n)$ is $BIBO$ stable iff $h(m, n)$ is absolutely summable, i.e., iff

$$\sum_{m=0,n=0}^{\infty,\infty} \|h(m, n)\| < \infty \tag{2.49}$$

Now, recall the system given by (2.42), where $A(z_1, z_2)$ and $B(z_1, z_2)$ are mutually prime. A point $(z_1, z_2) \ni B(z_1, z_2) = 0$ where $A(z_1, z_2) \neq 0$ will be called a pole or a nonessential singularity of the first kind (such a point is analogous to a pole in the one variable case). A point $(z_1, z_2) \ni B(z_1, z_2) = A(z_1, z_2) = 0$ will be called a nonessential singularity of the second kind (such points have no one variable analog) [1]. Clearly, if (z_1, z_2) is a pole, $H(z_1, z_2) = \infty$. If (z_1, z_2) is a nonessential singularity of the second kind, the value of $H(z_1, z_2)$ is undefined in any open neighborhood.
If the 2-D system is represented by a transfer function, then the stability of this sys-

tem is closely linked with the singularities of the transfer function, which are not in general isolated points as in 1-D digital filters. These singularities and their types are defined as follows.

Definition 2.8: Given a 2-D rational transfer function $H(z_1, z_2) = \frac{A(z_1,z_2)}{B(z_1,z_2)}$ where $A(z_1, z_2)$ and $B(z_1, z_2)$ are factor coprime polynomials. If $B(z_1, z_2) = 0$ and $A(z_1, z_2) \neq 0$, then (z_1, z_2) is said to be a pole or a nonessential singularity of the first kind of $H(z_1, z_2)$. If $A(z_1, z_2) = B(z_1, z_2) = 0$, then (z_1, z_2) is called a nonessential singularity of the second kind of $H(z_1, z_2)$ [1].

Based on the above definition, Shank's theorem states that $H(z_1, z_2)$ is BIBO stable iff $B(z_1, z_2) \neq 0 \ \forall (z_1, z_2) \in \bar{U}^2$ [1, 79, 80].

Theorem 2.8: [1, 21] **Shank's Theorem**

A 2-D digital filter characterized by a transfer function $H(z_1, z_2)$, as in (2.42), is BIBO stable if $H(z_1, z_2)$ has no singularities on the closed unit bidisc defined by $\bar{U}^2$.

Clearly, before applying this theorem, all irreducible factors common to $A(z_1, z_2)$ and $B(z_1, z_2)$ should first be cancelled to make the numerator and denominator mutually prime; this operation is analogous to cancelling all common poles and zeros in the 1-D case. A test for the existence of common factors is given in [81], and an algorithm for extraction of the greatest common factor is given in [82]. Shank's theorem is essentially correct except that cases may arise where $H(z_1, z_2)$ has a nonessential singularity of the second kind on T^2 but $\{h_{mn}\} \in \ l_1$ [1]. Interested readers can look at an example about that and the prove for sufficiency of Shank's theorem in [1].

We summarize this discussion by a few stability theorems from [1], followed by a table for the stability findings for $H(z_1, z_2) = \frac{A(z_1,z_2)}{B(z_1,z_2)}$, where $A(z_1, z_2)$ and $B(z_1, z_2)$ are mutually prime and $B(0, 0) \neq 0$.

Theorem 2.9: [1] If $H(z_1, z_2)$ represents a BIBO stable filter, then $H(z_1, z_2)$ has no poles in $\bar{U}^2$, and no nonessential singularities of the second kind on $\bar{U}^2$ except possibly on T^2.

Theorem 2.10: [1] If $H(z_1, z_2)$ has a bounded impulse response, then $H(z_1, z_2)$ is analytic in U^2 (i.e., $B(z_1, z_2) \neq 0$ in U^2).

Theorem 2.11: [1] If $H(z_1, z_2)$ is bounded in U^2, then h_{mn} is square summable.

Theorem 2.12: [1] Recall (2.42), if $B(z_1, z_2) \neq 0$ for $z_1 \in \bar{U} \triangleq \{z_1 \ni |z_1| \leq 1\}$, then for any fixed $n, h_{mn} \to 0$ geometrically in m and $\sum_{m=0}^{\infty} |h_{mn}| < \infty$.

Table 2.1 summarizes the stability results as discussed in [1]. The arrows $\Rightarrow$ and $\Leftarrow$ stand for "implies" and "is implied by," respectively.

a)	BIBO stability	$\Leftrightarrow$	$\{h_{mn} \in l_1\}$
b)	$B(z_1, z_2) \neq 0$ in $\bar{U}^2$	$\underset{\Rightarrow}{\not\Leftarrow}$	BIBO stability
c)	$B(z_1, z_2) \neq 0$ in $\bar{U}^2 - T^2$	$\underset{\not\Rightarrow}{\Leftarrow}$	BIBO stability
d)	$\{h_{mn}\} \in l_2$	$\underset{\not\Rightarrow}{\Leftarrow}$	BIBO stability
e)	$\lim h_{mn} = 0$	$\underset{\not\Rightarrow}{\Leftarrow}$	$\{h_{mn}\} \in l_1$ or $\{h_{mn}\} \in l_2$
f)	$B(z_1, z_2) \neq 0$ in U^2	$\underset{\not\Rightarrow}{\Leftarrow}$	$\lvert h_{mn}\rvert \leq M < \infty, \forall\ m, n$
g)	$\lvert H(z_1, z_2)\rvert \leq N < \infty$ in U^2	$\Rightarrow$	$\{h_{mn}\} \in l_2$
h)	$B(z_1, 0) \neq 0$ in $\bar{U}$	$\Rightarrow$	$\sum_{m=0}^{\infty} \lvert h_{mn}\rvert < \infty,\ \forall\ n$

Table 2.1: Stability results from [1]

2.6.2 Stability of 2-D IIR Digital Filters in State-Space

In addition to the above-mentioned stability conditions, it is also possible to analyze the stability characteristics of 2-D digital filters in terms of their state-space representation. The state-space representation offers certain benefits even if the results are the same as those discussed in the previous section. First, the stability of filters may be verified using ordinary matrix analysis techniques because all stability constraints are expressed in terms of the spectral characteristics of certain matrices. Second, the 2-D situation can be included in the generalized Lyapunov theory, which was proven to be highly helpful in 1-D stability analysis. The 2-D Lyapunov equation could be an important tool in the stability analysis and in the design of 2-D model reduction in the state-space where the stability of the reduced order model needs to be ensured given that the original model is also stable. Similar to the 1-D case, one can extend the Lyapunov matrix equation to the 2-D case. Although it has been shown in [9] that the existence of Lyapunov equations solutions is only a sufficient, not a necessary, condition for stability of 2-D systems, this condition is a useful test for the stability of 2-D systems [9].

Recall (2.47), and assume

$$B(z_1, z_2) = \det \begin{bmatrix} I_m - z_1 A_{11} & -z_1 A_{12} \\ -z_2 A_{21} & I_n - z_2 A_{22} \end{bmatrix} \neq 0 \quad \text{in } \bar{U}^2 \tag{2.50}$$

One can write $B(z_1, z_2)$ as follows
$B(z_1, z_2) = \det(z_1 I_m - A_{11}) \times \det\{z_2 I_n - [A_{22} + A_{21}(z_1 I_m - A_{11})^{-1} A_{12}]\}$
$= \det(z_2 I_n - A_{22}) \times \det\{z_1 I_m - [A_{11} + A_{12}(z_2 I_n - A_{22})^{-1} A_{21}]\}$
We provide some of the 2-D stability results as stated in terms of the following theorems and form the foundation of a number of stability criteria, as will be demonstrated in Theorem 2.16 below.

Theorem 2.14: Huang [21] A 2-D digital filter is BIBO stable if

1. $B(z_1, 0) \neq 0$ for $|z_1| \leq 1$.
2. $B(z_1, z_2) \neq 0$ for $|z_1| = 1$ and $|z_2| \leq 1$.

Theorem 2.15: DeCarlo, Murray, and Sacks [21] A 2-D digital filter is BIBO stable if

1. $B(z, z) \neq 0$ for $|z| \leq 1$.
2. $B(z_1, z_2) \neq 0$ for $(z_1, z_2) \in U^2$.

We bring to the attention of the reader that the Shank's, Huang's, and DeCarlo's theorems give a sufficient condition for BIBO stability for 2-D digital filters, and the necessity of these theorems may fail to apply, as [1] has shown. Based on Theorem 2.14 and 2.15 and the above expression of $B(z_1, z_2)$, state-space versions of the stability conditions can be stated in the following theorem.

Theorem 2.16: [21] The transfer function of (2.47) represents a BIBO-stable digital filter if and only if one of the following conditions holds:

1. (a) All the eigenvalues of matrix A_{11} are located on the open unit disc.
   (b) All the eigenvalues of matrix $A_{22} + A_{21}(z_1 I_m - A_{11})^{-1} A_{12}$ are located on the open unit disc for each $z_1 \in U_1 = \{z_1 : |z_1| = 1\}$.
2. (a) All the eigenvalues of matrix A_{22} are located on the open unit disc.
   (b) All the eigenvalues of matrix $A_{11} + A_{12}(z_2 I_n - A_{22})^{-1} A_{21}$ are located on the open unit disc for each $z_2 \in U_2 = \{z_2 : |z_2| = 1\}$.

3. (a) All the eigenvalues of matrix A of the model $\Sigma = (A, b, c, d)$ are located on the open unit disc.

   (b) Matrix A_{11} has no eigenvalues on the unit circle.

   (c) Matrix $A_{22} + A_{21}(z_1 I_m - A_{11})^{-1} A_{12}$ has no eigenvalues on the unit circle for each $z_1 \in U_1$

4. (a) All the eigenvalues of matrix A are located on the open unit disc.

   (b) Matrix A_{22} has no eigenvalues on the unit circle.

   (c) Matrix $A_{11} + A_{12}(z_2 I_n - A_{22})^{-1} A_{21}$ has no eigenvalues on the unit circle for each $z_2 \in U_2$.

2.7 Controllability and Observability Gramians of 2-D Systems

Controllability and observability gramians play a significant role in approximating a high-dimensional 2-D system with a lower-dimensional one while preserving its essential dynamics. As model reduction aims to capture the most relevant dynamics of a high-dimensional system while eliminating less significant modes, 2-D gramians provide insights into the energy distribution and controllability/observability properties of a 2-D system. By analyzing the singular values or eigenvalues of 2-D gramians, one can identify which modes contribute most to the system's behavior. This information guides the selection of modes to retain in the reduced-order model. Also, quantifying the error between the original high-dimensional system and the reduced-order model is crucial after model reduction. By contrasting the energy collected by the maintained modes with that of the rejected ones, 2-D gramians offer a technique to assess this inaccuracy. One can conclude that 2-D gramians are vital in the model reduction of 2-D systems. They provide insights into the system's energy distribution, controllability, and observability properties, guiding the selection of relevant modes for the reduced-order model. These gramians enhance the accuracy and efficiency of the model reduction process, making it an indispensable tool in dealing with complex, high-dimensional 2-D systems.

Now, considering the Roesser's state-space model given by (2.37) and (2.39), there are three types of gramians defined as follows [83]:

The first type of 2-D gramian, known as a pseudo-controllability and pseudo-observability gramian, is given by

$$P^p = \frac{1}{(2\pi j)^2} \oint_{|z_1|=1} \oint_{|z_2|=1} F(z_1, z_2) F^*(z_1, z_2) \frac{dz_2}{z_2} \frac{dz_1}{z_1} \tag{2.51}$$

$$Q^p = \frac{1}{(2\pi j)^2} \oint_{|z_1|=1} \oint_{|z_2|=1} G^*(z_1, z_2) G(z_1, z_2) \frac{dz_2}{z_2} \frac{dz_1}{z_1} \tag{2.52}$$

where

$$F(z_1, z_2) = [I(z_1, z_2) - A]^{-1} b \tag{2.53}$$

$$G(z_1, z_2) = c[I(z_1, z_2) - A]^{-1} \tag{2.54}$$

and $I(z_1, z_2) = z_1 I_m \oplus z_2 I_n$.
The second type of gramian, known as the structured controllability and observability gramian, is defined by the positive-definite solutions P^s and Q^s of the Lyapunov inequalities

$$AP^sA^T - P^s + bb^T < 0 \tag{2.55}$$

$$A^TQ^sA - Q^s + c^Tc < 0 \tag{2.56}$$

The matrices P^s and Q^s are block diagonal matrices, $P^s = diag(p_1, p_2)$ and $Q^s = diag(q_1, q_2)$, representing the solutions to the above Lyapunov inequalities.
The third type of gramian, known as the quasi controllability and observability gramian, is defined by the positive-definite block-diagonal matrices $P^q = diag(p_1, p_2)$ and $Q^q = diag(q_1, q_2)$ where p_i and q_i, $(i = 1, 2)$, satisfy the Lyapunov equations

$$A_{11}p_1A_{11}^T - p_1 + b_1b_1^T + A_{12}p_2A_{12}^T = 0 \tag{2.57}$$

$$A_{22}p_2A_{22}^T - p_2 + b_2b_2^T + A_{21}p_1A_{21}^T = 0 \tag{2.58}$$

$$A_{11}^Tq_1A_{11} - q_1 + c_1^Tc_1 + A_{21}^Tq_2A_{21} = 0 \tag{2.59}$$

$$A_{22}^Tq_1A_{22} - q_2 + c_2^Tc_2 + A_{12}^Tq_1A_{12} = 0 \tag{2.60}$$

There are several types of gramians of the system that can be properly defined for a given 2-D system and there are different types of balanced realizations for a 2-D discrete system, leading to different balanced approximations [83]. These balanced

approximations are pseudo-balanced approximation, structurally balanced approximations, and quasi-balanced approximations. The reduced-order model obtained by the first approximation maintains the stability if the original model has a separable denominators [84]. For the structurally-balanced approximation, the reduced model always preserves the stability which is not always true for the quasi-balanced approximation unless the original system has separable denominator [15, 83, 84]. Chapter 4 details the structurally-balanced approximation model reduction method for designing 2-D nearly linear-phase recursive digital filters including how to use a linear matrix inequality (LMI) method to compute controllability and observability gramians.

Chapter 3

Improved Design Method for Nearly Linear-Phase 1-D IIR Filter Using Constrained Optimization

Abstract: In this chapter, the design of nearly linear-phase recursive digital filters using a constrained optimization method is investigated. The method is based on existing constrained optimization techniques for nearly linear-phase IIR digital filters, and it is expected to be useful in applications where both magnitude and phase response specifications are required to be satisfied. Starting from an initial filter, the proposed method minimizes the group delay deviation under a set of linear constraints in terms of the magnitude response and filter stability. Improved sampling functions are introduced to the optimization problem, which are used to select the sampling points that are used for approximating the group delay and the rest of the constraints in various frequency bands. By using the proposed sampling functions we get an improved IIR filter response. The significance of this chapter lies in its exploration of constrained optimization techniques to shape the frequency response and characteristics of 1-D IIR filters. As we delve into this subject, we lay the foundation for our subsequent chapters by establishing the principles of IIR filter design and the power of optimization methodologies in achieving precision and specificity in filter response. Additionally, we introduce the concept of phase linearity and stability, which are crucial aspects in IIR filter design, setting the stage for a smooth transition into the multidimensional field of 2-D IIR filters.

3.1 Introduction

Digital filters with linear phase are important in several engineering applications where a flat group-delay characteristic is required [2,6]. Digital filters having linear-phase in the passband are very important in signal processing because they allow distortion-free transmission of waveforms. Perfectly linear-phase filters can be easily designed as nonrecursive digital filters by using various methods [6, 8]. The use of nonrecursive filters in these applications often entails increased computational effort, low throughput, and a large group delay [8]. To mitigate these problems, researchers have dedicated considerable effort in recent years developing quite a variety of methods for the design of recursive digital filters that have nearly linear-phase in the passband [2, 6, 8, 85–91]. In several applications, a perfectly linear-phase response is not required, and filters that have a nearly linear-phase response are quite acceptable [2,6]. In addition to control and communication systems, these filters find a place in some other applications, such as audio signal processing and speech coding [8, 87, 92]. Two main advantages make recursive digital filters more attractive than nonrecursive filters. Firstly, they can satisfy the required filter specifications with a much lower filter order, thereby reducing the computational requirement and/or the complexity of hardware, and secondly, they can have a lower overall group delay [2, 6, 35, 93]. The design of these filters is much more challenging than that of nonrecursive filters because zeros will typically end up both inside and outside of the unit circle, and we must, of course, constrain the poles to lie within the unit circle [94]. The optimization problem is usually highly nonlinear, thereby requiring highly sophisticated optimization methods [6, 35]. As recursive filters lack the inherent stability of their nonrecursive counterparts, the issue of stability introduces some complications in the design process since an unconstrained optimization can easily yield an unstable filter that would be of no use. Different design methods for general IIR filters exist in the literature [3, 95–104]. The classical equalizer approaches [90, 91, 105] used to alleviate the non-linear phase response involve an IIR filter satisfying the magnitude response requirements being firstly designed and then cascaded by an all-pass phase equalizer to the designed IIR filter. Using additional equalizers increases the computational and hardware overhead of the designed IIR filter. Another design method based on model reduction is introduced in [85]. The main steps of this method are to design a FIR filter that satisfies the magnitude specifications, convert that high-order FIR filter into state space, reduce the model order, and finally convert the lower-order

model to a reduced-order IIR filter. Other existing methods [89, 93, 94, 105, 106] minimize the frequency-response error of the filter to satisfy the design requirements for its magnitude and phase responses simultaneously. In these methods, the group-delay deviation is not well controlled and usually has a much larger value near the passband edges. Some other methods [107, 108] deal with the magnitude error and phase error independently by minimizing the magnitude and phase errors simultaneously or minimizing one of them subject to an upper-bound constraint on the other. These methods not only minimize the maximum phase error but also control the maximum magnitude error.

In this chapter, we propose a design method for a nearly linear-phase recursive digital filters. The proposed technique is used to improve the design of nearly linear-phase recursive digital filters originally proposed by Nongpiur, Shpak, and Antoniou in [2]. We introduce nonuniform variable sampling functions that control the number and frequencies of points in various frequency bands. The main objective is to facilitate the design by controlling the quality of the design specifications and implementing the design problem in a more efficient way. Using this proposed technique reduces the computation effort, reduces the passband ripple, improves transition and stopband responses, and also improves the convergence of the optimization algorithm. Developing these nonuniform variable sampling functions to impose constraints on the magnitude and phase responses to satisfy requirements on the magnitude and group-delay responses of the filter is the major contribution of this chapter. Design efficiency and the performance of the proposed method are evaluated to show the trade-off between minimum and maximum attenuation in the magnitude response with a group-delay quality factor Q_τ in the passband. The remaining sections are organized as follows: The constrained optimization problem is formulated in Section 3.2. In Section 3.3, we introduce a new function to control the number of points in various frequency bands. Section 3.4 addresses filter stability. Section 3.5 shows the design of the constrained optimization problem. Section 3.6 shows the simulation results of the lowpass filter presented as Example 5 in [2] and Example 4 in [3]. Section 3.7 is the conclusion.

3.2 Problem Formulation

As in [2], the filter is assumed to comprise a cascade of second-order sections (SOSs), which can be represented as a product of biquadratic transfer functions of the form:

$$H(z) = H_0 \prod_{m=1}^{J} \frac{a_{0m} + a_{1m} z + z^2}{b_{0m} + b_{1m} z + z^2} = H_0 \prod_{m=1}^{J} \frac{N_m(z)}{D_m(z)}, \tag{3.1}$$

where $z = e^{j\omega}$, $\omega = 2\pi f$, f is the frequency in (Hz), J is the number of second-order sections, $N = 2J$ is the filter order, and H_0 is a positive multiplier constant.
Let $c = [a_{01}\, a_{11}\, b_{01}\, b_{11}\, \ldots\, b_{0J}\, b_{1J}\, H_0]^T$ be a variable vector that includes the transfer function coefficients, where the superscript T represents the transpose operation. The corresponding frequency response $H(e^{j\omega})$ can be obtained by substituting $z = e^{j\omega}$ in $H(z)$ above. The group-delay, $\tau_h(c, z)$, corresponding to the transfer function in (3.1) is given by [105]:

$$\tau_h(c, z) = -\sum_{i=1}^{J} \frac{\alpha_n(c, z, i)}{\beta_n(c, z, i)} + \sum_{i=1}^{J} \frac{\alpha_d(c, z, i)}{\beta_d(c, z, i)}, \tag{3.2}$$

where

$$\begin{aligned}
\alpha_n(c, z, i) &= 1 - a_{0i}^2 + a_{1i}(1 - a_{0i}) \cos\omega, \\
\beta_n(c, z, i) &= a_{0i}^2 + a_{1i}^2 + 1 + 2a_{0i}(2\cos^2\omega - 1) \\
&\quad + 2a_{1i}(a_{0i} + 1) \cos\omega, \\
\alpha_d(c, z, i) &= 1 - b_{0i}^2 + b_{1i}(1 - b_{0i}) \cos\omega, \\
\beta_d(c, z, i) &= b_{0i}^2 + b_{1i}^2 + 1 + 2b_{0i}(2cos^2\omega - 1) \\
&\quad + 2b_{1i}(b_{0i} + 1) \cos\omega.
\end{aligned}$$

The objective is to minimize the error function of the group-delay deviation, $e_g(x, e^{j\omega})$, at frequency ω as:

$$e_g(x, e^{j\omega}) = \tau_h(c, e^{j\omega}) - \tau, \tag{3.3}$$

where τ approximates the passband group delay, which can be initially assigned a value equal to the average group delay of the initial filter at the start of the optimization, but after the first iteration τ is also adjusted along with the parameters of the filter so as to minimize the group delay deviation. The end result will be that τ will tend to track the average value of the passband group-delay. By including the

element τ, the filter-coefficient vector becomes:

$$x = [a_{01}\, a_{11}\, b_{01}\, b_{11}\, \ldots\, b_{0J}\, b_{1J}\, H_0\, \tau]^T \tag{3.4}$$

If x_k is the value of x at the start of the k_{th} iteration and δ is the update to x_k, the updated value of the group-delay deviation can be estimated by using the linear Taylor approximation as follows:

$$e_g(x_k\, +\, \delta,\, e^{j\omega}) \approx e_g(x_k, e^{j\omega})\, +\, \nabla e_g(x_k, e^{j\omega})^T \delta, \tag{3.5}$$

where ∇ is the gradient operator. To control the step size during the optimization process and thereby yield a more accurate and reliable result, $\|\delta\|_2$ in (3.5) is constrained to be small [2, 8].

3.3 Proposed Sampling Function

The computational effort required to complete a design is directly proportional to the number of frequency sample points used for each frequency band. The nonuniform sampling technique can be used to reduce the computational effort and also improve the convergence of the optimization algorithm by controlling the number of sampling points [8, 109, 110]. In this section, we introduce a nonuniform variable sampling function $f(n)$ based on the Riemann approximation.

Definition 3.1: Let f:$[\omega_l, \omega_h] \rightarrow \mathbb{R}$ be a function defined on a closed interval $[\omega_l, \omega_h]$ of the real numbers, $\mathbb{R}$, and $\mathbf{P} = \{[\omega_0, \omega_1], [\omega_1, \omega_2], \cdots, [\omega_{n-1}, \omega_n]\}$, be a partition of the interval I, and $\omega_l = \omega_0 < \omega_1 < \omega_2 < \cdots < \omega_n = \omega_h$, where ω_l and ω_h are the lower and upper edges of the frequency band, and n is the number of points.

The Riemann sum of f over I with partition $\mathbf{P}$ is defined as $\mathbf{S} = \sum_{i=1}^{n} f(\omega_i^*)\Delta\omega_i$ where $\Delta\omega_i = \omega_i - \omega_{i-1}$ and $\omega_i^* \in [\omega_{i-1}, \omega_i]$.

The choice of ω_i^* in the interval $[\omega_{i-1}, \omega_i]$ is arbitrary, so for any given function f defined on an interval I and a fixed partition $\mathbf{P}$, one might produce different Riemann sums depending on which ω_i^* is chosen, as long as $\omega_{i-1} \leq \omega_i^* \leq \omega_i$ holds true.

Using the Riemann sum approximation of an integral, the L_p-norm of the group-delay deviation at the k_{th} iteration is computed as follows:

$$E_p(k) = \left[\int_{\omega_l}^{\omega_h} |e_g(x_{k+1}, e^{j\omega})|^p d\omega\right]^{1/p} \tag{3.6}$$

$$\approx \left[\sum_{i=1}^{N} |e_g(x_{k+1}, e^{j\omega_i})|^p \Delta\omega_i\right]^{1/p}$$
$$= \kappa_g \left[\sum_{i=1}^{N} |e_g(x_{k+1}, e^{j\omega_i})|^p f(i)\right]^{1/p} \tag{3.7}$$

where the value of p in the above expression can be any positive integer and the most significant values for p are 2 and ∞, f is called a *sampling function* from $\mathbb{N}$ to $\mathbb{R}^+$ that determines the length of each $\Delta\omega_i$, and κ_g is a constant given by:

$$\kappa_g = \frac{\omega_h - \omega_l}{\sum_{i=1}^{N} f(i)}. \tag{3.8}$$

For the Riemann sum to converge to the integral, each $\Delta\omega_i$ has to converge to 0 as N goes to $+\infty$. Therefore, the sampling functions have to satisfy the following condition:

$$\lim_{N\to\infty} \frac{f(i)}{\sum_{j=1}^{N} f(j)} = 0, \forall i = 1, \ldots, N. \tag{3.9}$$

The space of sampling functions that satisfy the above condition will be denoted by $\mathbb{S}$. It is easy to see that $f(n) = 1$, $f(n) = n$, and $f(n) = 1/n$ are in $\mathbb{S}$. The sampling points ω_i can be chosen according to f based on the midpoint rule approximation and can be computed recursively as follows:

$$\begin{aligned} \Delta\omega_i &= \kappa_g f(i), \\ v_i &= v_{i-1} + \Delta\omega_i, \\ \omega_i &= v_{i-1} + \frac{\Delta\omega_i}{2}, \\ v_0 &= \omega_l \end{aligned} \tag{3.10}$$

The v_i are the boundary points, and the ω_i are the middle points. If we take $f(i) = 1, \forall i \in \{1, \ldots, N\}$, we obtain the same expression as in [2]. Using (3.5), we can rewrite (3.6) as follows:

$$E_p(k) \approx \kappa_g \left[\sum_{i=1}^{N} \left|e_g(x_k, e^{j\omega_i}) f(i) \; + \; \nabla e_g(x_k, e^{j\omega_i})^T f(i)\delta\right|^p\right]^{1/p} \tag{3.11}$$

By writing the above expression $E_p(k)$ in matrix form, we get:

$$E_p(k) \approx \|d_k + C_k\delta\|_p, \tag{3.12}$$

where

$$d_k = \begin{bmatrix} \kappa_g e_g(x_k, e^{j\omega_1}) f(1) \\ \kappa_g e_g(x_k, e^{j\omega_2}) f(2) \\ \vdots \\ \kappa_g e_g(x_k, e^{j\omega_N}) f(N) \end{bmatrix},$$

$$\text{and } C_k = \begin{bmatrix} \kappa_g \nabla e_g(x_k, e^{j\omega_1})^T f(1) \\ \kappa_g \nabla e_g(x_k, e^{j\omega_2})^T f(2) \\ \vdots \\ \kappa_g \nabla e_g(x_k, e^{j\omega_N})^T f(N) \end{bmatrix}$$

Doing the same calculations as above and following the same procedures as in [2], we obtain similar expressions but with two extra matrix operations, as shown below:

$$d_k = \begin{bmatrix} \kappa_g e_g(x_k, e^{j\omega_1}) \\ \kappa_g e_g(x_k, e^{j\omega_2}) \\ \vdots \\ \kappa_g e_g(x_k, e^{j\omega_N}) \end{bmatrix} \circ \begin{bmatrix} f(1) \\ f(2) \\ \vdots \\ f(N) \end{bmatrix},$$

where $\circ$ is the Hadamard product operator and

$$C_k = \begin{bmatrix} f(1) & & \\ & \ddots & \\ & & f(N) \end{bmatrix} \begin{bmatrix} \kappa_g \nabla e_g(x_k, e^{j\omega_1})^T \\ \kappa_g \nabla e_g(x_k, e^{j\omega_2})^T \\ \vdots \\ \kappa_g \nabla e_g(x_k, e^{j\omega_N})^T \end{bmatrix}$$

For the passband error, if we consider $H_d(\omega)$ to be the desired frequency response of the filter and c_k is the value of vector c at the start of the k_{th} iteration, a passband

error function at frequency ω can be defined as

$$e_h(c_k,\, e^{j\omega}) \approx |H(c_k, e^{j\omega})\,|^2 - |H_d(\omega)|^2, \tag{3.13}$$

Assuming that the desired amplitude response is unity in the passband, the passband error function becomes

$$e_h^{(pb)}(c_k,\, e^{j\omega}) \approx |H(c_k, e^{j\omega})\,|^2 - 1, \tag{3.14}$$

Using the same approach as in the group-delay case, we can write the passband error in matrix form as follows:

$$E_p^{(pb)}(k) \approx \|D_k^{(pb)}\delta + f_k^{(pb)}\|_p, \tag{3.15}$$

where

$$f_k^{(pb)} = \begin{bmatrix} \kappa_a e_g(x_k, e^{j\omega_1}) \\ \kappa_a e_g(x_k, e^{j\omega_2}) \\ \vdots \\ \kappa_a e_g(x_k, e^{j\omega_N}) \end{bmatrix} \circ \begin{bmatrix} f_a(1) \\ f_a(2) \\ \vdots \\ f_a(N) \end{bmatrix}, \text{ and}$$

$$D_k^{(pb)} = \begin{bmatrix} f_a(1) & & \\ & \ddots & \\ & & f_a(N) \end{bmatrix} \begin{bmatrix} \kappa_a \nabla e_g(x_k, e^{j\omega_1})^T \\ \kappa_a \nabla e_g(x_k, e^{j\omega_2})^T \\ \vdots \\ \kappa_a \nabla e_g(x_k, e^{j\omega_N})^T \end{bmatrix}$$

The updated frequency response of the filter at the k_{th} iteration is given by

$$H(c_k \,+\, \delta,\, e^{j\omega}) \approx H(c_k, e^{j\omega}) \,+\, \nabla H(c_k, e^{j\omega})^T \delta, \tag{3.16}$$

In the same manner, we can approximate the L_p-norm of the transition-band error for the filter as follows:

$$E_p^{(tb)}(k) \approx \|D_k^{(tb)}\delta + f_k^{(tb)}\|_p, \tag{3.17}$$

where

$$f_k^{(tb)} = \begin{bmatrix} \kappa_t e_g(x_k, e^{j\omega_1}) f_t(1) \\ \kappa_t e_g(x_k, e^{j\omega_2}) f_t(2) \\ \vdots \\ \kappa_t e_g(x_k, e^{j\omega_N}) f_t(N) \end{bmatrix},$$

$$D_k^{(tb)} = \begin{bmatrix} \kappa_t \nabla e_g(x_k, e^{j\omega_1})^T f_t(1) \\ \kappa_t \nabla e_g(x_k, e^{j\omega_2})^T f_t(2) \\ \vdots \\ \kappa_t \nabla e_g(x_k, e^{j\omega_N})^T f_t(N) \end{bmatrix}$$

and equivalently,

$$f_k^{(tb)} = \begin{bmatrix} \kappa_t e_g(x_k, e^{j\omega_1}) \\ \kappa_t e_g(x_k, e^{j\omega_2}) \\ \vdots \\ \kappa_t e_g(x_k, e^{j\omega_N}) \end{bmatrix} \circ \begin{bmatrix} f_t(1) \\ f_t(2) \\ \vdots \\ f_t(N) \end{bmatrix},$$

$$D_k^{(tb)} = \begin{bmatrix} f_t(1) & & \\ & \ddots & \\ & & f_t(N) \end{bmatrix} \begin{bmatrix} \kappa_t \nabla e_g(x_k, e^{j\omega_1})^T \\ \kappa_t \nabla e_g(x_k, e^{j\omega_2})^T \\ \vdots \\ \kappa_t \nabla e_g(x_k, e^{j\omega_N})^T \end{bmatrix}$$

In the same way, the L_p-norm of the stopband error for the filter can be given by

$$E_p^{(sb)}(k) \approx \|D_k^{(sb)}\delta + f_k^{(sb)}\|_p, \tag{3.18}$$

where

$$f_k^{(sb)} = \begin{bmatrix} \kappa_s e_g(x_k, e^{j\omega_1}) \\ \kappa_s e_g(x_k, e^{j\omega_2}) \\ \vdots \\ \kappa_s e_g(x_k, e^{j\omega_N}) \end{bmatrix} \circ \begin{bmatrix} f_s(1) \\ f_s(2) \\ \vdots \\ f_s(N) \end{bmatrix},$$

$$D_k^{(sb)} = \begin{bmatrix} f_s(1) & & \\ & \ddots & \\ & & f_s(N) \end{bmatrix} \begin{bmatrix} \kappa_s \nabla e_g(x_k, e^{j\omega_1})^T \\ \kappa_s \nabla e_g(x_k, e^{j\omega_2})^T \\ \vdots \\ \kappa_s \nabla e_g(x_k, e^{j\omega_N})^T \end{bmatrix}$$

The expressions above are similar to those in [2], except for the Hadamard product and the scaling matrix factor.

3.4 Stability Constraints of the 1-D IIR Filter

To meet the stability constraints of the filter, all of the poles have to be located inside the unit circle $\mathbf{U}$ of the z-plane [2, 111–113]. Given that the denominator of each SOS has the form:

$$p_m(z) = b_{0m} + b_{1m} z + z^2 \tag{3.19}$$

where m is the section number, and b_{0m}, b_{1m} are real-valued coefficients, the Jury-Marden stability criterion implies that the polynomial $p_m(z)$ is stable if and only if:

$$\begin{aligned} b_{0m} &< 1 \\ b_{1m} - b_{0m} &< 1 \\ -b_{1m} - b_{0m} &< 1 \end{aligned}$$

To ensure robust stability of the filter, a small positive stability margin is introduced and is defined as $\varepsilon_s = 1 - r_{max}^{(p)}$, where $r_{max}^{(p)}$ is the maximum pole radius allowed. The

stability margin ε_s can be incorporated into the above stability conditions as follows:

$$\begin{aligned} b_{0m} &< 1-\gamma \\ b_{1m} - b_{0m} &< 1-\gamma \\ -b_{1m} - b_{0m} &< 1-\gamma \end{aligned}$$

where $\gamma = 1-(1-\varepsilon_s)^2$. Expressing the above stability conditions for the k_{th} iteration in matrix form yields

$$\mathbf{B}\delta < \mathbf{b^{(k)}}, \tag{3.20}$$

where the matrix $\mathbf{B}$ is given by:

$$\mathbf{B} = \begin{bmatrix} 0 & 0 & \beta & 0 & \cdots & 0 & 0 \\ \vdots & \vdots & \mathbf{0} & \ddots & \vdots & \vdots & \\ 0 & 0 & \cdots & 0 & \beta & 0 & 0 \end{bmatrix}$$

and

$$\beta = \begin{bmatrix} 1 & 0 \\ -1 & 1 \\ -1 & -1 \end{bmatrix}, \; b^{(k)} = \begin{bmatrix} b_1^{(k)} \\ \vdots \\ b_J^{(k)} \end{bmatrix}, \; b_m^{(k)} = \begin{bmatrix} 1-\varepsilon_s - b_{0m}^{(k)} \\ 1-\varepsilon_s - b_{1m}^{(k)} + b_{0m}^{(k)} \\ 1-\varepsilon_s + b_{1m}^{(k)} + b_{0m}^{(k)} \end{bmatrix}$$

where $J = N/2$. Note that since the stability depends only on the poles of the second-order sections of the filter, the first two columns for the stability matrix $\mathbf{B}$ have to be zero, which was not satisfied by the matrix $\mathbf{B}$ found in [2].

For the stability constraints, the stability margin ε_s is defined in terms of the maximum pole radius allowed $r_{max}^{(p)}$. A smaller value of the maximum pole radius $r_{max}^{(p)}$ than necessary has a significant effect on the behavior of the filter [8, 106, 114]. This small value of $r_{max}^{(p)}$ can increase the passband ripple and/or reduce the minimum stopband attenuation and, therefore, affect the performance of the filter. However, a reduced pole radius also reduces sensitivity to coefficient quantization because the effect of pole perturbation is smaller for poles that are farther away from the unit circle [2, 8, 113, 115].

3.5 The Constrained Optimization Problem

An IIR filter design that uses the proposed sampling functions can be expressed, at each iteration k, as a constrained minimization problem. To solve this problem, the

group-delay deviation is minimized under the constraints that the passband error, stopband attenuation, and transition band attenuation are within prescribed levels. The problem at hand can be stated as the standard constrained optimization problem:

$$\begin{aligned} &\text{minimize} \|e_g(x, e^{j\omega})\|_p \\ &\text{subject to :} \\ &\qquad \text{passband error} \leq \Gamma_{pb} \\ &\qquad \text{transition-band gain} \leq \Gamma_{tb} \\ &\qquad \text{stopband gain} \leq \Gamma_{sb} \\ &\qquad \text{stability margin} = \varepsilon_s \end{aligned} \tag{3.21}$$

where Γ_{pb}, Γ_{tb}, and Γ_{sb} are the maximum prescribed levels for the passband error, transition-band gain, and stopband gain, respectively. Using (3.12), (3.15), (3.17), (3.18), and (3.20) in (3.21), the iterative problem to be solved becomes

$$\begin{aligned} &\min_{\delta} \|C_k \delta + d_k\|_p \\ &\text{subject to :} \ \ \|D_k^{(pb)} \delta + f_p^{(pb)}\|_p \leq \Gamma_{pb}, \\ &\qquad \|D_k^{(tb)} \delta + f_k^{(tb)}\|_p \leq \Gamma_{tb}, \\ &\qquad \|D_k^{(sb)} \delta + f_k^{(sb)}\|_p \leq \Gamma_{sb}, \\ &\qquad \|\delta\|_2 \leq \Gamma_{small}, \\ &\qquad \mathbf{B}\delta \leq b^k, \end{aligned} \tag{3.22}$$

where δ is the optimization variable vector and Γ_{small} is a small positive constant. The value of δ is used to update the parameters of the filter for the next iteration. The bound on the L_2-norm of the updated vector, δ, assures the validity of the linear approximation and, at the same time, eliminates the need for a linear step that is required in most optimization algorithms [8]. To solve the optimization problem in (3.22), an initial filter has to be given. The model reduction approach based on impulse-response Gramians proposed by Sreeram and Agathoklis [85] is employed to generate an initial filter. The initial filter may satisfy only the stopband and transition band constraints but not the passband. In order to handle such a situation, the objective function and constraints for the passband error and the norm of the parameter update are relaxed by adding a so-called *relaxation* variable δ_{rlx} which is

also minimized while its value is constrained to be positive. As a consequence, the constrained optimization problem formulated in (3.22) for the case $p = \infty$ can be expressed as:

$$\begin{aligned} & \min_{\delta, \delta_{rlx}} \|C_k \delta + d_k\|_\infty + W \delta_{rlx} \\ \text{subject to : } & \|D_k^{(pb)} \delta + f_k^{(pb)}\|_\infty \leq \Gamma_{pb} + \delta_{rlx}, \\ & \|D_k^{(sb)} \delta + f_k^{(sb)}\|_\infty \leq \Gamma_{sb}, \\ & \|D_k^{(tb)} \delta + f_k^{(tb)}\|_\infty \leq \Gamma_{tb}, \\ & \|\delta\|_2 \leq \Gamma_{small} + \delta_{rlx}, \\ & \delta_{rlx} \geq 0, \\ & \mathbf{B}\delta \leq b^k, \end{aligned} \tag{3.23}$$

where δ_{rlx} is a relaxation variable and $W > 0$ is a weighting factor that helps speed up the convergence of the optimization problem. The objective function and the constraints on passband, transition band, and stopband in (3.23) are convex because they are linear, and each of them is an L_∞-norm and every norm is convex. The fourth constraint on δ in (3.23) is also convex since it includes the L_2-norm and a linear function. The last two constraints in (3.23) are also linear functions, and thus both are convex. Under these linear constraints, the feasible region is convex, and, therefore, the problem in (3.23) is a convex programming problem. This constrained optimization problem can be solved efficiently by using modern optimization tools such as CVX, which is a Matlab-based modeling system for convex optimization. The quality of the group-delay characteristic of the obtained filter can be measured by using the normalized maximum variation of the filter group-delay τ over the passband as a percentage [6, 35].

$$Q_\tau = \frac{(\tau_{max} - \tau_{min})}{(\tau_{max} + \tau_{min})} \times 100\% \tag{3.24}$$

For implementation and to handle the complexity of the optimization above, we chose the sampling functions from a small discrete space of $\mathbb{S}$ containing the following sampling functions: $f_g(n) = 1$ for the group delay, $f_a(n) = 1/(1 + \log(n))$ for the passband, $f_t(n) = 1$ for the transition band, and $f_s(n) = 1 + \log(n)$ for the stopband.

3.6 Design Examples and Comparisons

In this section, the proposed design method is compared with the state-of-the-art method of [2] and the more recent method of [3]. These new methods aim to design nearly linear-phase IIR filters and achieve better filters than earlier methods in the literature.

3.6.1 Lowpass Filter

For comparison purposes, an IIR filter with the design specifications given in Table 1 is designed. This lowpass filter of order $(n, r) = (12, 12)$ was designed in Example 1 in [89, 90] and used as Example 5 in [2] and Example 4 in [3]. Using the same IIR filter design specifications here as in the previous publications allows the comparison of results from the proposed method with the results of the earlier methods.

Table 3.1: Lowpass filter design specifications

Parameters	Values
Max. PB ripple, dB	0.266
Min. SB attenuation, dB	37
PB edge, rad/s	0.5π
SB edge, rad/s	0.6π
Max. pole radius	0.98
Group delay (samples)	15.9

The optimization parameters in (3.23) were set as in [2], including the maximum pole radius, which was set to the value of 0.98, and that leads to $\varepsilon_s = 0.02$. The MATLAB Symbolic Math Toolbox and the CVX package were used to implement the constrained optimization problem. In this example, a model reduction algorithm based on the Impulse-Response Gramian [85] is used to design a stable IIR initial filter of order $(n, r) = (12, 12)$. Having the initial filter's frequency response close to the desired frequency response aids the convergence to a filter that satisfies specifications. The performance of the obtained IIR filter is compared with the results of Example 5 in [2], Example 4 in [3], and the results of the lowpass filter example in Section E of [89]. In Table 2, the performance of the filter is evaluated in terms of passband ripple, transition-band gain, stopband attenuation, average deviation of the group delay in the passband, and quality factor Q_τ.

Table 3.2: Results of the designed lowpass filters

Parameters	Proposed method	Design A-1 in [2]	Method in [3]	Method in [89]
Total order	12	12	12	12
Max. PB ripple, dB	0.057	0.265	0.265	0.266
Min. SB atten., dB	38.200	36.145	36.145	36.146
Max. TB gain, dB	0.2928	4.37	4.37	-0.136
τ_{avg}	11.29	10.92	7.554	16.26
Q_τ	4.237×10^{-1}	4.49×10^{-3}	3.67×10^{-4}	4.5400

Figure 3.1 shows the magnitude response of the filter designed by the proposed method (blue), the filter designed in [2] (red) and the filter designed in [3] (yellow). The peak-to-peak passband for these three filters is shown in Figure 3.3 using the same color code. It is clear that the obtained filter has a smaller peak-to-peak ripple in the passband region compared with the same filter presented in [2] and [3]. In Figure 3.1, we can also see a good improvement in the transition-band, where instead of having overshoot in the magnitude response in this frequency range, the magnitude in the transition-band is monotonically decreasing, resulting in less noise gain in the transition band. The required stopband attenuation of 37 dB is met as shown in Figure 3.1, which is not the case in [2] and [3]. The group-delay of the filter in passband is shown in Figure 3.2. The quality of the group-delay characteristic of the filter is $Q_\tau = 4.237 \times 10^{-1}$ in our case versus $Q_\tau = 4.49 \times 10^{-3}$ in [2] and $Q_\tau = 3.67 \times 10^{-4}$ in [3]. All of these filters have a maximum group-delay deviation quality factor Q_τ less than 1. For most applications, a perfectly linear-phase response is not required, and a value of quality factor Q_τ in the range of 1 to 10, depending on the application, would be entirely acceptable [8]. The filter is stable and Figure 3.4 shows the pole/zero locations of the filter in the z-plane, where all of the poles are located inside the unit circle with a maximum pole radius of 0.95. Analysis of the results shows that the obtained filter has considerable performance improvements in peak-to-peak passband ripple, transition-band and stopband attenuation over the

filters in [2] and [3]. The obtained results are summarized in Table 3.2. The design was done using an Intel (R) Core (TM) i7-7700 CPU at 3.60 GHz and 16 GB of RAM. The algorithm converged in 23 iterations with a CPU time of 1186.57 sec.

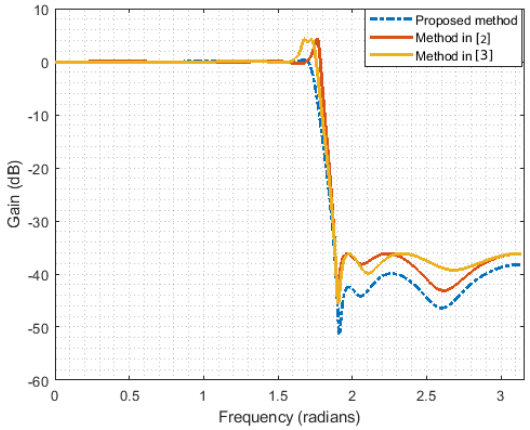

Figure 3.1: Magnitude response: proposed method (blue), method A-1 in [2] (red) and method in [3] (yellow)

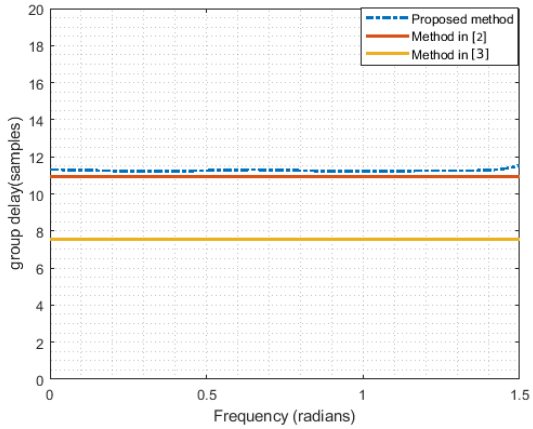

Figure 3.2: Group delay: proposed method (blue), method A-1 in [2] (red) and method in [3] (yellow)

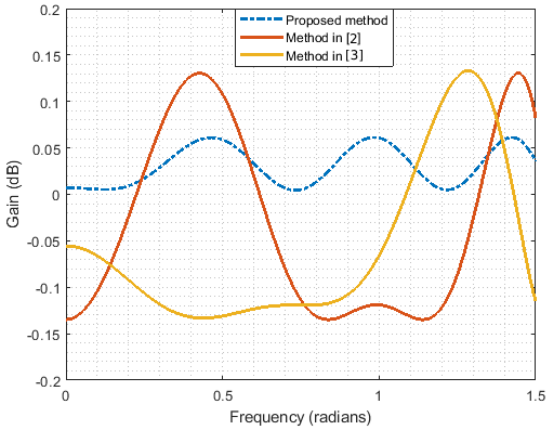

Figure 3.3: Passband ripple: proposed method (blue), method A-1 in [2] (red) and method in [3] (yellow)

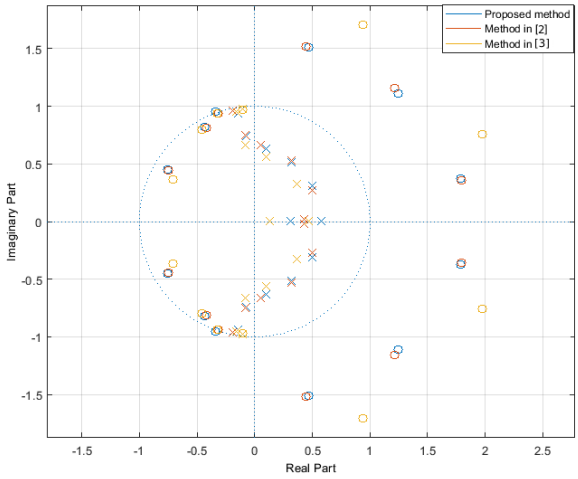

Figure 3.4: Pole/zero map: proposed method (blue), method A-1 in [2] (red) and method in [3] (yellow)

3.7 Conclusion

In this chapter, we introduced a new sampling function for a constrained optimization method that can yield improved results when designing IIR filters with nearly linear-phase response in the passband. The filter being designed by this method satisfied the prescribed magnitude response specifications and met a specified degree of flatness in the passband group-delay of the filter. The results show that the performance of the obtained filter has improved, particularly in the magnitude response. The proposed method yields improvements in peak-to-peak passband ripple, transition-

band monotonicity, and stopband attenuation compared with the state-of-the-art method of [2] and a recently published method in [3].

Chapter 4

LMI-based Design of Nearly Linear-Phase 2-D Recursive Digital Filters Using Balanced Realization Model Reduction

Abstract: Building upon the principles outlined in the 1-D filter design in the previous chapter, we now proceed into the world of 2-D IIR digital filters. The natural progression from 1-D to 2-D filtering necessitates a shift in our approach, and we introduce the balanced realization model reduction technique as a means to tackle the challenges associated with designing stable and efficient 2-D IIR filters. By extending our understanding of 1-D IIR filter design into the multidimensional domain, we demonstrate the adaptability and versatility of our optimization-based approach. This chapter serves as a bridge between the 1-D and 2-D worlds, emphasizing the importance of efficient filter designs, reduced computational complexity, and the ability to handle multidimensional signals. We present a design method for 2-D IIR digital filters with nearly linear phase in the passband. This method is based on a balanced-realization model reduction technique for 2-D separable-denominator recursive digital filters. The initial design is a linear-phase 2-D FIR filter which is represented using a 2-D separable-denominator system which leads to the 2-D IIR filter design using 2-D model reduction. The model reduction method is based on structured controllability P^s and structured observability Q^s gramians which are block-diagonal positive-definite matrices satisfying 2-D Lyapunov inequalities. An efficient method

is developed to compute these matrices by minimizing the trace of P^s and the trace of Q^s under Linear Matrix Inequalities (LMI) constraints. The use of these gramians ensures that the resulting 2-D IIR filter is a 2-D stable filter and can be implemented using a separable denominator 2-D filter with fewer coefficients than the original 2-D FIR filter. The numerical examples show that the proposed method compares favourably with existing techniques.

4.1 Introduction

Two-dimensional digital filters have been used in many signal processing applications such as image processing, video signal filtering, satellite image processing, beam filters, X-ray, TV transmission, and biomedical imaging [12, 17, 21–23]. Many methods have been proposed for their design, see, e.g., [4, 15, 24–38]. 2-D FIR filters have several advantages. They are simple and involve only localized computations [25]. They are always stable and can have a constant group delay. The main drawback is that a large 2-D FIR filter order is often required to satisfy performance requirements with good selectivity when compared with 2-D IIR filters [25]. On the other hand, stability problems of nearly linear-phase 2-D IIR filters are one of the main difficulties to deal with in their design [26]. Some methods confined the filters to have denominators in the form of cascaded low-order factors [26], for which sufficient and necessary stability conditions are available [28], [29], [116]. Other methods used a state space approach to investigate the stability of 2-D discrete systems using the sufficiency of the 2-D Lyapunov equation to ensure 2-D stability. Although studying the stability problems in state space might lead to strong stability constraints, it has been shown in [117] that the existence of a positive definite solution pair to the 2-D Lyapunov equation is a sufficient but not necessary condition for 2-D stability.

For 2-D IIR filters with separable denominator $D(z_1, z_2) = D_1(z_1)D_2(z_2)$, the stability is much easier to guarantee than the stability of a 2-D IIR filter with nonseparable denominator [25, 118]. 2-D IIR filters with separable denominators have received attention because, in addition to fewer stability constraints, the complexity of the implementation is reduced due to fewer coefficients with a separable denominator than with a nonseparable denominator of the same order [25, 119, 120]. The process of designing separable denominator filters often results in filters that have high order. For various reasons it is desirable to represent a high-order filter by a lower-order one to reduce the implementation cost and improve the computational

efficiency. As a solution to this problem, balanced realization model reduction techniques for 2-D digital filters have been investigated by many researchers during the past several years, and the results obtained have been found to be useful in digital filter design [24, 121]. Since a balanced realization is essentially determined by the controllability and observability gramians of the system, there are several types of gramians which can be properly defined for a given 2-D system. Accordingly, there are different types of balanced realizations for a given 2-D discrete system, leading to different balanced approximations [83].

This chapter is concerned with a balanced realization model reduction of 2-D digital filters based on the structured controllability gramian P^s and the structured observability gramian Q^s, where P^s and $Q^s \in \mathbb{R}^{n\times n}$. In other words, to use balanced truncation, the controllability gramian P and the observability gramian Q are needed. In the MATLAB environment, one can use LMI to compute these gramian matrices. The theory of LMI has been attracting the attention of research communities for a decade, especially from researchers in the control systems community [26,31,122–125]. The concept of LMI and its applications are based on the fact that LMIs can be reduced to linear programming problems which can be easily solved by computers [124, 125]. Some of the earlier design work using LMI include the work of Li and Paganini [126], and Vandendorpe [127]. In [127], frequency-weighted balanced and closed-loop balanced truncation are used to solve the same problem. In addition, block-diagonal solutions of linear matrix inequalities have long been used in model reduction of uncertain systems where the state partitions correspond to different frequency variables [128]. A crucial step in obtaining a coordinate system wherein the realization is balanced is to compute the leading diagonal block matrices of the gramians of the given 2-D system [16].

In this chapter, a balanced realization model reduction for the design of 2-D IIR filters with nearly linear-phase in the passband is proposed. The proposed method is based on structured controllability and structured observability gramians. First, we propose a LMI-based algorithm to compute the structured controllability and observability gramians for 2-D discrete systems, where the problem is formulated as a minimization problem that can be solved numerically by minimizing the trace of gramian matrices, P^s and Q^s, under LMI constraints. Using this algorithm, the gramians, $P^s \in \mathbb{R}^{n\times n}$, $Q^s \in \mathbb{R}^{n\times n}$, are constrained to be positive definite $P^s > 0$, $Q^s > 0$, symmetric $P^s = P^{sT}$, $Q^s = Q^{sT}$, and block diagonal $P^s = diag(p_1, p_2)$, $Q^s = diag(q_1, q_2)$.

This chapter is organized as follows: In Section 4.2, the definitions of the three types of controllability and observability gramians of 2-D discrete systems are presented. In Section 4.3, a LMI-based algorithm for computing the structured controllability P^s and structured observability Q^s gramians is proposed. Section 4.4 provides a design procedure for a balanced realization technique for separable denominator 2-D IIR digital filters. In section 4.5, several examples are presented to illustrate the effectiveness of the proposed algorithm. Section 4.6 is the conclusion.

4.2 Gramians of 2-D Discrete Systems

Consider a 2-D discrete state-space system realization $\Sigma = (A, b, c, d)$ described by the Roesser model [49]:

$$\begin{bmatrix} x^h(i+1,j) \\ \\ x^v(i,j+1) \end{bmatrix} = \begin{bmatrix} A_{11} & A_{12} \\ \\ A_{21} & A_{22} \end{bmatrix} \begin{bmatrix} x^h(i,j) \\ \\ x^v(i,j) \end{bmatrix} + \begin{bmatrix} b_1 \\ \\ b_2 \end{bmatrix} u(i,j) \tag{4.1}$$

$$\equiv \mathbf{A}\mathbf{x}(i,j) + \mathbf{b}\mathbf{u}(i,j) \tag{4.2}$$

$$y(i,j) = [c_1 \quad c_2]x(i,j) + du(i,j) \tag{4.3}$$

$$\equiv \mathbf{c}\mathbf{x}(i,j) + \mathbf{d}\mathbf{u}(i,j) \tag{4.4}$$

where $x^h(i,j) \in \mathbb{R}^{m\times 1}$ is the horizontal state vector, $x^v(i,j) \in \mathbb{R}^{n\times 1}$ is the vertical state vector, $u(i,j) \in \mathbb{R}$ is the input, $y(i,j) \in \mathbb{R}$ is the output, and $A_{11}, A_{12}, A_{21}, A_{22}, b_1, b_2, c_1, c_2$, and d are real matrices with appropriate dimensions.
The first type of 2-D gramian, known as a pseudo-controllability and pseudo-observability gramian [83], is given by

$$P^p = \frac{1}{(2\pi j)^2} \oint_{|z_1|=1} \oint_{|z_2|=1} F(z_1, z_2) F^*(z_1, z_2) \frac{dz_2}{z_2} \frac{dz_1}{z_1} \tag{4.5}$$

$$Q^p = \frac{1}{(2\pi j)^2} \oint_{|z_1|=1} \oint_{|z_2|=1} G^*(z_1, z_2) G(z_1, z_2) \frac{dz_2}{z_2} \frac{dz_1}{z_1} \tag{4.6}$$

where

$$F(z_1, z_2) = [I(z_1, z_2) - A]^{-1} b \tag{4.7}$$

$$G(z_1, z_2) = c[I(z_1, z_2) - A]^{-1} \tag{4.8}$$

and $I(z_1, z_2) = z_1 I_m \oplus z_2 I_n$ and $\oplus$ is the direct sum of matrices.
The second type of gramians, known as the structured controllability and observability gramians [83], are defined by the positive-definite solutions P^s and Q^s of the Lyapunov inequalities:

$$AP^sA^T - P^s + bb^T < 0 \tag{4.9}$$

$$A^TQ^sA - Q^s + c^Tc < 0 \tag{4.10}$$

The matrices P^s and Q^s are block diagonal matrices, $P^s = diag(p_1, p_2)$ and $Q^s = diag(q_1, q_2)$, representing the solution to the above Lyapunov inequalities.
The third type of gramians, known as the quasi controllability and observability gramians [83], are defined by the positive-definite block-diagonal matrices $P^q = \text{diag}(p_1, p_2)$ and $Q^q = \text{diag}(q_1, q_2)$ where p_i and q_i, $(i = 1, 2)$, satisfy the Lyapunov equations:

$$A_{11}p_1A_{11}^T - p_1 + b_1b_1^T + A_{12}p_2A_{12}^T = 0 \tag{4.11}$$

$$A_{22}p_2A_{22}^T - p_2 + b_2b_2^T + A_{21}p_1A_{21}^T = 0 \tag{4.12}$$

$$A_{11}^Tq_1A_{11} - q_1 + c_1^Tc_1 + A_{21}^Tq_2A_{21} = 0 \tag{4.13}$$

$$A_{22}^Tq_1A_{22} - q_2 + c_2^Tc_2 + A_{12}^Tq_1A_{12} = 0 \tag{4.14}$$

There are several types of gramians of the system that can be properly defined for a given 2-D system and there are different types of balanced realizations for a 2-D discrete system, leading to different balanced approximations [83]. In the next section a method to obtain the structural controllability and observability gramians using LMI is presented. The benefits of using the second type of gramians over the others is that the resulting positive-definite block-diagonal gramians satisfy the 2-D Lyapunov equations and are, therefore, sufficient for 2-D stability [117]. Further, they can be used to obtain a block diagonal similarity transformation which will lead, as it will be discussed in Section 4.4, to a guaranteed stable 2-D reduced order system.

4.3 Proposed Computation Method for Structured Gramians

Several problems arising in control system analysis and design involve minimizing the rank of a matrix variable subject to LMI constraints. LMIs have emerged as a powerful computational design tool in systems and control engineering because of their computational efficiency and flexibility for treating a large class of system design problems [123, 129–132].
In general, an LMI has the form

$$F(x) \triangleq F_0 + \sum_{i=1}^{m} x_i F_i > 0, \tag{4.15}$$

where $x = (x_1, ..., x_m)$ is a vector of m real numbers called the decision variables, i.e., $x_i \in \mathbb{R}^m$, for $i = 0, ..., m$ and $F_i \in \mathbb{R}^{m \times m}$ are given symmetric matrices. The problem is to determine if there exists a vector x that satisfies the matrix inequality. In [133, 134], it has been shown that for certain special cases, the rank minimization problem can be reduced to a semi-definite problem. Under these hypotheses, it is possible to say that the solution can be obtained by solving the associated LMI. One effective heuristic, applicable when the matrix variable is symmetric and positive semi-definite, is to minimize the trace instead of the rank [123, 129]. This results in a semi-definite problem (SDP) which can be efficiently solved. This heuristic obviously does not apply to problems in which the matrix is non-square, since the trace is not even defined [123, 129, 135]. In the following, we propose a LMI-based algorithm to compute the gramian matrices P^s and Q^s of a 2-D discrete system represented by Roesser's model. Given a 2-D system in state space form represented by Roesser's model, $\Sigma = (A, b, c, d)$, then the block-diagonal positive-definite solutions P^s and Q^s of the Lyapunov inequalities

$$AP^sA^T - P^s + bb^T < 0 \tag{4.16}$$

$$A^TQ^sA - Q^s + c^Tc < 0 \tag{4.17}$$

are the structured controllability and structured observability gramians. The existence of such P^s and Q^s ensure the stability of the system Σ, but the converse does not hold as it was shown in [117] and [4]. Finding P^s and Q^s satisfying (4.16) and (4.17) can be solved by formulating an optimization problem using the traces of P^s

and Q^s.
Given a 2-D system realization $\Sigma = (A, b, c, d)$, we can find P^s by minimizing

$$min\ tr(P^s) \tag{4.18}$$

subject to

$$\begin{aligned} AP^sA^T - P^s + bb^T < 0 \\ P^s > 0 \qquad (4.19) \\ P^s = P^{s^T} \qquad (4.20) \\ P^s = diag(p_1, p_2) \end{aligned}$$

and

$$min\ tr(Q^s) \tag{4.21}$$

subject to

$$\begin{aligned} A^TQ^sA - Q^s + c^Tc < 0 \\ Q^s > 0 \qquad (4.22) \\ Q^s = Q^{s^T} \qquad (4.23) \\ Q^s = diag(q_1, q_2) \end{aligned}$$

This problem can be solved as a linear objective minimization problem under LMI constraints [136].
The gramian matrices P^s and Q^s can be computed using MATLAB as follows:

1. Initialize the creation of a system of LMIs using `setlmis([ ])`
2. Define the LMI constraints of (4.19) and (4.22) by the appropriate sequence of commands and get the controllability gramian using `ctrgram=getlmis`.
3. For the structured controllability gramian P^s, write the objective $tr(P^s)$ as c^Tp where p is a vector of free entries of P^s.

4. Call the minimize linear objectives under LMI constraints `mincx` to compute the minimizer P^s_{opt} and the global minimum $c_{opt} = c^T P^s_{opt}$ of the objective function.

5. `mincx` also returns the optimizing vector of decision variables P^s_{opt}. The corresponding optimal value of the matrix variable P^s is given by P^s=`dec2mat`$(ctrgram, P^s_{opt}, p)$.

6. In the same manner, apply all the above steps to find the observability gramian Q^s.

The controllability and observability gramian matrices P^s and Q^s obtained by using this method are block-diagonal positive-definite matrices. We refer the reader to Appendix A where several numerical examples including separable and non-separable denominator 2-D systems are presented to illustrate the proposed LMI technique to solve 2-D Lyapunov inequalities.

4.4 Balanced Realization of 2-D Digital Filters

Balanced realizations are known to be useful realizations for model reduction. The internally-balanced realization gives an indication of the dominance of the system states in the input/output behavior [137]. The balanced realization is an asymptotically stable minimal realization in which the controllability and observability gramians are equal and diagonal. The idea of a balanced realization model reduction, in general, is to remove from the system matrices (in the balanced realization) the blocks corresponding to the smaller Hankel singular values [35, 36, 52, 138].

4.4.1 Design Procedure

We now present the design steps for nearly linear-phase 2-D IIR digital filters with separable denominators. For a 2-D IIR filter with a separable denominator, it is assumed that $A_{12} = 0$ or $A_{21} = 0$. The design steps can be described as follows:

1. Design a linear phase 2-D FIR digital filter that approximates the required frequency response

2. Realize the designed 2-D FIR filter $H(z_1, z_2)$ in state space Roesser's model [4, 49] as follows

$$\begin{bmatrix} X^h(i+1,j) \\ X^v(i,j+1) \end{bmatrix} = \begin{bmatrix} A_{11} & A_{12} \\ A_{21} & A_{22} \end{bmatrix} \begin{bmatrix} x^h(i,j) \\ x^v(i,j) \end{bmatrix} + \begin{bmatrix} b_1 \\ b_2 \end{bmatrix} u(i,j) \tag{4.24}$$

$$y(i,j) = \begin{bmatrix} c_1 & c_2 \end{bmatrix} \begin{bmatrix} x^h(i,j) \\ x^v(i,j) \end{bmatrix} + du(i,j). \tag{4.25}$$

where $A_{12} = 0$ or $A_{21} = 0$. $A_{11}, A_{12}, A_{21}, A_{22}, b_1, b_2, c_1, c_2$, and d are real matrices with appropriate dimensions which can be built as in [4].

3. Compute the structured controllability gramian $P^s > 0$ and structured observability gramian $Q^s > 0$ using the LMI-based algorithm proposed in Section 4.3. Note that since either A_{12} or A_{21} is zero, the equations are simplified and the computational cost is reduced. The obtained structured controllability and structured observability gramians are block-diagonal matrices where $P^s = diag(p_1, p_2)$ and $Q^s = diag(q_1, q_2)$

4. Find the invertible matrices T_1 and T_2 such that

$$\begin{aligned} T_i^{-1} p_i (T_i^{-1})^T = \Sigma_i &= T_i^T q_i T_i \\ &= diag(\sigma_{1i}, \sigma_{2i}, ...\sigma_{n_i i}), \quad i = 1, 2 \end{aligned} \tag{4.26}$$

   - Decompose the matrices $[u_i, s_i, v_i] = svd(\sqrt{p_i}\ q_i \sqrt{p_i}),\ i = 1, 2$
     where $x = \sqrt{p_i}$ is a matrix so that $xx^T = p_i$ and svd is the full singular value decomposition of an m-by-n matrix involves [139]:
     $m \times m$ matrix u
     $m \times n$ matrix s
     $n \times n$ matrix v
   - Compute the matrices $T_i = \sqrt{p_i}\ u_i\ (s_i^{1/4})^{-1}, \quad i = 1, 2$

5. Obtain the similarity transformation matrix
   $T := diag(T_1, T_2)$

6. Form the balanced realization model $\Sigma_b = (T^{-1}AT, T^{-1}b, cT)$

7. Obtain the reduced order (r_1, r_2) filter by partitioning the balanced realization obtained in the above step $\Sigma_r = (A_r, b_r, c_r)$.

It is important to note that, there is no specific method can be used to predict the lowest order of the reduced model. Usually, the trial-and-error method is used to obtain the lowest order of the filter that still meets the design specifications.

4.5 Illustrative Examples and Evaluation

In this section, we present several design examples to illustrate the effectiveness of the proposed method. In these examples, lowpass, bandstop, and fan 2-D FIR filters are first designed using window methods and then the 2-D IIR reduced-order approximation filters are obtained by using the proposed balanced truncation method. The implementation of the resulting filter designs is investigated and evaluated with respect to the maximum ripple in passband region Δ_p, the maximum ripple in stopband region Δ_s and number of arithmetic operations.

4.5.1 2-D Lowpass Filters

For the sake of comparison, we carried out a study of two examples for a 2-D lowpass filter with separable denominator. The first example was presented by Xiao and Agathoklis in [4] and the second example was presented in [140]. For the first example, it is required to design a 2-D lowpass filter to satisfy the following specification:

$$| H(\omega_1, \omega_2) | = \begin{cases} 1 & {\omega_1}^2 + {\omega_2}^2 \leq w_p^2 \\ 0 & {\omega_1}^2 + {\omega_2}^2 \geq w_s^2 \end{cases} \tag{4.27}$$

where the passband edge $\omega_p = 0.4\pi$ and stopband edge $\omega_s = 0.6\pi$. First, the linear-phase 2-D FIR filter prototype of order (24,24) was designed using the window method. The proposed algorithm is guaranteed to yield a stable 2-D IIR filter and the solution was computable in a reasonable amount of time. On a PC Intel(R) Core(TM) i5-2450M CPU @ 2.50GHz and RAM 6.00 GB, the computation time for the controllability gramian P^s and the observability gramian Q^s was 7.46 seconds. The magnitude response of the full order, (24,24), 2-D FIR lowpass filter is shown in Figure 4.1a. The magnitude response of the (13,13) reduced order 2-D IIR filter presented in [4] is shown in Figure 4.1b. The magnitude response of the (13,13) reduced order 2-D IIR filter obtained using the proposed method is illustrated in Figure 4.1c. The magnitude contour of the obtained filter is shown in Figure 4.1d. Figures 4.1e and 4.1f show the group delays, τ_1 and τ_2, of the reduced order 2-D IIR filter over

the passband region. Table 4.1 summarizes the results of the designed filter using the proposed method and the filter obtained in [4] and the results reported in [141] in terms of the reduced order, obtained group delays τ_1 and τ_2, maximum ripple Δ_p in the passband region and the maximum ripple in the stopband region Δ_s. We can see that the proposed method gives a filter with a comparable performance to that of the same order filter obtained in [4] and [141] with improvements in the maximum passband ripple Δ_p and the stopband Δ_s as shown in Table 4.1 below.

Table 4.1: Comparison results of the designed 2-D IIR filters

	Proposed Method	Method in [4]	Method in [141]
Orders	(13,13)	(13,13)	(18,18)
Group Delay	(12,12)	(12,12)	(12,12)
Δ_p	0.0102	0.0124	0.0128
Δ_s	0.0060	0.0111	0.0350

We also analyze the complexity of the implementation based on the number of non-zero coefficients of the transfer function of the filter. When implementing a general $N_1 \times N_2$ 2-D FIR filter, the number of filter coefficients C is $(N_1 + 1)(N_2 + 1)$ so the cost of implementation increases rapidly as N_1 or N_2 increases. In this example, for the 2-D FIR filter of order (24,24), C is 625, whereas for the reduced-order (13,13) 2-D IIR filter with a separable denominator, C is 14×14 for the numerator plus 2×14 for the denominator (i.e., $C = 224$). We can see that implementing the obtained 2-D IIR filter designed by the proposed method requires less than half of the number of coefficients required by the 2-D FIR filter.

The second example in this section is the 2-D lowpass filter that has the design specifications given in [140]. The 2-D lowpass FIR filter of order (20,20) shown in Figure 4.2a is designed first using a window method to be used as an initial filter. Then the reduced 2-D lowpass IIR filter of order (12,12) is obtained by using the proposed method. The magnitude response of the reduced order 2-D IIR lowpass filter is shown in Figure 4.2b. The impulse responses of the 2-D FIR and IIR filters are shown in Figure 4.2c and Figure 4.2d, respectively. Figure 4.2e shows the magnitude contour of the reduced order 2-D IIR lowpass filter. It has been shown that the proposed method works very well when compared with other methods.

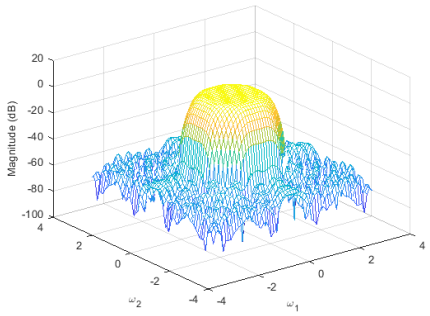

(a) 2-D FIR lowpass filter of order (24,24)

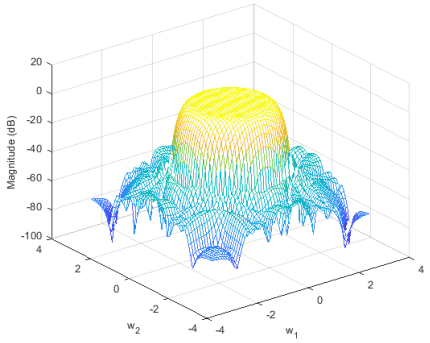

(b) 2-D IIR of reduced order (13,13) in [4]

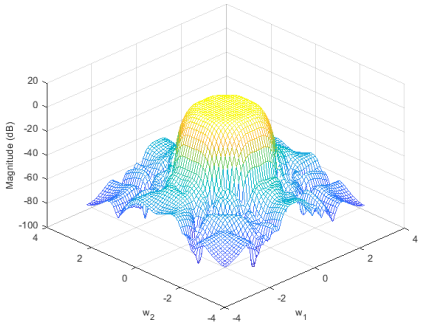

(c) 2-D IIR of reduced order (13,13) using LMI

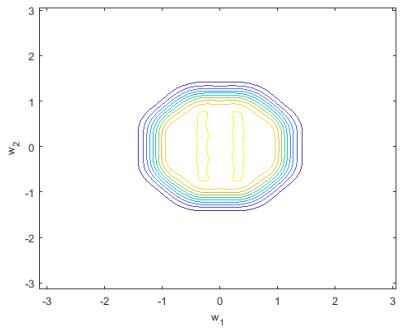

(d) Magnitude contour of the reduced order filter

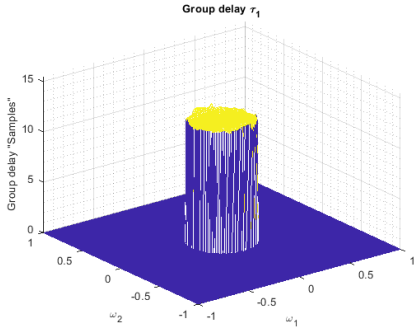

(e) Group delay τ_1 of the reduced order (13,13)

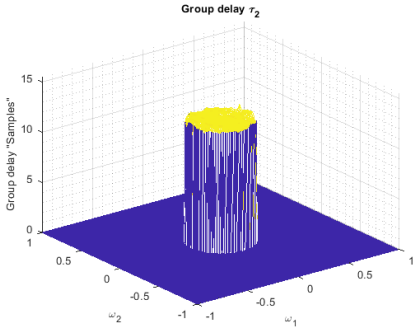

(f) Group delay τ_2 of the reduced order (13,13)

Figure 4.1: Magnitude response and group delay of 2-D lowpass FIR and IIR filters discussed in Section 4.5.1

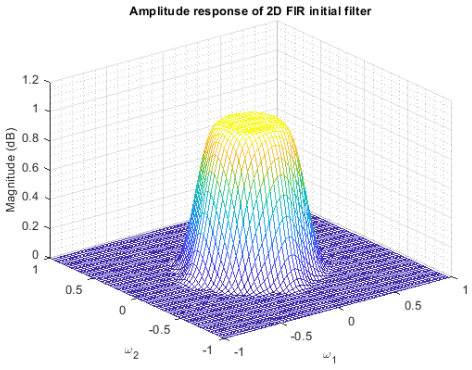

(a) 2-D FIR lowpass filter of order (20,20)

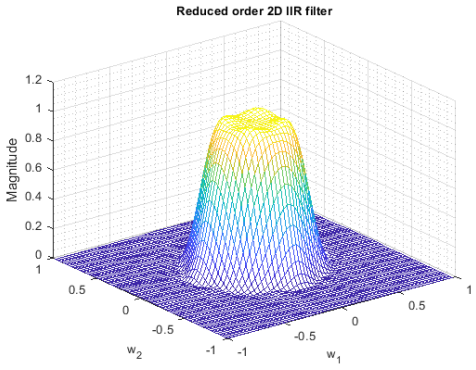

(b) 2-D IIR of reduced order (12,12)

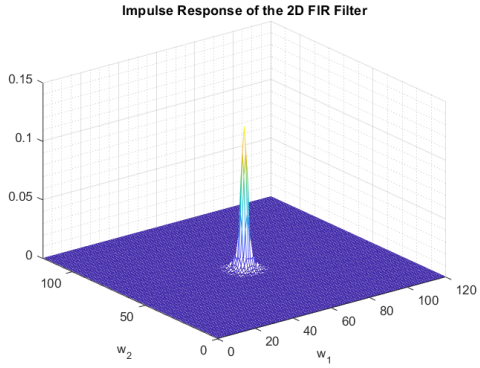

(c) Impulse response of the 2-D FIR filter

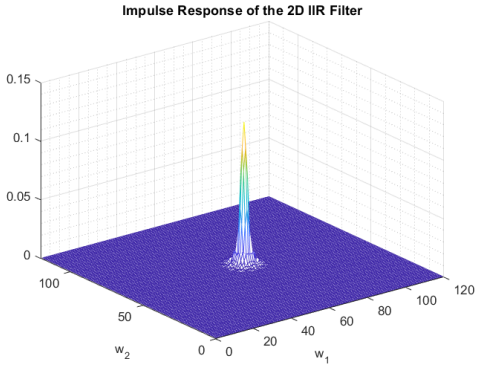

(d) Impulse response of the 2-D IIR filter

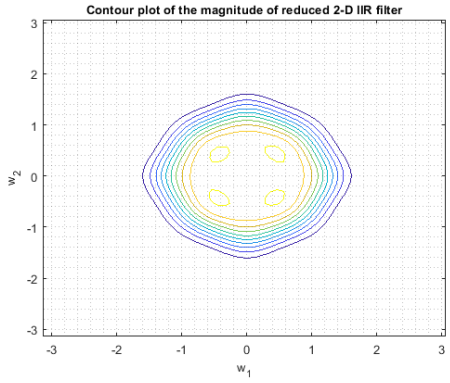

(e) Magnitude contour of the 2-D IIR filter

Figure 4.2: Magnitude and impulse response of 2-D FIR and IIR lowpass filters discussed in Section 4.5.1

4.5.2 2-D Bandpass Filter

In this example, we design a 2-D bandpass filter satisfying the following specification:

$$| H(\omega_1, \omega_2) | = \begin{cases} 1 & \omega_{p1}^2 \leq {\omega_1}^2 + {\omega_2}^2 \leq \omega_{p2}^2 \\ 0 & otherwise \end{cases} \tag{4.28}$$

where $\omega_{p1} = 0.2\pi$ and $\omega_{p2} = 0.5\pi$. First, a linear-phase 2-D FIR filter of order (24,24) is designed using a window method to satisfy the design specifications. After that a 2-D IIR bandpass filter of a reduced order (13,13) is obtained by using the proposed method. In this example, the computation time for the controllability gramian P^s and the observability gramian Q^s was 6.88 sec. The number of coefficients for the FIR filter of order $(24, 24)$ is $(N_1 + 1) \times (N_2 + 1) = 625$ while the obtained IIR filter of a reduced order of $(13, 13)$ has a reduced number of coefficients equal 224.
The magnitude response of the full order (24,24) 2-D FIR bandpass filter is shown in Figure 4.3a. The obtained filter is stable and the magnitude response of the reduced 2-D IIR filter of order (13,13) is shown in Figure 4.3b. The impulse responses for the 2-D FIR initial filter and the 2-D IIR reduced order filter are shown in Figures 4.4a and 4.4b, respectively. The group delay of the reduced 2-D IIR bandpass filter over the passband region is illustrated in Figure 4.5.

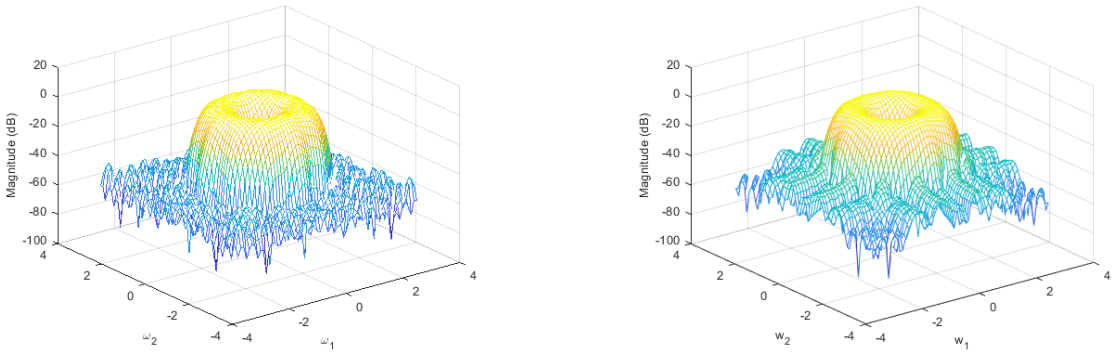

(a) 2-D FIR filter of order (24,24)

(b) 2-D IIR filter of reduced order (13,13)

Figure 4.3: Magnitude of 2-D FIR and IIR bandpass filters discussed in Section 4.5.2

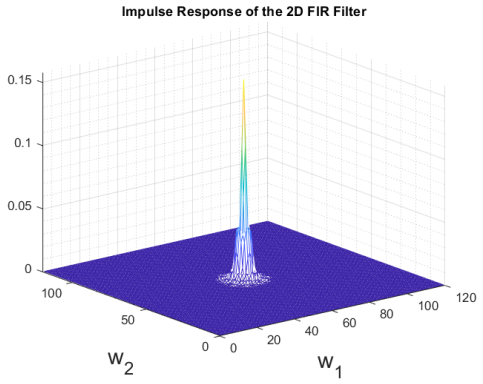

(a) Impulse response of the 2-D FIR

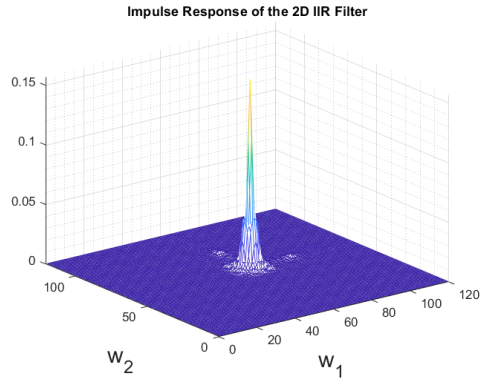

(b) Impulse response of the 2-D IIR

Figure 4.4: Impulse response of the 2-D FIR and IIR bandpass digital filters

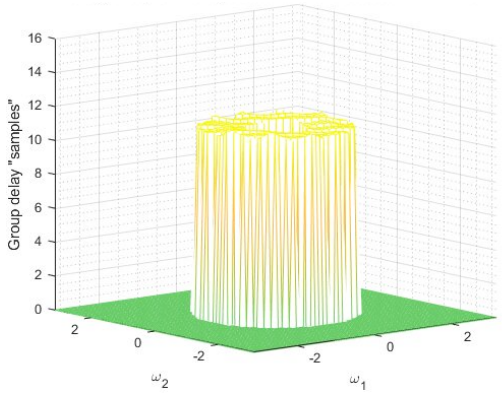

Figure 4.5: Group delay of the reduced order 2-D IIR bandpass filter

4.5.3 Two-Dimensional Fan Filter

Fan filters constitute an important class of 2-D filters that find applications, for example, in geological and seismological data processing and beamforming [142,143]. This type of 2-D filters has the capability of directional filtering where the signal is passed or rejected according to its direction. In general, fan filters represent a fundamental component of 2-D signal processing, offering valuable capabilities for directional filtering in diverse applications ranging from geological data analysis to beamforming in communication systems. Their ability to selectively pass or reject signals based on directionality provides a powerful tool for extracting meaningful information and enhancing system performance in complex signal environments. In this example, the proposed method is applied for the design of a 2-D fan filter having an amplitude

response described in [144], with ω_1 and ω_2 as the two frequency variables where $-\pi \leq \omega_1, \omega_2 \leq \pi$.

$$| H(\omega_1, \omega_2) | = \begin{cases} 1 & |\omega_2| \leq |\omega_1| \\ 0 & otherwise \end{cases} \tag{4.29}$$

A linear-phase FIR fan filter of order (49,49) is first designed. Figure 4.6a shows the magnitude response of this 2-D fan filter. A reduced-order nearly linear-phase 2-D IIR fan filter of order (34,34) is obtained by using the proposed method. The magnitude response of the reduced-order 2-D IIR fan filter is illustrated in Figure 4.6b. The number of multiplications and additions for the 2-D FIR filter of order $(49, 49)$ is $(N_1 + 1) \times (N_2 + 1) = 2500$ and 2499, respectively. For implementation purpose, the obtained 2-D IIR fan filter with a reduced-order of $(34, 34)$ has fewer computations: 1295 multiplications and 1294 additions. The computation time for controllability gramian P^s and observability gramian Q^s is 6.53 sec. As can be seen, the designed 2-D IIR fan filter has lower order, which would lead to reduced computational complexity in the implementation of the filter.

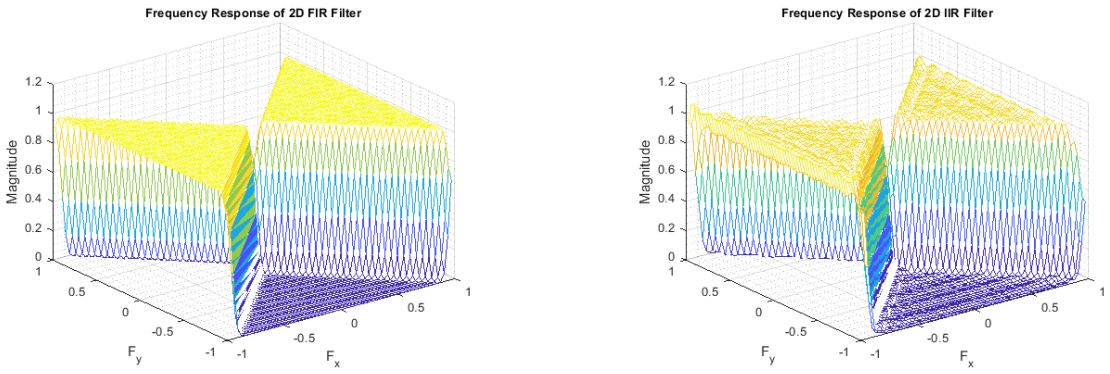

(a) Initial 2-D FIR fan filter of order (49,49)

(b) Reduced 2-D IIR fan filter of order (34,34)

Figure 4.6: Magnitude of 2-D FIR and IIR fan filters described in Section 4.5.3

4.5.4 Fan Filtering of Plane Waves Image

In this section, we generate an image via sum of plane waves with two angles $\theta_1 = 80°$ and $\theta_2 = 100°$ measured counter clockwise from the horizontal. The wave has $\omega_1 = 100/512 \times 2\pi$ rad/pixels and $\omega_2 = 53/512 \times 2\pi$ rad/pixels over the size $N = 512$

pixels of the output image. 2-D FIR and IIR fan filters are designed to be applied on this plane wave image where it is required to design a reduced order 2-D IIR fan filter to satisfy the following design specifications:

$$| H(\omega_1, \omega_2) | = \begin{cases} 1 & |{\omega_1}^2| \leq 0.57|\omega_2^2| \\ 0 & |{\omega_1}^2| > 0.57|\omega_2^2| \end{cases} \tag{4.30}$$

Figure 4.7a shows the magnitude response of the initial 2-D FIR filter of order (24,24) designed using the window method. The reduced 2-D IIR filter of order (17,17) obtained by using a balanced realization model reduction method is shown in Figure 4.7b.

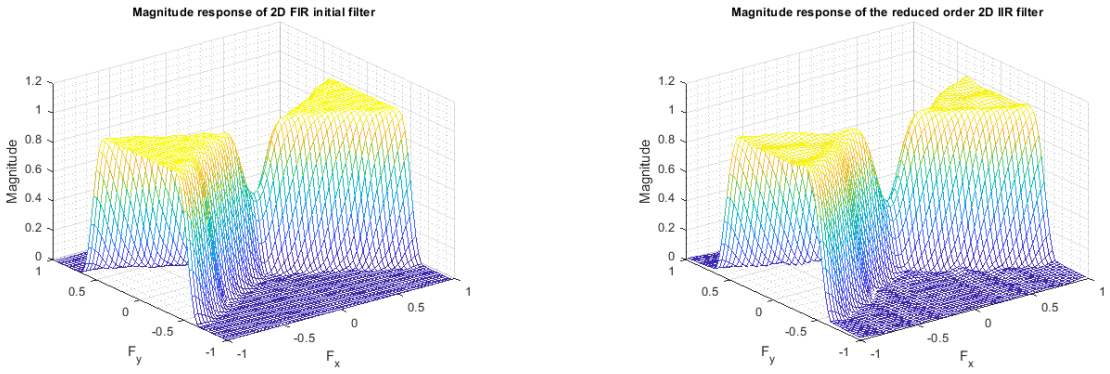

(a) FIR fan filter of order (24,24)

(b) Reduced IIR fan of order (17,17)

Figure 4.7: Magnitude of 2-D FIR and IIR fan filters described in Section 4.5.4

For comparison, the 2-D FIR filter of order (24,24) shown in Figure 4.7a is applied to this plane wave image first, where Figure 4.8 shows the original and filtered images and their 2-D spectrum. The reduced order 2-D IIR fan filter of order (17,17) shown in Figure 4.7b is then applied to the same image and the obtained result is shown in Figure 4.9. In terms of the computation complexity, the 2-D FIR filter of order (24,24) has number of coefficients C is 625, whereas for the reduced-order (17,17) 2-D IIR filter, C is 18×18 for the numerator plus 2×18 for the denominator (i.e., $C = 360$) which is reduced to less than 58%. We can see that implementing the obtained 2-D IIR filter designed by the proposed method requires less than half of the number of coefficients required by the 2-D FIR filter. The results show that the reduced order 2-D IIR fan filter designed using the proposed method has a good filtering performance

to the plane wave image as well as the advantage of a low implementation cost in terms of adders and multipliers over 2-D FIR fan filter.

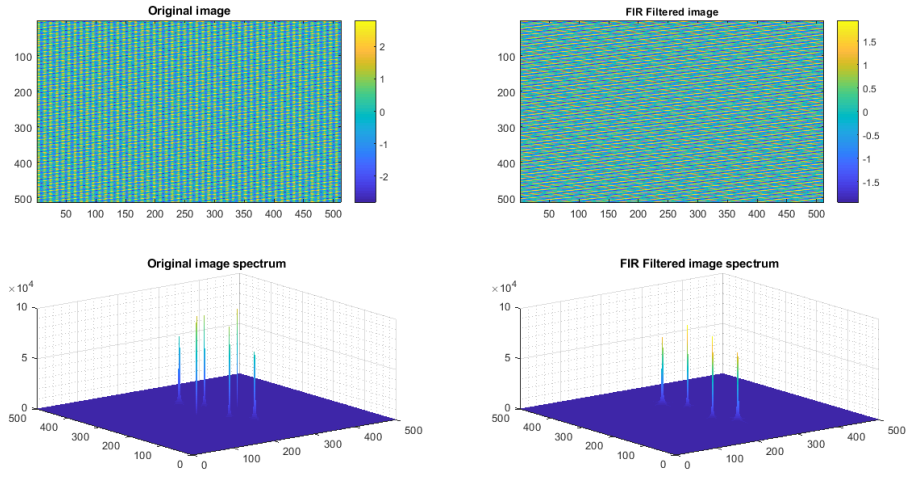

Figure 4.8: Original and filtered PWs using 2-D FIR fan filter and their spectrum

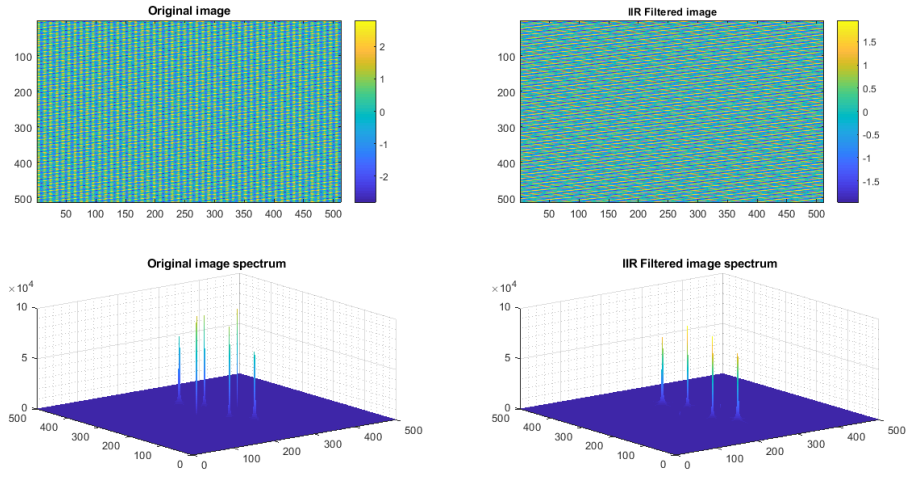

Figure 4.9: Original and filtered PWs using 2-D IIR fan filter and their spectrum

4.6 Conclusion

A method to design nearly linear-phase 2-D recursive digital filters has been presented. The method is based on the 2-D model order reduction of 2-D filters using balanced realization. The design method starts with the design of a 2-D linear-phase FIR filter and its state-space representation as a 2-D system with separable denominator. The balanced realization of this system can be obtained using the 2-D structural controllability and structural observability gramians of the system. These block-diagonal gramians satisfy a set of Lyapunov inequalities which are solved using an optimization approach under linear matrix inequalities constraints. The use of the structural gramians ensures that the resulting reduced-order filter satisfies a 2-D Lyapunov equation and is, therefore, 2-D stable. The proposed method is illustrated by numerical examples which have shown that the method is suitable for the design of reduced order 2-D IIR filters with nearly linear-phase in the passband. The performance of the obtained 2-D IIR filters compares favorably with existing techniques, while at the same time they can be implemented using a separable-denominator filter with less computational complexity than the original 2-D FIR filter. Although, the phase of the reduced order 2-D IIR filter is only nearly linear, we can see that the reduced order 2-D IIR filter offers good selectivity and computational efficiency and reduced system delay when compared to the corresponding 2-D FIR filter.

Chapter 5

A Nonlinear Optimization Design Algorithm for Nearly Linear-Phase 2-D IIR Digital Filters

Abstract: In this chapter, a new optimization method for the design of nearly linear-phase two-dimensional infinite impulse (2-D IIR) digital filters with a separable denominator is proposed. A design framework for 2-D IIR digital filters is formulated as a nonlinear constrained optimization problem where the group delay deviation in the passband is minimized under prescribed soft magnitude constraints and hard stability requirements. To achieve this goal, sub-level sets of the group delay deviations are utilized to generate a sequence of filters, from which the one with the best performance is selected. The quality of the obtained filter is evaluated using three quality factors, namely, the passband magnitude quality factor Q_h and the group delay deviation quality factor Q_τ, while the third one is a new quality factor Q_s that assesses the performance in the stopband relative to the minimum filter gain in the passband. The proposed framework is implemented using the interior-point (IP) method in a MATLAB environment, and the experimental results show that filters designed using the proposed method have good magnitude response and low group-delay deviation. The performance of the resulting filters is compared with the results of other methods. In Chapter 3, we laid the groundwork for our exploration, emphasizing the precision and specificity achievable through constrained optimization. In this chapter, we demonstrate the versatility of this approach by navigating the complexities of nearly linear-phase 2-D IIR digital filter design. These two chapters thus form a

seamless continuum, illustrating the consistent application of optimization principles from 1-D to 2-D IIR digital filters. Through this research, we showcase not only the transformative power of constrained optimization but also our ability to create a unified framework that effortlessly extends across dimensions, paving the way for innovative solutions in digital filters design.

5.1 Introduction

Two-dimensional digital filters have found many signal processing applications, such as image processing, video signal filtering, beamforming systems, and remote sensing. As already mentioned, digital filters are broadly classified into two main categories, namely, finite impulse response (FIR) filters and infinite impulse response (IIR) filters [6]. An FIR filter is one whose impulse response is of finite duration. The output of such a filter is calculated solely from the current and previous input values. This type of filter is hence said to be non-recursive. On the other hand, an IIR filter is one whose impulse response (theoretically) continues forever in time. They are also termed as recursive filters. In addition to the current and previous input values, the current output of such a filter depends on the previous output values.

FIR filters are generally easier to implement, as they are non-recursive, always stable (by definition), and can be designed to have a linear phase characteristic. They are, however, not well-suited for very sharp (narrow transition band) frequency responses. IIR filters, on the other hand, are much more difficult to design due to their non-linear phase and their stability constraints. However, they can effectively accommodate very narrow transition band frequency responses, which makes them suitable for a broad range of applications. Moreover, selective IIR filters are much more efficient than selective FIR filters, as the latter require higher orders (i.e., more multiplications) [5–7, 12, 21–23, 145–147]. The efficiency of IIR filters stems from their ability to satisfy the required filter specifications with a much lower filter order, thereby reducing the computational requirements. In addition, IIR filters can have a much smaller group delay compared with FIR filters [2, 6, 35, 148]. Due to these advantages, IIR filters find extensive applications in the domains of de-noising of digital images, biomedical imaging and digital mammography, X-ray image enhancement, and seismic data processing.

Since many signal and image processing applications are very sensitive to phase non-linearity, the design of IIR filters needs to take into consideration not only the am-

plitude requirements but also the phase constraints. Therefore, for most of these applications, the designed IIR filters should have a nearly linear-phase response. Moreover, hard constraints on the location of the poles of IIR filters must be enforced to ensure the stability of the obtained filters [9–11, 17, 26, 38, 45, 86, 89, 123, 124, 138, 149–152]. These and other design requirements usually lead to highly nonlinear constrained optimization problems that require highly sophisticated optimization methods [6, 25, 26, 32, 34, 35]. Research on 2-D IIR filters has produced many constrained and nonconstrained optimization problems, depending on the researchers' design objectives. Moreover, each researcher has designed specialized algorithms and techniques to handle their optimization problems. Most of these methods can be classified into linear and nonlinear techniques. In linear design techniques, the nonlinear optimization problem is approximated by a sequence of linear optimization problems [2, 6], which are then solved using linear programming. Starting from an initial filter that satisfies most of the design specifications, the algorithm linearizes the nonlinear optimization around this initial filter to produce a linear optimization problem. Solving this problem leads to an improved filter, around which the linearization is carried out. This iterative process is repeated until an acceptable filter is achieved. Although the linear methods can be very fast, and the designer might be able to find an initial filter satisfying most of the design specifications, there is no guarantee that it will converge or produce accurate solutions. As such, nonlinear techniques are preferred. Some researchers have attempted to develop design methods based on modern optimization algorithms.

In [26], the Sequential Partial Optimization algorithm was proposed to convert the minmax design problem into a sequence of smaller sub-problems, each updating only a single second-order denominator factor.

In [41], a modern optimization methodology known as semi-definite programming (SDP) is utilized. This SDP method includes minmax and weighted least-squares designs of FIR filters as well as minmax formulations of stable separable-denominator IIR filters. The work reported in [41] describes how SDP has the potential to serve as a unified optimization engine for designing a wide range of 2-D digital filters.

The Quasi-Newton method has been applied to design 2-D IIR digital filters [21], but it may result in unstable filters. Neural networks were used in [153] to design 2-D IIR filters, which can guarantee the stability of the designed filters with low computational time. Some researchers have employed the genetic algorithm (GA) to design 2-D IIR digital filters [27, 34, 154–156]. Others have proposed hybrid methods that

combine different evolutionary algorithms, such as biogeography-based optimization and particle swarm optimization in [157], to tackle the nonlinear 2-D IIR optimization design.

In this chapter, a robust nonlinear optimization method for the design of nearly linear-phase 2-D IIR digital filters with separable denominators is proposed. This design problem is formulated as a nonlinear constrained optimization problem where the group delay deviation is minimized under prescribed soft magnitude constraints and hard stability requirements. We also rely on sub-level sets of the group delay deviations to obtain a sequence of filters, from which we choose the most optimal one. The performance of the obtained 2-D IIR filters is evaluated using three quality factors. These first two quality factors are the usual passband magnitude quality factor Q_h and the group delay deviation quality factor Q_τ, while the third one is a new quality factor Q_s that assesses the performance of the filter within the stopband relative to the minimum filter gain in the passbands, which is because amplitude response anomalies in transition regions are undesirable [110]. The obtained results show that these quality factors are all necessary to judge the optimality of the filter. The proposed framework is implemented using the interior-point (IP) method in a MATLAB environment, and the results are very promising.

The chapter is organized as follows. The constrained optimization problem for 2-D IIR digital filters is formulated in Section 5.2. Section 5.3 is for the stability requirements for the 2-D IIR digital filters with a separable denominator. Section 5.4 presents the constrained optimization design problem for a 2-D IIR digital filters. Section 5.5 is dedicated to the quality of the design, and Section 5.6 to the experimental results. Section 5.7 concludes with a brief summary and future work directions.

5.2 Formulation of the Design Problem

Much attention has been paid to the optimal design of 2-D filters with separable denominators [26, 32, 41, 42, 89, 158, 159]. The stability of such 2-D filters can be easily guaranteed by ensuring the roots of both denominators are within the unit bi-disc independently. As such, the internal stability triangles for 1-D second-order factors are used as stability constraints [160]. In addition, separable denominators reduce the complexity of the 2-D filter and the induced optimization problem and also result in fewer coefficients [26, 161]. Although the phase of the optimized 2-

D IIR filter is only nearly linear, one can see that the separable-denominator 2-D IIR filter offers good selectivity and computation efficiency and reduced system delay without compromising the required amplitude specifications when compared with the corresponding other 2-D filters [161]. As such, we will assume in this design problem that the filters of interest have separable denominators. The desired 2-D IIR filter can then be represented by the following transfer function [30, 162–164]:

$$H(a,b,z_1,z_2) = \frac{N(z_1,z_2,b)}{D(z_1,z_2,a)} \tag{5.1}$$

$$= H_0 \frac{N(z_1,z_2,b)}{D_1(z_1,a_1)D_2(z_2,a_2)},$$

where b is a vector of the form $[b_{00}\, b_{01} \ldots b_{N_1 N_2}]$, and $N(z_1,z_2,b)$ is a multivariate polynomial of the form:

$$N(z_1,z_2,b) = \sum_{j=0}^{N_2}\sum_{i=0}^{N_1} b_{ij} z_1^{-i} z_2^{-j}, \tag{5.2}$$

$D_1(z_1,a_1)$ and $D_2(z_2,a_2)$ are polynomials in z_1 and z_2, respectively, of the form

$$D_1(z_1,a_1) = \prod_{n=1}^{J_1}(1 + a_{1n,1}z_1^{-1} + a_{1n,2}z_1^{-2}), \tag{5.3}$$

$$D_2(z_2,a_2) = \prod_{n=1}^{J_2}(1 + a_{2n,1}z_2^{-1} + a_{2n,2}z_2^{-2}), \tag{5.4}$$

where $J_1 = N_1/2$ and $J_2 = N_2/2$ and N_1 and N_2 are even.
The vectors a_1 and a_2 are given by:

$$a_1 = [a_{11,1}\, a_{11,2}\, a_{12,1}\, a_{12,2}\, \ldots\, a_{1J_1,1}\, a_{1J_1,2}], \text{ and} \tag{5.5}$$

$$a_2 = [a_{21,1}\, a_{21,2}\, a_{22,1}\, a_{22,2}\, \ldots\, a_{2J_2,1}\, a_{2J_2,2}]. \tag{5.6}$$

We then construct a vector c by concatenating the vectors b, a_1, and a_2 as follows [160]:

$$c = [b\, a_1\, a_2\, H_0]^T.$$

Using the same notation symbol, the transfer function can be written as follows:

$$H(c, z_1, z_2) = \frac{N(z_1, z_2, b)}{D(z_1, z_2, a)}. \tag{5.7}$$

Now, the main design problem is to determine the coefficients in the numerator and denominator of (5.7) in such a way that the obtained transfer function $H(z_1, z_2)$ satisfies all the desired specifications as explained in the following sections.

5.2.1 Passband Group Delay Deviations

Let $\phi(c, \omega_1, \omega_2)$ and $\psi(c, \omega_1, \omega_2)$ be the phase angles of $N(e^{j\omega_1}, e^{j\omega_2}, b)$ and $D(e^{j\omega_1}, e^{j\omega_2}, a)$, respectively. The group delay of the transfer function $H(c, z_1, z_2)$ is given as a partial derivative with respect to ω_1 and ω_2 as follows:

$$\begin{aligned}
\tau_1(c, \omega_1, \omega_2) &= \frac{\partial \phi(c, \omega_1, \omega_2)}{\partial \omega_1} - \frac{\partial \psi(c, \omega_1, \omega_2)}{\partial \omega_1}, \text{ and} \\
\tau_2(c, \omega_1, \omega_2) &= \frac{\partial \phi(c, \omega_1, \omega_2)}{\partial \omega_2} - \frac{\partial \psi(c, \omega_1, \omega_2)}{\partial \omega_2}.
\end{aligned}$$

Letting τ_{10} and τ_{20} be the intended average passband group delays of the initial filter in each dimension over a domain Ω_{pb}, the deviation can be computed as follows:

$$\begin{aligned}
e_{g_i}(x, \omega_1, \omega_2) =& \tau_i(x, \omega_1, \omega_2) - \tau_{i0}, \\
& \text{for } i = 1, 2, \forall (\omega_1, \omega_2) \in \Omega_{pb},
\end{aligned} \tag{5.8}$$

where $x = [c^T \, \tau_{10} \, \tau_{20}]^T$, and Ω_{pb} is the passband region [160].

At the start of the optimization, τ_{10} and τ_{20} can be assigned values equal to the average group delays of the initial filter. As the optimization progresses, their values can be adjusted along with the coefficients of the filter so as to minimize the group delay deviation. The end result will be that τ_{10} and τ_{20} will track the average value of the group delays in each dimension. As such, we have added them to the vector of variables to be optimized.

5.2.2 Passband Amplitude Error

For the passband error, if we consider $H_d(\omega_1, \omega_2)$ to be the desired frequency response of the filter and that c_k is the value of the vector c at the start of the k_{th} iteration,

then the passband error function at frequencies ω_1 and ω_2 can be defined as:

$$e_h(x,\, \omega_1, \omega_2) \approx |H(c_k, \omega_1, \omega_2)\,| - |H_d(\omega_1, \omega_2)|.$$

Assuming that the desired amplitude response is unity in the passband, therefore, the passband error function becomes:

$$e_h(x,\, \omega_1, \omega_2) \approx |H(c_k, \omega_1, \omega_2)\,| - 1, \forall(\omega_1, \omega_2) \in \Omega_{pb}. \tag{5.9}$$

The expression above can be used as is in the case of the nonlinear approach.
For the transition and stopband regions, the magnitude response is subject to prescribed levels of transition-band and stopband gains, as explained in Section 5.4.

5.3 Filter Stability

One of the major problems underlying the design task is satisfying the stability criterion for the 2-D IIR filter transfer function. For the stability constraints of the 2-D IIR filter, since the filter transfer function is separable in the denominator, the stability analysis is similar to the 1-D case used in Chapter 3, where all the poles of $D_1(z_1, a_1)$ and $D_2(z_2, a_2)$ have to be located inside the unit circle $\mathbf{U}$ of the z-plane for both z_1 and z_2.

5.4 The Constrained Optimization Problem

To solve the design problem, the group delay deviation is minimized under hard and soft constraints. Hard constraints are the requirements that the filter must satisfy. These requirements must include at least the stability constraints of the filter. On the other hand, soft constraints are the requirements that the filter should try to satisfy. These can, for example, include the passband ripple constraint, transition-band gain. and stopband attenuation.

The general constrained optimization problem at hand can be stated as follows:

$$\min_{x} \max_{\omega_1,\omega_2 \in \Omega_{pb}} \{|e_{g1}(x,,\omega_1,\omega_2)|, |e_{g2}(x,\omega_1,\omega_2)|\} \tag{5.10}$$

subject to :

$$\begin{aligned} &\text{passband error} \leq \Gamma_{pb}, \\ &\text{transition-band gain} \leq \Gamma_{tb}, \\ &\text{stopband gain} \leq \Gamma_{sb}, \\ &\text{stability margin} \geq \varepsilon_s, \end{aligned} \tag{5.11}$$

where Γ_{pb}, Γ_{tb}, and Γ_{sb} are the maximum prescribed levels for the passband error, transition-band gain, and stopband gain, respectively. The stability margin, ε_s, is defined as $\varepsilon_s = 1 - r_{max}^{(p)}$ where $r_{max}^{(p)}$ is the maximum pole radius allowed [2]. The above general optimization problem for the nearly linear-phase 2-D IIR digital filters can now be expressed as follows:

$$\min_{x} \max_{\omega_1,\omega_2 \in \Omega_{pb}} \{|\tau_1(x,\omega_1,\omega_2) - \tau_{10}|, |\tau_2(x,\omega_1,\omega_2) - \tau_{20}|\} \tag{5.12}$$

s.t :

$$\begin{aligned} &|e_h(x,\omega_1,\omega_2)| \leq \Gamma_{pb}, \forall(\omega_1,\omega_2) \in \Omega_{pb}, \\ &|H(x,\omega_1,\omega_2)| \leq \Gamma_{tb}, \forall(\omega_1,\omega_2) \in \Omega_{tb}, \\ &|H(x,\omega_1,\omega_2)| \leq \Gamma_{sb}, \forall(\omega_1,\omega_2) \in \Omega_{sb}, \\ &|\tau_1 - \tau_{10}| \leq \Gamma_{g_1}, \forall(\omega_1,\omega_2) \in \Omega_{pb}, \\ &|\tau_2 - \tau_{20}| \leq \Gamma_{g_2}, \forall(\omega_1,\omega_2) \in \Omega_{pb}, \\ &\mathbf{B}_1 x \leq 1 - \gamma, \\ &\mathbf{B}_2 x \leq 1 - \gamma, \end{aligned} \tag{5.13}$$

where Γ_{g_1} and Γ_{g_2} are the maximum errors between the group delays of the actual and the initial filters. $\gamma = 1 - (1 - \varepsilon_s)^2$, $\mathbf{B_1}$ and $\mathbf{B_2}$ are the stability matrices for $D_1(z_1, a_1)$ and $D_2(z_2, a_2)$, respectively [2, 160]. The 2-D IIR filter design problem can be readily solved using interior-point method. This is because the interior-point method is efficient from a computational point of view and also highly efficient in

practice [165, 166]. To make our implementation easier, we used $\Gamma_g = \Gamma_{g_1} = \Gamma_{g_2}$. By varying Γ_g, and therefore Γ_{g_1} and Γ_{g_2}, we obtain different filters from which we choose the best filter by looking at the quality factors that will be discussed in the next section. The proposed framework is implemented using the interior-point method in a MATLAB environment and the flowchart of the optimization process is shown in Figure 5.1.

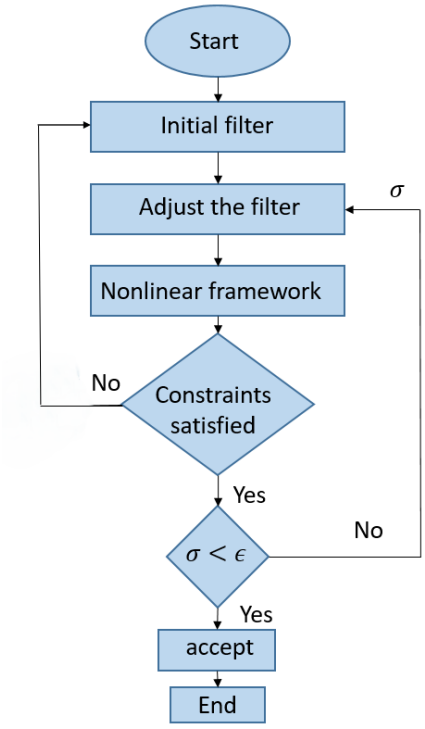

Figure 5.1: Flowchart of the optimization process.

5.5 Quality of the Design

Design efficiency and the performance of the proposed method are evaluated in terms of the quality of the group delay characteristic Q_τ, the quality of the magnitude response in the passband Q_h, and a new quality factor Q_s for the magnitude attenuation in the stopband. We introduced this new factor, Q_s, to measure the quality of the magnitude in the stopband. It is important to know that, as these quality factors are inverse measures, they have to be small to obtain a good filter that satisfies prescribed specifications. The quality of the group delay characteristic of the 2-D filter will be measured by using the normalized maximum variation of the filter group delay over

the passband as a percentage as follows:

$$Q_\tau = \max\left\{\frac{\tau_{1max} - \tau_{1min}}{\tau_{1max} + \tau_{1min}}, \frac{\tau_{2max} - \tau_{2min}}{\tau_{2max} + \tau_{2min}}\right\} \times 100\%, \tag{5.14}$$

To measure the quality of the magnitude in the passband, we use:

$$Q_h = \frac{H_{max} - H_{min}}{H_{max} + H_{min}} \times 100\%, \tag{5.15}$$

where H_{max} and H_{min} are the maximum and minimum magnitudes in the passband, respectively. We observe that when we design the filter, we improve the passband ripple and the group delays, but sometimes the stopband attenuation is not good enough. Based on this observation, we introduced a new quality factor for the stopband attenuation, which is measured in terms of the minimum variation of the passband ripple and the maximum variation of the stopband attenuation. Therefore, to measure the quality of the magnitude response in the stopband, one can use:

$$Q_s = \frac{H^s_{max}}{H_{min} - H^s_{max}}, \tag{5.16}$$

where H^s_{max} is the maximum magnitude in the stopband region, and H_{min} is the minimum magnitude in the passband. This quality factor, Q_s, is valid for $H_{min} > H^s_{max}$, i.e., negative values are excluded. Note that these quality factors are inverse measures, and, therefore, a good filter is the one where these quality factors are small.

5.6 Experimental Results

This section is dedicated to implementing (5.12) and (5.13) to optimize the design of 2-D IIR filters with nearly linear-phase. Our proposed approach will be evaluated against other methods described in the literature. Specifically, we will compare the designs obtained using the proposed method to the ones presented in [5]. Some of these examples are discussed in [167, 168] as well. The desired frequency response will be defined in each example, and the group delays τ_1 and τ_2 along the ω_1 and ω_2 directions are considered to be the same, i.e., $\tau_1 = \tau_2 = \tau$. In each of the designed examples, the starting values for τ_{10} and τ_{20} are set as the mean values of the passband group delays of the initial filter, and the stability margin ε_s is set to 0.02, unless otherwise mentioned in the design example. The MATLAB environment is used to

solve the proposed constrained optimization problem. The MATLAB Symbolic Math Toolbox and the interior-point method (IP) were used to implement the constrained optimization problem.

5.6.1 2-D Highpass Filter

In this example, it is required to design a 2-D highpass filter with the ideal filter specifications shown in Figure 5.2, where $\theta_i = \omega_i T$. In addition to the given design specifications, we are including the transition band in our design, which aligns with the filter obtained in [5]. To assess the performance of our filter and the one proposed by [5], we have calculated the maximum transfer function magnitude in the transition band $H^t_{\max}$ for both filters, as presented in Table 5.1.

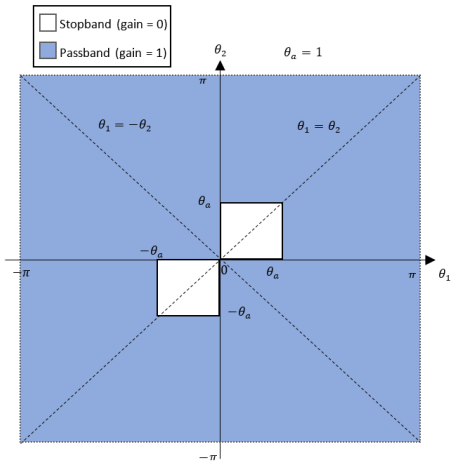

Figure 5.2: Ideal specifications for 2-D highpass filter presented in [5].

In this example, we let the maximum iterations=140, $\epsilon = 1 \times 10^{-7}$, $\varepsilon_s = 0.1$, $\Gamma_{pb} = 0.01$, $\Gamma_{tb} = 1.5$, $\Gamma_{sb} = 0.1$, $H_0 = 1$. We implement the proposed algorithm for various values of Γ_g starting from 0.1 to 4.0. Using the quality factors defined in Section 5.5, the filter with $\Gamma_g = 1.65$ is the most optimal filter among the filters obtained. Figure 5.3 shows the magnitude response of the designed filter using the proposed method, and the filter presented in [5]. Figure 5.4 and Figure 5.5 show the group delays τ_1 and τ_2 of the designed 2-D IIR highpass filter obtained using the proposed method and the filter presented in [5], respectively. Table 5.1 compares the results of the highpass filter designed by the proposed algorithm with the highpass filter presented in [5].

Table 5.1: Comparison results for highpass filters.

	Proposed Method	Method in [5]
Orders	(4,4)	(4,4)
$H_{\min}$	0.437	0.262
$H_{\max}$	1.338	1.066
Q_h	50.76	60.54
$H^t_{\max}$	0.664	0.849
$H^s_{\max}$	0.389	0.426
Q_s	8.104	-2.598
$\tau_{\min}$	0.962	0.009
$\tau_{\max}$	4.397	11.614
Q_τ	64.09	99.84

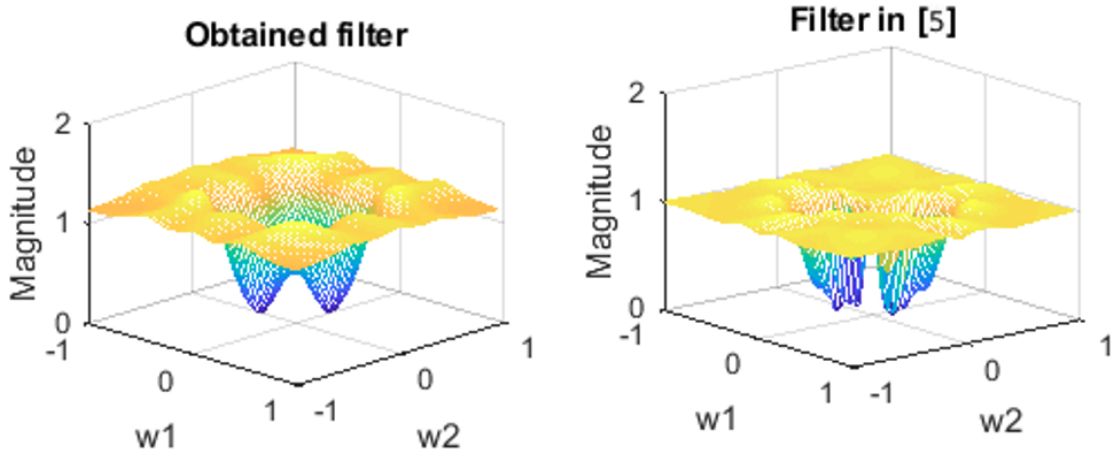

Figure 5.3: Magnitude responses of the 2-D highpass filters.

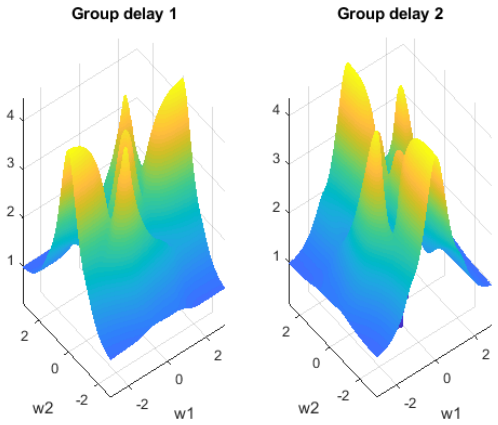

Figure 5.4: Group delays in the passband of the obtained highpass filter ($\Gamma_g = 1.65$).

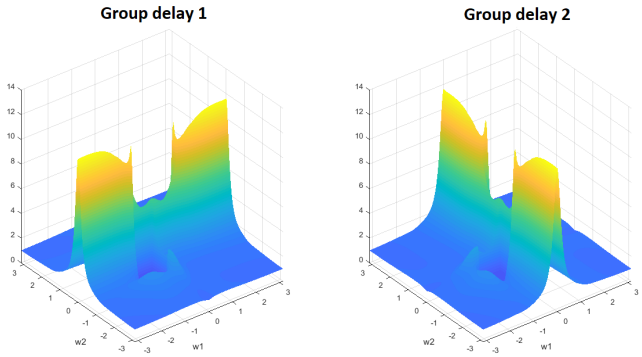

Figure 5.5: Group delays in the passband of the highpass filter presented in [5].

We can see that the quality of the group delay characteristic, defined by (5.14), of the 2-D highpass filter designed by the proposed method is better than the one designed in [5]. It can be seen that $Q_\tau = 64.09$, where $\tau_{min} = 0.962$ and $\tau_{max} = 4.397$ for the filter obtained by using the proposed method, and $Q_\tau = 99.84$ for the filter designed in [5], whereas $\tau_{min} = 0.009$ and $\tau_{max} = 11.614$. The quality measure of the magnitude response in the passband, defined by (5.15), of the obtained 2-D IIR highpass filter is $Q_h = 50.76$, where $H_{min} = 0.437$ and $H_{max} = 1.338$. In the same manner, the quality measure of the magnitude response in the passband of the filter presented in [5] is $Q_h = 60.54$, where $H_{min} = 0.262$ and $H_{max} = 1.066$. The quality of the magnitude response in the stopband defined by (5.16) is $Q_s = 8.104$ for the filter obtained by the proposed method and for the filter presented in [5], Q_s is negative, indicating too low stopband attenuation compared with the minimum gain in the passband.

5.6.2 2-D Lowpass Filter

The proposed method is used to design a 2-D IIR lowpass filter with the ideal design specifications shown in Figure 5.6. The filter was presented in [5], and its order was selected as (4,4). The transition band constraint is included in this example, and H^t_{max} is computed for both filters, where the results are shown in Table 5.2.

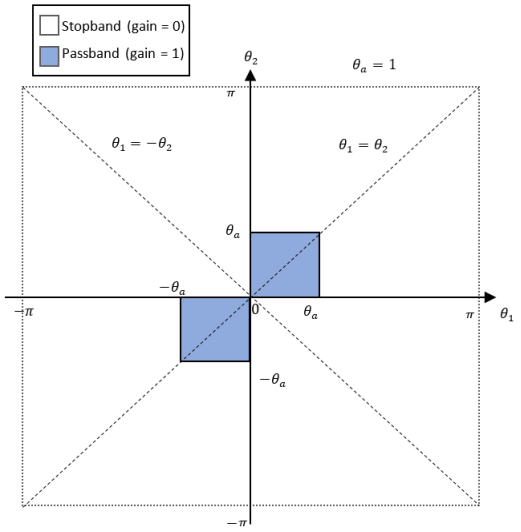

Figure 5.6: Ideal specifications for 2-D lowpass filter presented in [5].

This 2-D lowpass filter is designed by the proposed method using the following values: Maximum iterations = 140, $\epsilon = 1 \times 10^{-7}$, $\varepsilon_s = 0.1$, $\Gamma_{pb} = 0.0001$, $\Gamma_{tb} = 1$, $\Gamma_{sb} = 0.01$, $H_0 = 1$, $\tau_{10} = \tau_{20} = 2$. The algorithm is implemented for different values of Γ_g, starting from 0.1 to 4. The filter with $\Gamma_g = 2.35$ has the best quality in this example.

Figure 5.7 shows the magnitude response of the filter obtained by using the proposed method and the filter presented in [5]. Figures 5.8 and 5.9 show the group delays, τ_1 and τ_2, of the obtained 2-D lowpass filter for $\Gamma_g = 2.35$. The group delays, τ_1 and τ_2, of the 2-D lowpass filter presented in [5] are shown in Figure 5.10 and Figure 5.11, respectively. Table 5.2 compares the results of the filter designed by the proposed method and the filter obtained in [5]. The quality of the group delay characteristic, defined by (5.14), for the 2-D lowpass filter obtained by the proposed method is $Q_\tau = 47.650$, where $\tau_{min} = 2.217$ and $\tau_{max} = 6.864$. The same quality measure for the 2-D lowpass filter presented in [5] is found to be $Q_\tau = 93.774$, where $\tau_{min} = 1.738$ and $\tau_{max} = 54.091$. The quality measure of the magnitude response in

the passband, defined by (5.15) of the 2-D lowpass filter obtained by the proposed method is $Q_h = 14.25$, where $H_{min} = 0.843$ and $H_{max} = 1.120$, and for the filter presented in [5] is $Q_h = 25.26$, where $H_{min} = 0.642$ and $H_{max} = 1.069$. The quality of the magnitude response in the stopband defined by (5.16) is $Q_s = 0.916$ for the filter designed by the proposed method, and $Q_s = 2.275$ for the filter presented in [5]. We can see that the filter designed with the proposed method is better than the one designed in [5], especially with respect to the passband phase linearity.

Table 5.2: Comparison results for 2-D IIR lowpass filters.

	Proposed Method	**Method in [5]**
Orders	(4,4)	(4,4)
$H_{\min}$	0.843	0.642
$H_{\max}$	1.120	1.069
Q_h	14.25	25.26
$H^t_{\max}$	1.0079	1.020
$H^s_{\max}$	0.403	0.446
Q_s	0.916	2.275
$\tau_{\min}$	2.217	1.738
$\tau_{\max}$	6.864	54.091
Q_τ	47.650	93.774

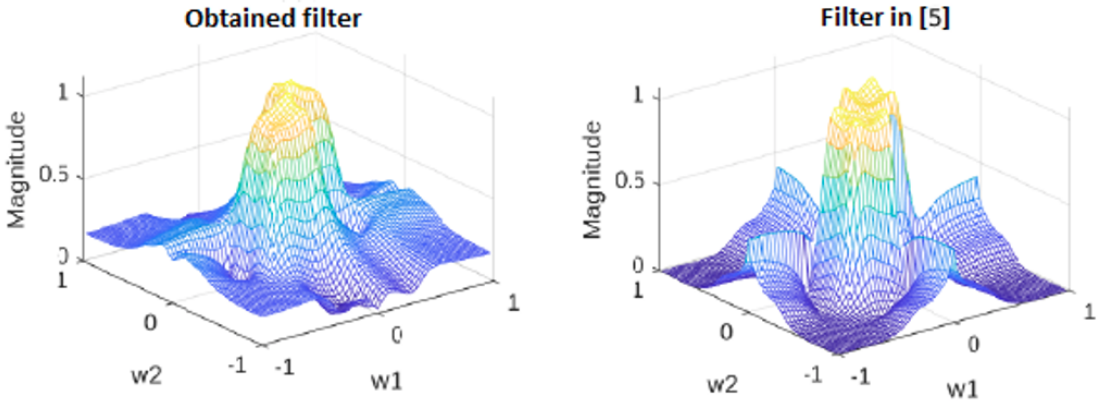

Figure 5.7: Magnitude responses of the 2-D lowpass filters.

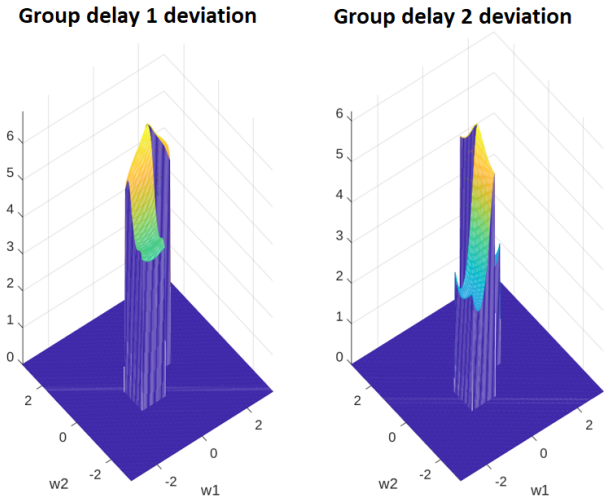

Figure 5.8: Passband group delays of the obtained lowpass filter ($\Gamma_g = 2.35$).

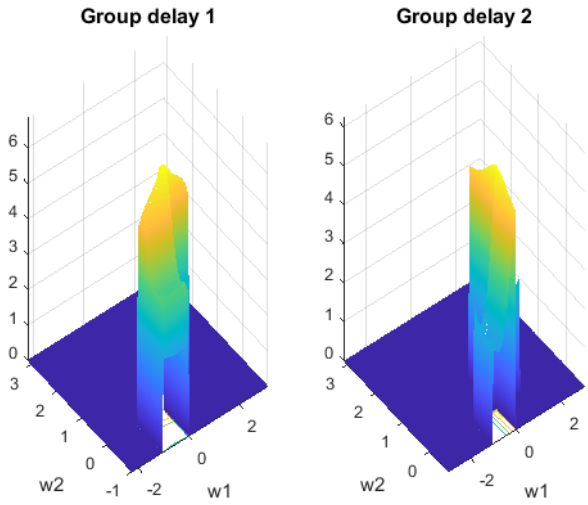

Figure 5.9: First quadrant group delays for 2-D IIR lowpass filter ($\Gamma_g = 2.35$).

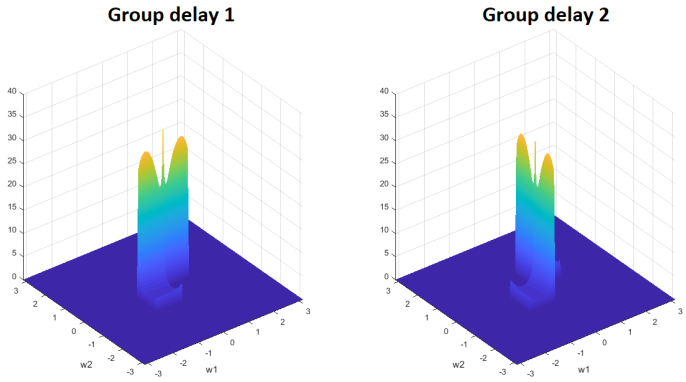

Figure 5.10: Passband group delays of the 2-D lowpass filter presented in [5].

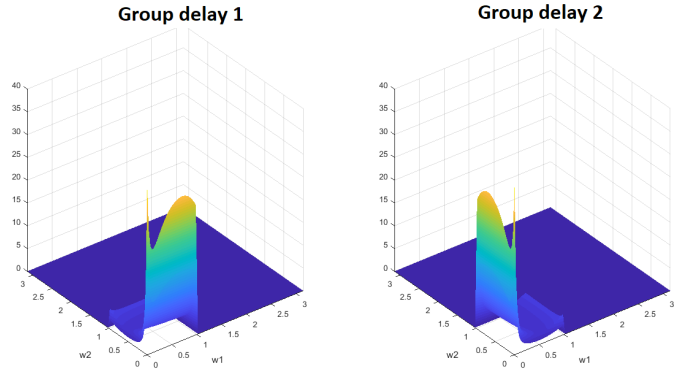

Figure 5.11: First quadrant group delays of the 2-D lowpass presented in [5].

5.6.3 2-D Bandpass Filter

In this example, a 2-D IIR bandpass filter with the design specifications shown in Figure 5.12 is presented. It is also required that the order of this filter remain low, specifically $(4, 4)$ as in [5]. In addition to these design specifications and to assess the performance of our filter and the one proposed in [5], we have included the transition band constraint in our design. As a result, we calculated the max. transfer function magnitude $H^t_{\max}$ for both filters, as presented in Table 5.3. The algorithm is implemented with various values of Γ_g, starting from 0.1 to 4, and the resulting filter with $\Gamma_g = 1.6$ has the best quality.

The magnitude response of the 2-D IIR bandpass filter obtained using the proposed method and the filter designed in [5] are shown in Figure 5.13. The group delays τ_1 and τ_2 of the designed 2-D bandpass filter are illustrated in Figure 5.14. Figure 5.15 shows the group delays of the same filter in the first quadrant. The group

delays of the 2-D bandpass filter presented in [5] are illustrated in Figure 5.16. The first quadrant plot of the group delays τ_1 and τ_2 for the same filter is shown in Figure 5.17. Table 5.3 compares the results of the bandpass 2-D IIR filter designed by the proposed algorithm and the bandpass filter presented in [5]. The quality of the group delay characteristic, defined by (5.14), of the 2-D IIR bandpass filter obtained by the proposed method is $Q_\tau = 47.150$, where $\tau_{min} = 1.822$ and $\tau_{max} = 5.073$. The same measure is applied to the 2-D IIR bandpass filter designed in [5], which gives $Q_\tau = 57.315$, where $\tau_{min} = 1.828$ and $\tau_{max} = 6.737$. The quality measure of the magnitude response in the passband, defined by (5.15), of the 2-D IIR bandpass filter obtained by the proposed method is $Q_h = 19.09$, where $H_{min} = 0.809$ and $H_{max} = 1.191$. In the same manner, the quality measure of the magnitude in the passband region of the 2-D IIR bandpass filter presented in [5] is $Q_h = 29.667$, where $H_{min} = 0.633$ and $H_{max} = 1.167$. The quality of the magnitude response in the stopband defined by (5.16) is $Q_s = 0.668$ for the filter obtained by the proposed method, and $Q_s = 0.734$ for the filter presented in [5].

In this example, we can see that the filter obtained by using the proposed algorithm has a better passband quality factor, Q_h, stopband quality factor, Q_s, and group delay quality factor, Q_τ, than the filter presented in [5].

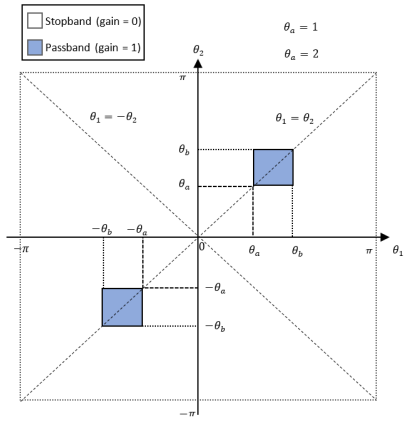

Figure 5.12: Ideal specifications for the 2-D bandpass filter presented in [5].

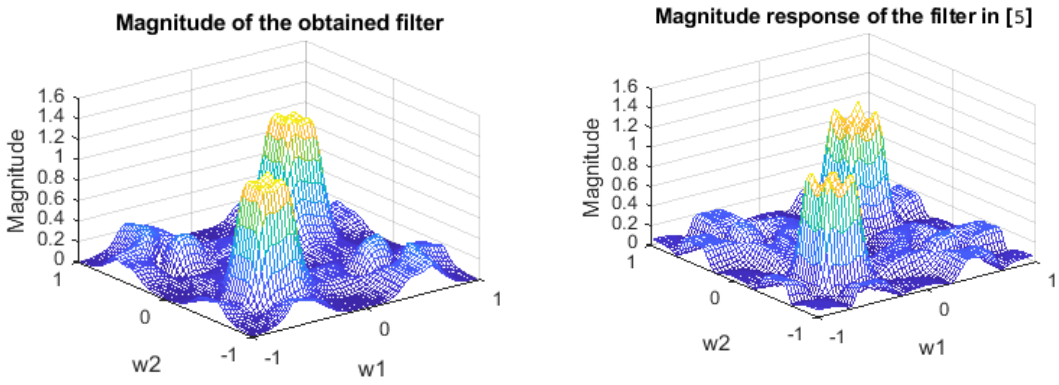

Figure 5.13: Magnitude responses of the 2-D Bandpass filters.

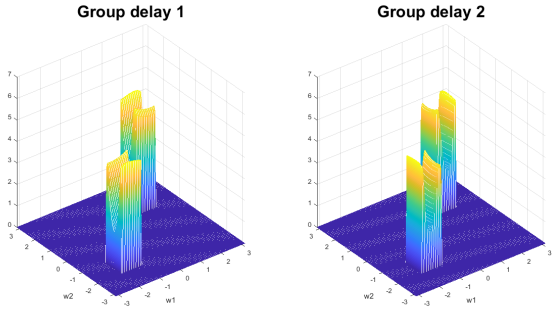

Figure 5.14: Passband group delays of the obtained 2-D bandpass filter.

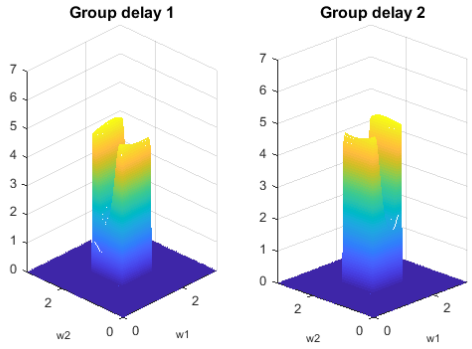

Figure 5.15: Group delays of the obtained bandpass filter in the first quadrant.

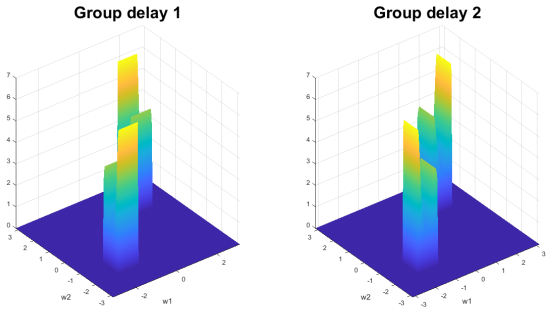

Figure 5.16: Passband group delays of the bandpass filter presented in [5].

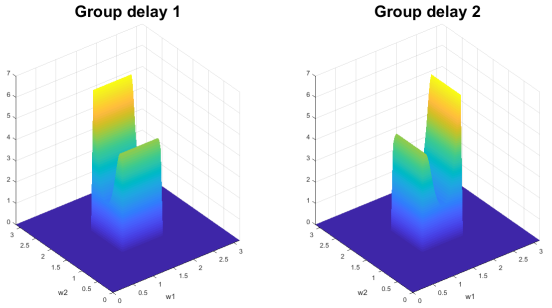

Figure 5.17: Group delays of the bandpass filter in [5] in the first quadrant.

Table 5.3: Comparison results for 2-D bandpass filters.

	Proposed Method	**Method in [5]**
Orders	(4,4)	(4,4)
$H_{\min}$	0.809	0.633
$H_{\max}$	1.191	1.167
Q_h	19.100	29.667
$H^t_{\max}$	0.855	0.798
$H^s_{\max}$	0.324	0.268
Q_s	0.668	0.734
$\tau_{\min}$	1.822	1.828
$\tau_{\max}$	5.073	6.737
Q_τ	47.150	57.315

5.7 Conclusions

In this chapter, a new framework for a nonlinear optimization design method for nearly linear-phase 2-D IIR digital filters with separable denominators is presented. The method is used to solve the design problem, expressed as a nonlinear constrained optimization problem. In our implementation, we distinguish two kinds of constraints: soft and hard constraints. Meeting the soft constraints is not compulsory and, therefore, not decisive in rejecting the filter. The hard constraints, however, must be satisfied to accept the filter. The designed filters are evaluated with three quality factors, namely passband amplitude and group delay quality factors, and a new quality factor for the stopband magnitude response. Compared with other 2-D IIR filters designed with other methods, the results show that the framework produces very good results for different filter specifications.

By evaluating the resulting filters, we see that this method improves the linearity of the phase in the passband along with magnitude improvements, generally without significant deterioration in the magnitude response. The method is also flexible enough to be used after any other 2-D IIR design algorithm by taking the resulting filter as the initial filter and running this method to obtain possible further improvements.

Chapter 6

Broadband Beamforming and Interference Rejection of Plane Waves using 2-D FIR and IIR Digital Filters

Abstract: This chapter explores and compars the application of 2-D FIR and IIR digital filters as beamformers, leveraging their frequency-domain characteristics to extract and enhance spatio-temporal (ST) broadband plane waves (PWs) arriving from specific Direction of Arrivals (DOAs). 2-D FIR and IIR fan filters with a pass-band that precisely aligns with the Region of Support (ROS) corresponding to the desired PWs are designed. These fan filters act as spatial frequency-domain selectors, effectively passing signals of interest (SOI) while attenuating interference and noise from other directions.

Experimental results show that both FIR and IIR fan filters are capable of extracting and enhancing 2-D broadband ST PWs according to their DOAs in the presence of severe cochannel interference and noise. The performance of these filters is evaluated by examining the Signal-to-Noise-plus-Interference Ratio (SNIR) and the Signal SOI to Error Ratio after applying the filter. The comparison shows that 2-D IIR filters, when designed using advanced model order reduction techniques, achieve similar performance to their FIR counterparts but with significantly lower computational overhead.

6.1 Introduction

In the field of array signal processing, 2-D digital filters emerge as powerful tools, particularly when employed as beamformers in scenarios where the DOAs of desired broadband PWs are known. The process involves the design of a 2-D filter, carefully made to act as a beamformer, utilizing knowledge about the DOAs of the broadband PWs. This strategy is rooted in the frequency domain, where the filter is configured to have a passband that precisely encloses the Region of Support (ROS) corresponding to the desired PW [169, 170].

The resulting 2-D filter functions as a spatial filter in the frequency domain, selectively passing the signals associated with the desired PW while attenuating all other PWs received from any other DOA. This targeted filtering process allows for enhanced signal isolation and improved reception of the SOI, mitigating interference from signals arriving from unintended directions [169].

In this chapter, we focus specifically on the applications of 2-D FIR and IIR digital filters as beamformers, benefiting from the knowledge of DOAs for desired broadband PWs. By manipulating the frequency response in the passband region, these filters demonstrate a capability to enhance selectivity and isolate the signals of interest [22]. In addition, these filters are used to suppress interference and reduce noise corrupting the SOI, which arrives from a known direction, while the interference arrives from different directions that are often unknown.

It is well know that FIR filters offer several good properties, such as guaranteed stability and exact linear phase, but also that they require a higher filter order to fulfill the given specifications compared to IIR filters, especially when the transition band is relatively narrow. In addition, as we use IIR instead of FIR, the complexity of IIR filters can be reduced in comparison with FIR. Examples will demonstrate that the 2-D IIR filter obtained by the proposed model order reduction method presented in Chapter 4 has lower arithmetic complexity compared to the 2-D FIR filter while fulfilling the same specification.

6.2 Plane Waves and Directional Filter Pattern

The PW model shown in Figure 6.1 forms the basis of traditional beamforming techniques which assumes that the source is in the far field. When the distance between the array and the source is significantly greater than the size of the aperture, this

condition is met and the propagating energy may be described as a PW. If this condition is not met, consideration must be given to the wave front curvature of impinging signals (near-field) [171, 172].

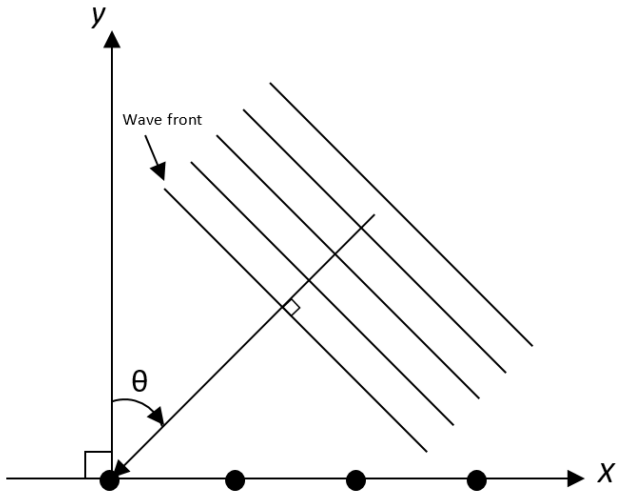

Figure 6.1: Plane wave in space

For the far field case, a continuous-domain (CD) temporal signal propagating through the 2-D space can be expressed as [22]:

$$pw(x, y, t) = \omega(c^{-1}(d_x x + d_y y) + t) \tag{6.1}$$

where $\mathbf{d} = [d_x \; d_y]$ is the unit vector specifying the DOA in the 2-D space $(x, y) \in \mathbb{R}^2$, c is the constant speed of propagation and $\omega(l) \mid \forall l \in \mathbb{R}^1 \; ; \; l = c^{-1}(d_x x + d_y y) + t$ is the 1-D temporal intensity function in the DOA [22, 170]. The angle $\theta = (\cos^{-1}(d_x))$ between the normal to the x-axis and the normal to the 2-D wave fronts defines the DOA of $pw(x, t)$. If $\omega(t)$, the broadband temporal intensity function, is the signal received at the origin then the PW received at the position $\mathbf{p} = [x, y]$ is a delayed version of $\omega(t)$ namely $\omega(t - \tau_p)$ where $\tau_p = \mathbf{a^T p}/c$ and $\mathbf{a}= [\cos\theta \;\; \sin\theta]^T$ [22, 169, 172, 173]. Therefore, we can write

$$\omega(t - \tau_p) = \omega(c^{-1}(x\cos\theta + y\sin\theta) + t) \tag{6.2}$$

Assuming $pw(x, y, t)$ is received by sensors located on the x-axis ($y = 0$) then the received signal is given by [172]:

$$pw(x,y,t) = \omega(c^{-1}d_x x + t) \tag{6.3}$$

The 2-D CD Fourier transform of $pw(x,t)$ is defined by [172]:

$$\begin{aligned}\boldsymbol{\Omega}(\omega_x,\omega_{ct}) = \int_{ct=-\infty}^{\infty}\int_{x=-\infty}^{\infty} \omega(c^{-1}\cos\theta x + t)e^{-j2\pi\omega_x x}e^{-j2\pi\omega_{ct}ct}dxd(ct) \\ = c\delta(\omega_x - \cos(\theta\omega_{ct})\boldsymbol{\Omega}(c\omega_{ct})\end{aligned} \tag{6.4}$$

where δ is a 1-D unit impulse function, ω_{ct} is equal to $c^{-1}\omega_t$ (ω_t and ω_x represent the temporal and spatial frequency, respectively), and $\boldsymbol{\Omega}(\mathbf{c}\omega_{\mathbf{ct}})$ is 1-D CD Fourier transform of $\omega(t)$. It follows from (6.4) that the ROS of $pw(\omega_x,\omega_{ct})$, shown by the two solid line segments in Figure 6.2, is on the line $\omega_x - \cos(\theta)\omega_{ct} = 0$ which passes through the origin and makes an angle equal to $\phi = \tan^{-1}(\cos\theta)$ with the ω_{ct} axis as shown in Figure 6.2. The spectral ROSs of all possible CD 2-D PWs with $|\theta| \leq 90°$ are constrained to a double-fan area with $|\phi| \leq 45°$ as the half-fan angle [22]. The passband area of the desired 2-D fan filter in (ω_x,ω_{ct}) plane can be defined by the following equations [173]:

$$\omega_x - \tan(\phi-\varepsilon)\omega_{ct} \geq 0, \quad \text{for } \beta_2\pi \leq \omega_{ct} \leq \beta_1\pi \tag{6.5}$$

$$\omega_x - \tan(\phi+\varepsilon)\omega_{ct} \leq 0, \quad \text{for } -\beta_1\pi \leq \omega_{ct} \leq -\beta_2\pi \tag{6.6}$$

where ϕ is obtained from the DOA of the desired signal, i.e., $\phi = \tan^{-1}(\cos\theta)$, and ε is called a selectivity parameter that controls the selectivity around the DOA. The two coefficients β_1 and β_2 are used to control the upper and lower bounds along ω_{ct}-axis. These equations will be used for the creation of a directional filter pattern, similar to a fan, which selectively passes signals originating from a specified range of directions and attenuates signals arriving from other undesired directions.

The utilization of a 2-D fan filter aligns with the fundamental objective of beamforming, enabling the extraction and enhancement of the signals of interest while suppressing interference from undesired directions.

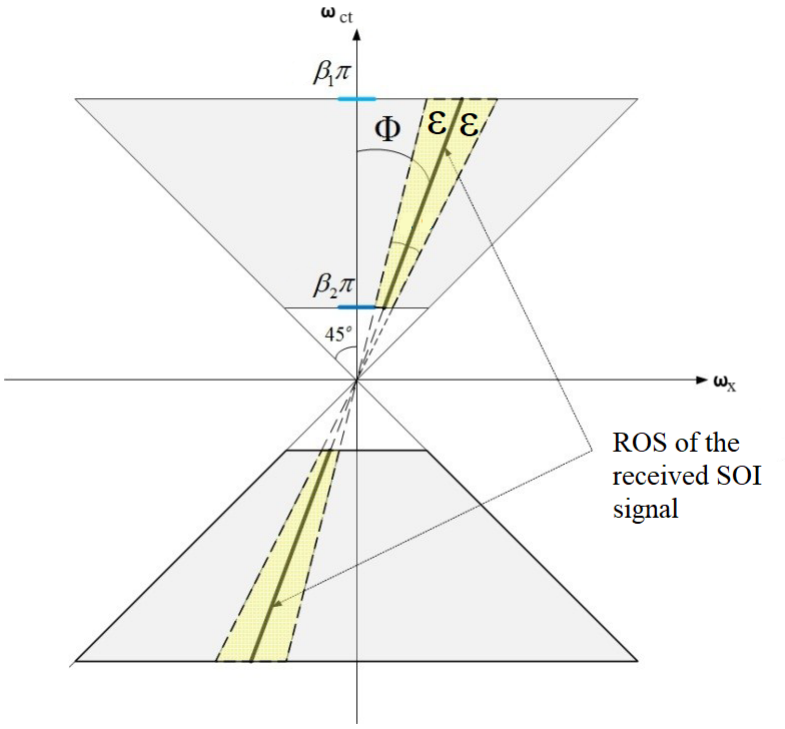

Figure 6.2: Region of support of the SOI.

6.3 Beamforming and Plane Wave Filtering

We consider now a typical application where three broadband PWs are received by a uniform linear array (ULA) having sensors aligned on the x-axis. The SOI and the plane wave interference are arriving from different directions. Moreover, a 2-D additive white Gaussian noise (AWGN) signal is added to the discrete-domain 2-D signal in order to model any received noise. More importantly in this example, the energy of the SOI is selected to be lower than the energy of the interference and AWGN in order to represent a weak SOI. When the interference and noise are much stronger than the SOI signal, the 2-D fan filter provides very effective rejection of the interference and reduces the noise. We demonstrate two cases to illustrate the functioning of and evaluate the performance of 2-D FIR and IIR filters in enhancing broadband PWs. The first scenario illustrates how a 2-D FIR fan filter is proposed as a beamformer and used to extract the SOI. The second case is to use the reduced-order 2-D IIR filter to extract the same SOI and then provide a comparison between 2-D FIR and IIR fan filters in terms of computational complexity. Firstly, a 2-D FIR

fan filter is designed using a 1-D Kaiser window. For the 2-D IIR fan filter, the model order reduction design method described in the previous chapter will be used. In both cases, we illustrate how these filters are used in beamforming applications and filtering of 2-D PWs in array signal processing, particularly in the selective processing of 2-D PWs received from desired directions while mitigating interference and noise from other sources.

6.4 Using a 2-D FIR Fan Filter

As mentioned above, consideration is given to the beamforming and filtering of three distinct PWs, each originating from a different direction and exhibiting varying magnitudes and frequencies. It is assumed that these waves cross the array elements at time equal to zero. We generate a 2-D signal consisting of multiple chirps having a specified frequency range, direction, onset delay, and duration. Using the sampling frequency $f_s = 3000Hz$ and zero delay, the resulting 2-D signal is $N \times N$ with duration equals $N \times T_s$, where $N = 512$ in this example. The parameters characterizing each PW are summarized in Table 6.1, providing a comprehensive overview of their respective attributes. Figure 6.3 shows these three PWs propagating in a 2-D space and the 2-D Fourier transform of these waves is shown in Figure 6.4.

Table 6.1: Three different PWs.

	θ	ϕ	**Freq.**	**Mag.**
1^{st} PW (SOI)	55	29.84	[200 1200]	10
2^{nd} PW (Int.)	10	44.65	[500 1250]	40
3^{rd} PW (Int.)	85	4.98	[350 1000]	40

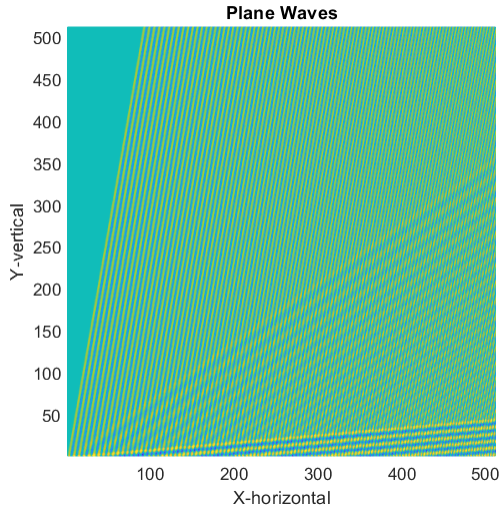

Figure 6.3: Three PWs propagating in space.

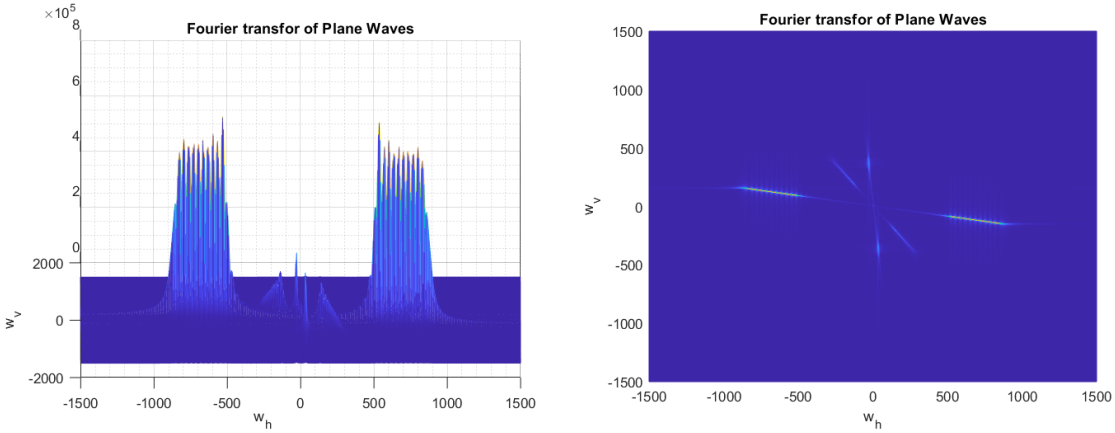

(a) Axonometric view

(b) Top view

Figure 6.4: Fourier transform of three PWs in space.

The first PW in Table 6.1 considered as the SOI, which is received by the sensors placed on the x-axis, is shown in Figure 6.5. The 2-D Fourier transform of the SOI is visually depicted in Figure 6.6. Designating the first PW as the SOI and the remaining waves as the interference, Figure 6.7 shows the 2-D Fourier transform of the noisy SOI and the interference received by the same sensors. Figure 6.8 shows the SOI, interference, and the noise received by the sensors deployed on the x-axis. In the next section, we apply the 2-D FIR fan filter to extract the SOI, eliminate the interference, and reduce the effect of the noise on the desired signal.

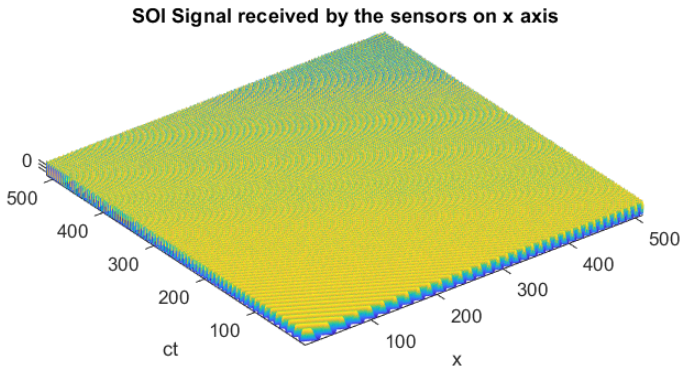

Figure 6.5: The SOI signal received by the sensors placed on x-axis.

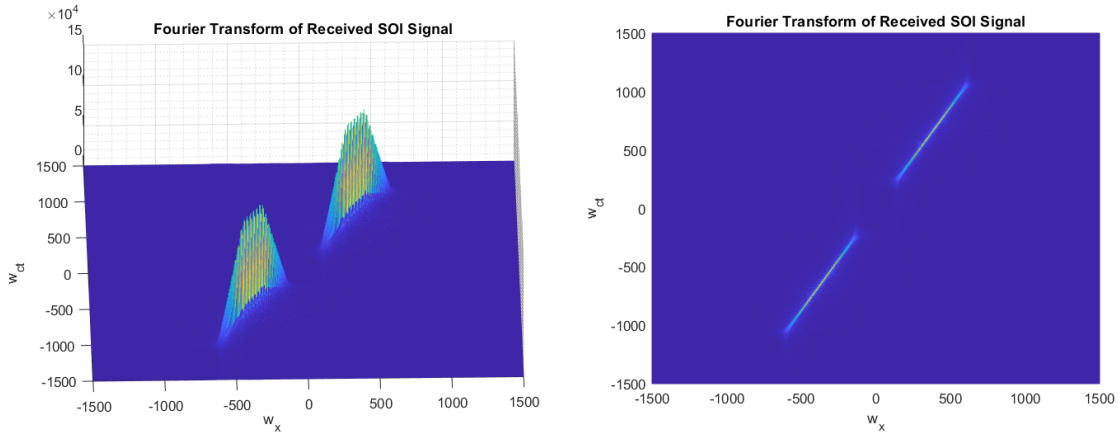

(a) Axonometric view (b) Top view

Figure 6.6: 2-D Fourier transform of the SOI.

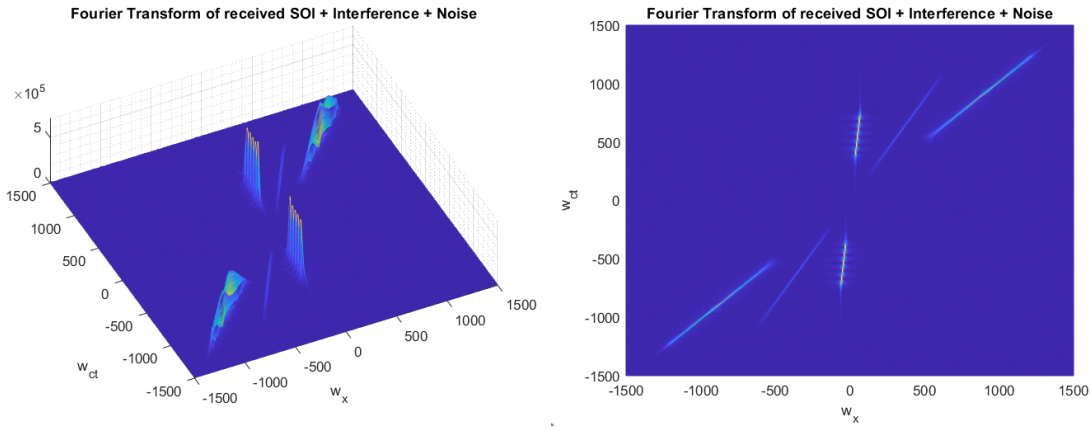

(a) Axonometric view (b) Top view

Figure 6.7: 2-D Fourier transform of the noisy SOI and interference.

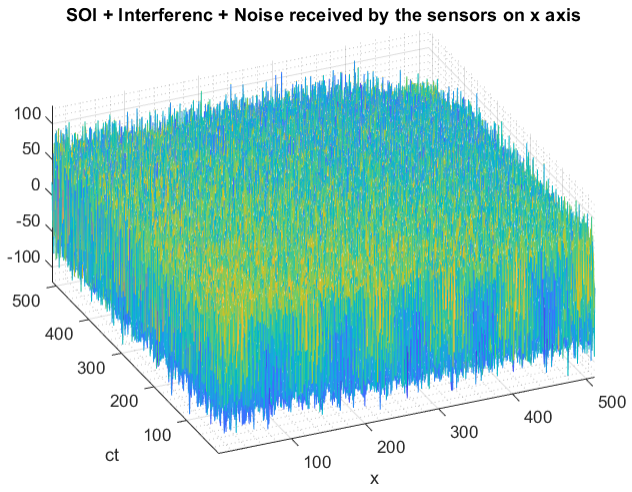

Figure 6.8: SOI plus interference and noise received by the sensors on x-axis.

6.4.1 Applying the 2-D FIR Fan Filter

In this subsection, a 2-D FIR fan filter of order M=29 is designed to be applied to the set of PWs shown in Figure 6.8. The 2-D FIR filter is configured with unity gain within the defined passband area and zero gain outside this region. To perform beamforming and filtering 2-D PWs, the objective is to design a 2-D FIR fan filter that selectively passes the SOI while attenuating the other signals. The passband area of the filter must enclose the whole ROS of the desired PW received from the desired

DOA and reject interference signals with different DOAs. Employing Equations 6.5 and 6.6, the passband of the desired 2-D FIR fan filter for isolating the signal of interest can be defined by the following four parameters: ϕ, ε, β_1, and β_2. The parameter ϕ serves as a key parameter, i.e., $\phi = \tan^{-1}(\cos\theta)$, and is derived from the DOA of the SOI, ε controls the selectivity of the filter around the DOA, while β_1 and β_2 dictate the upper and lower bounds along the frequency axis. We have $\theta = 55°$ and we used $\varepsilon = 4$, $\beta_1 = 0.8$, $\beta_2 = 0.1$ for the passband of the 2-D FIR fan filter. The axonometric and top views of the magnitude response of this filter are shown in Figure 6.9.

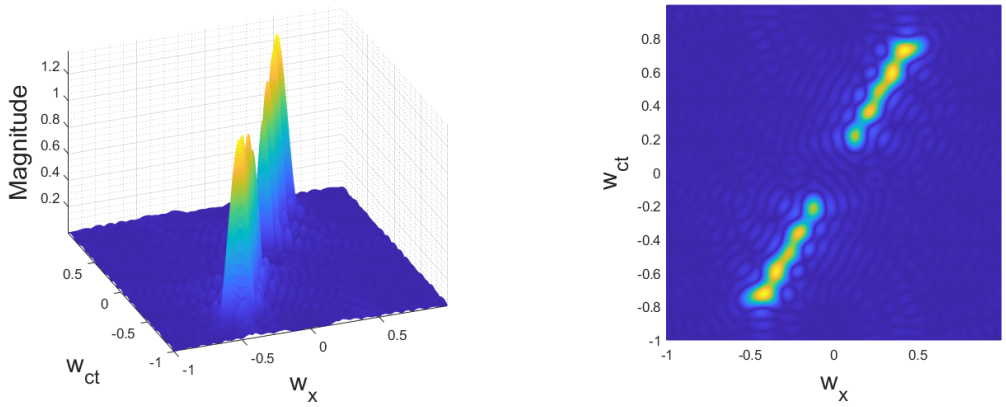

(a) Axonometric view (b) Top view

Figure 6.9: Magnitude response of 2-D FIR fan filter.

To verify the reliability of the filter's performance, testing its design specifications is vitally important. The validation process ensures that the SOI is indeed placed within the designated passband region of the filter. By evaluating the filter to its specified design parameters, including the directional parameters ϕ, ε, and the upper and lower bounds along the frequency axis β_1, and β_2, the testing phase provides essential confirmation that the filter operates as intended. This careful verification process is useful for guaranteeing the filter's accuracy and effectiveness in isolating the desired SOI within the complex frequency spectrum. Figure 6.10 shows the results of this test for a 2-D FIR filter which confirms that the SOI is situated within the passband region of the filter.

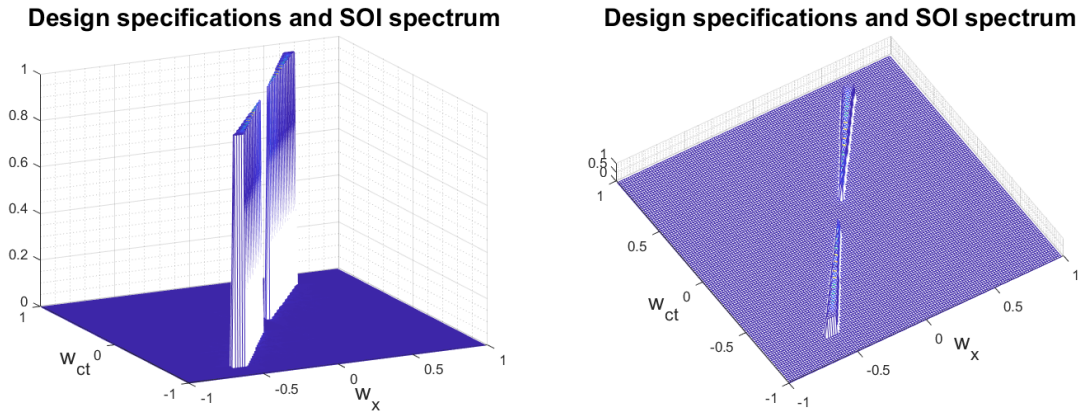

(a) Axonometric view (b) Top view

Figure 6.10: Design specifications of the fan filter and SOI spectrum.

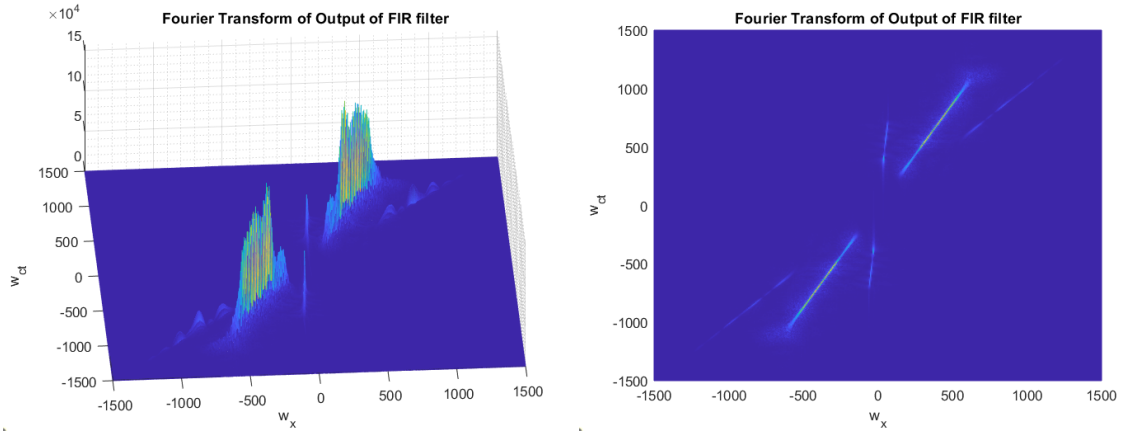

(a) Axonometric view (b) Top view

Figure 6.11: Output of the 2-D FIR fan filter.

By comparing Figure 6.11 with Figure 6.7 in the process of using the 2-D FIR fan filter, we can see that the second and third PWs undergo strong attenuation, demonstrating the efficacy of the 2-D fan filter in extracting the desired SOI signal. This observation holds significant implications, showing the effectiveness of the filter in extracting the desired PW while attenuating undesired signals. The suppression of the second and third PWs emphasize the precision and selectivity achieved by the 2-D FIR fan filter in this example, confirming its capability to discriminate between different directional PWs. The performance of this filter is evaluated by examining the Signal-to-Noise-plus-Interference Ratio (SNIR) of the signals before applying the

filter and the Signal to Error ratio after using the filter. The error is defined as the difference between the filter output and the original SOI signal in dB. The power of the SOI in this example is 16.9897 dB, and for the interference and noise are 32.0275 dB and 20.0075 dB, respectively. Table 6.2 provids more information about the power of these signals and the SNIR of the SOI before filtering and the Signal to Error Ratio after using the 2-D FIR fan filter.

Table 6.2: Results using the 2-D FIR filter

Mag. of PWs	SOI Pwr (dB)	Inter. Pwr (dB)	Noise Pwr (dB)	SNIR before filtering (dB)	Signal to Error Ratio (dB)
10 40 40	16.99	32.04	20.00	-15.29	9.08

Figure 6.12 shows the extracted SOI using the 2-D FIR fan filter. For illustration, Figure 6.13 shows the original SOI (black), SOI plus interference and noise (yellow), and the output signal of the FIR filter (red) observed at the sensor that has the maximum SNIR.

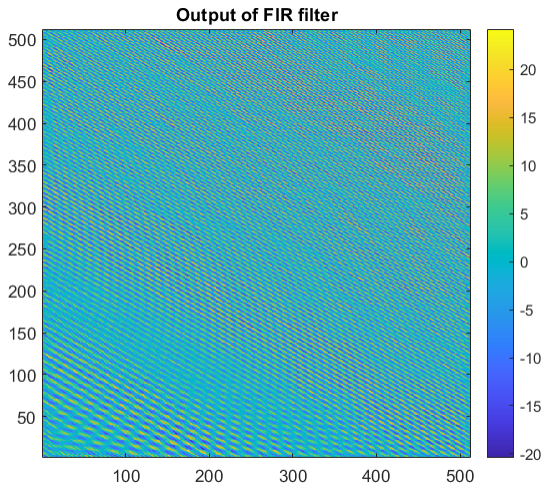

Figure 6.12: Output of the 2-D FIR fan filter.

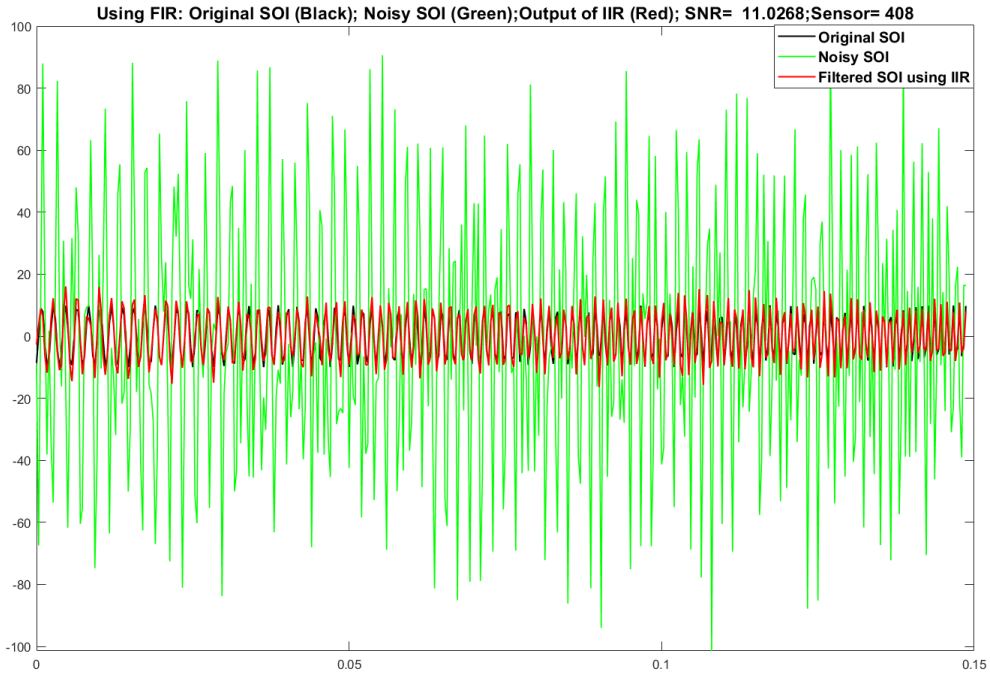

Figure 6.13: Original SOI (black), SOI plus interference and noise (green), and output of the FIR filter (red).

We can see that the efficacy of the designed 2-D FIR fan filter is particularly highlighted in its ability to enhance the SOI signal, which had been obscured by strong interference and AWGN signals. By mitigating the influence of interfering PWs, the filter succeeds in extracting the SOI from the received signals, showing its effectiveness in signal enhancement and noise reduction.

6.4.2 Applying the Reduced Order 2-D IIR Fan Filter

In this subsection, we are using the 2-D FIR filter presented in the previous section in generating the reduced 2-D IIR fan filter of order M=15. This filter is designed by using the proposed balanced realization model reduction method presented in Chapter 4 and will be applied to the same set of PWs shown in Figure 6.8. The magnitude response of this 2-D IIR fan filter is shown in Figure 6.14. Similar to the FIR case, when we compare Figure 6.7 with Figure 6.15, the results obtained by using the reduced 2-D IIR filter of order M=15 indicates that the second and third PWs exhibit much stronger attenuation than the SOI, demonstrating the efficacy of the

reduced 2-D IIR fan filter in extracting the desired SOI signal.

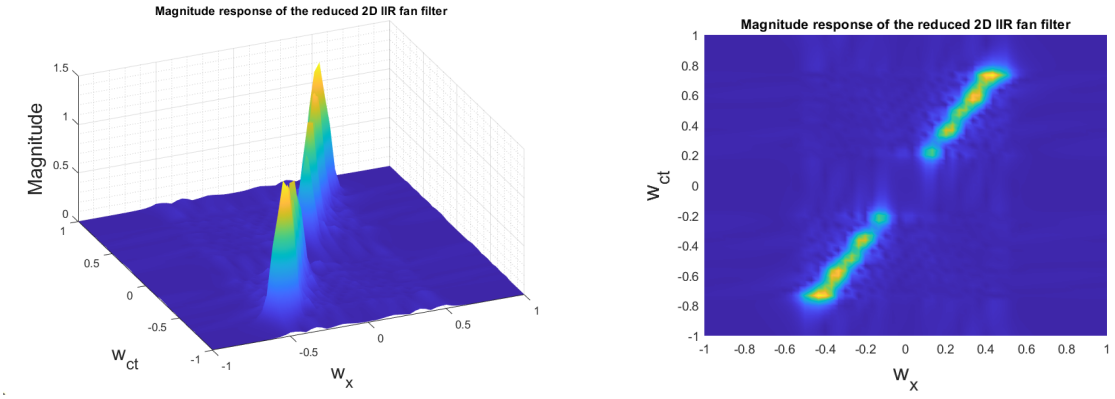

(a) Axonometric view (b) Top view

Figure 6.14: Magnitude response of the 2-D IIR fan filter.

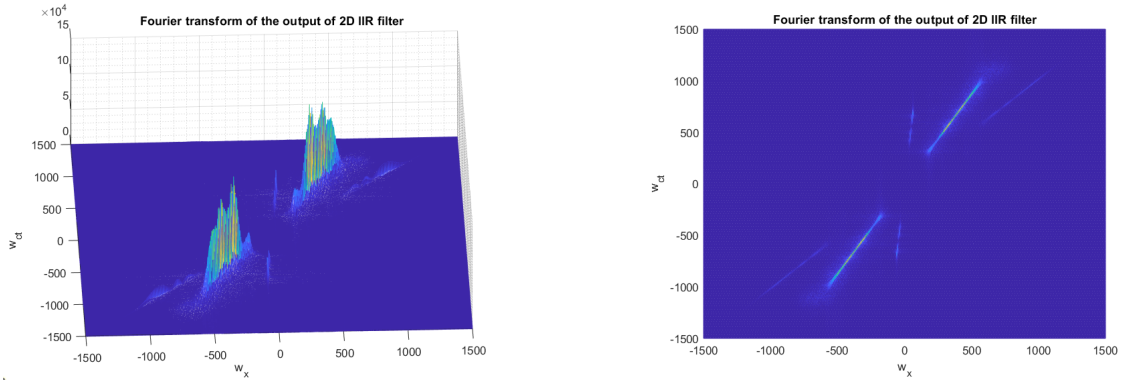

(a) Axonometric view (b) Top view

Figure 6.15: Output of the 2-D IIR fan filter.

This observation, which demonstrates how well the filter isolates the desired signal while attenuating unwanted signals, has significant implications. The suppression of the second and third PWs highlights the 2-D IIR fan filter's selectivity and precision in this case, demonstrating its ability to distinguish between PWs with different directions. Figure 6.16 shows the extracted SOI using the reduced order 2-D IIR fan filter. For illustration, Figure 6.17 shows the original SOI (black), SOI plus interference and noise (yellow), and the output signal of the IIR filter (red) observed at the sensor that has the maximum SNIR. As in the FIR case, in this example also

the power of the SOI is 16.99 db, the power of interference and noise are 32.04 db and 20.00 db, respectively.

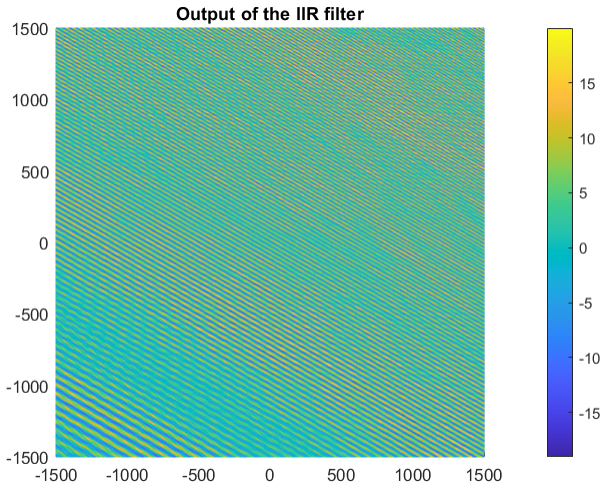

Figure 6.16: Output of the 2-D IIR fan filter.

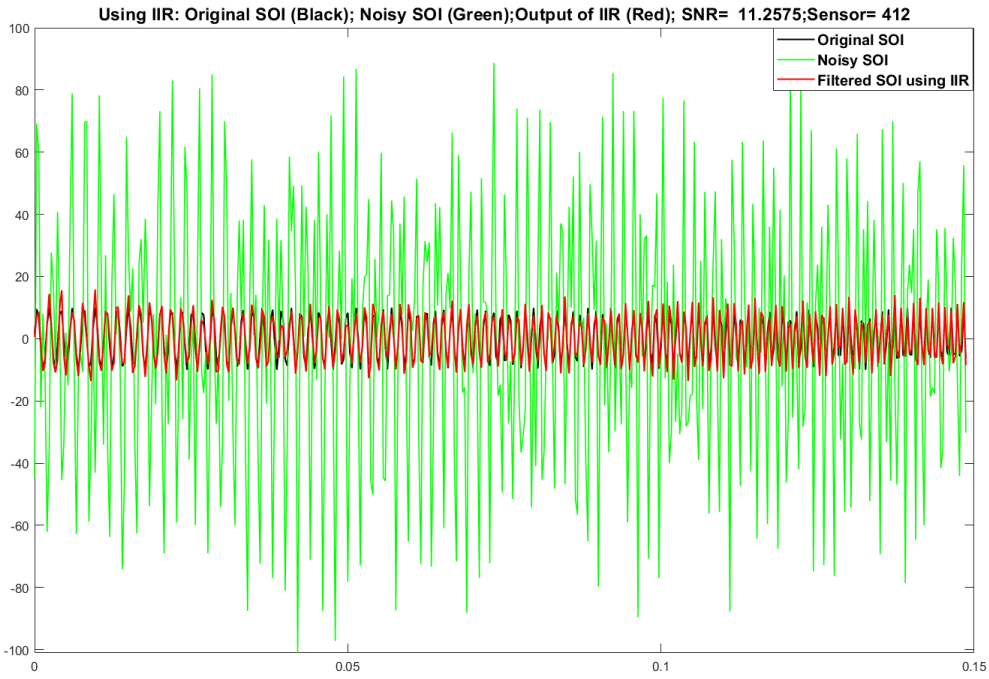

Figure 6.17: Original SOI (black), SOI plus interference and noise (green), and output of the IIR filter (red).

Similar to the 2-D FIR case, the performance of the 2-D IIR filter is evaluated by examining the Signal-to-Noise-plus-Interference Ratio (SNIR) and the Signal SOI to Error Ratio after applying the filter. Table 6.3 provides comparison results for using 2-D FIR and IIR filters.

Table 6.3: Results using 2-D FIR and IIR filters

	Mag. of PWs	SOI Pwr (dB)	Inter. Pwr (dB)	Noise Pwr (dB)	SNIR before filtering (dB)	Signal to Error Ratio (dB)
FIR	10 40 40	16.99	32.04	20.00	-15.29	9.08
IIR	10 40 40	16.99	32.04	20.00	-15.29	8.98

Concerning the number of arithmetic operations, which are controlled by the number of coefficients presented in the transfer function of both 2-D FIR and IIR filters, it is evident that the implementation cost increases rapidly with the increase in the orders of the filter. For a general $N_1 \times N_2$ 2-D FIR filter, the total number of coefficients C is computed as $(N_1+1)(N_2+1)$, signifying a rapid rise in implementation cost as either N_1 or N_2 increases. To illustrate, in the case of a 2-D FIR filter with an order of (29,29), the total number of coefficients C is 900. In contrast, for a separable denominator 2-D IIR filter with a reduced order of (15,15), the number of coefficients count $(N_1 + 1)(N_2 + 1)$ for the numerator comprises 256 and $(N_1 + N_2 + 2)$=32 for the denominator, summing up to C=288.

6.5 Discussion and Computational Analyses

6.5.1 Arithmetic Operations and Coefficient Count in 2-D FIR and IIR Filters

When discussing the computational complexity of 2-D FIR and IIR filters, a primary consideration is the number of arithmetic operations required for implementation. This complexity is directly influenced by the number of non-zero coefficients present in the filter's transfer function.

- For 2-D FIR filters, the total number of coefficients C for a general filter of size (N_1, N_2) is calculated as:

$$C = (N_1 + 1) \times (N_2 + 1)$$

This formula shows an exponential growth in the number of coefficients as the filter dimensions N_1 and N_2 increase. In the above example, a 2-D FIR filter of order (29,29) results in:

$$C = (29 + 1) \times (29 + 1) = 900 \text{ coefficients.}$$

This rapid increase in coefficients implies a significant rise in the implementation cost, making high-order 2-D FIR filters computationally expensive, particularly in real-time applications.

- In contrast, a 2-D IIR filter, especially when designed with a separable denominator, often requires fewer coefficients due to its recursive nature. For instance, the computation complexity of the 2-D IIR filter with an order of (15,15) presented in the above example will have:

$$C = (N_1 + 1) \times (N_2 + 1) + N_1 + N_2 + 2 = 288 \text{ coefficients.}$$

Comparing this result with the 900 coefficients of the 2-D FIR filter, it is evident that the 2-D IIR filter requires only 32% of the total number of coefficients used by the FIR filter without any deterioration in the performance. This significant reduction highlights the computational efficiency of 2-D IIR filters, particularly for applications requiring high performance and fast time response.

6.5.2 Beamforming and Filtering with 2-D FIR and IIR Filters

The chapter proceeds to discuss an example involving the use of both 2-D FIR and IIR filters for beamforming and filtering in 2-D plane waves (PWs):

- In both cases (FIR and IIR), the filters were able to:
  - Extract the signal of interest (SOI) by attenuating the interference coming from other directions.

  - Reduce the effect of AWGN, thereby maintaining the overall signal quality.

- However, the reduced-order 2-D IIR filter demonstrated a key advantage:
  - It required fewer coefficients compared to its FIR counterpart, directly reducing the computational complexity.
  - The IIR filter presented in this example achieved this result with only 32% of the coefficients needed by the FIR filter, making it a more efficient choice for practical applications.

6.5.3 Interference Cancellation and Filter Order

A key observation is the relationship between the filter order and its performance in interference cancellation:

- When the angle of arrival and frequency of interference are near that of the SOI, increasing the number of filter coefficients can significantly enhance the filter's ability to distinguish between the desired signal and the interference.
- However, this improvement in filtering performance comes at the cost of higher computational complexity, as each increase in filter order requires additional arithmetic operations.

This trade-off demonstrates a positive correlation between the computational cost and the interference cancellation performance. In practical applications, we must balance the need for effective interference cancellation with the constraints of computational resources.

6.5.4 Model Reduction and Practical Advantages of IIR Filters

The subsection concludes by highlighting the advantages of the proposed model reduction method for 2-D IIR filters:

- The method effectively reduces the filter order without compromising performance, maintaining or even improving the filtering capabilities of the reduced-order IIR filter.

- This positions reduced-order IIR filters as a favorable alternative to FIR filters, especially in applications where computational efficiency is paramount.
- While FIR filters offer simplicity and stability (since they are inherently stable), their high coefficient count and computational complexity make them less suitable for high-dimensional applications.
- IIR filters, which require extra design effort to ensure stability, offer significant reductions in implementation cost due to their lower coefficient count. The proposed model reduction method can mitigate stability concerns while preserving the performance of IIR filters.

6.6 Conclusion

Beamforming and a plane wave filtering technique using 2-D FIR and reduced-order IIR digital filters for 2-D signals received by a uniform linear array of sensors placed on the x-axis was presented. In both cases (FIR and IIR), we can extract the SOI, eliminate the interference, and reduce the effect of the noise by using 2-D FIR and IIR digital fan filters. The implementation of the reduced order 2-D IIR filter designed by using model order reduction method requires fewer coefficients when compared to its FIR counterpart, thereby reducing the computational complexity associated with the filter. Consequently, the adoption of the proposed model reduction method for designing 2-D IIR filters presents a viable strategy for reducing the computational load inherent in 2-D signal processing tasks, facilitating greater efficiency in practical applications. The efficacy of the reduced-order 2-D IIR fan filter with a low number of coefficients is of particular interest due to its capability to extract the SOI, which is often surrounded by strong interference and AWGN signals. The filter effectively eliminates the impact of interfering PWs and reduces the noise, thereby clarifying the presence of the SOI component within the received signals. This confirms its effectiveness in extracting the SOI signal while simultaneously mitigating and attenuating unwanted signals, illustrating the proficiency of the reduced-order 2-D IIR filter in signal extraction and noise reduction tasks. This claim is confirmed by the filter's ability to selectively suppress unwanted signal components, allowing the SOI to become visible in challenging environmental conditions characterized by substantial interference and noise. Furthermore, the reduced-order 2-D IIR filter not only

reduces the computational cost but also minimizes the memory and processing resources required, thereby enhancing overall efficiency in 2-D signal processing tasks. Also, it is apparent that as the interference becomes closely spaced over the SOI, additional number of filter coefficients will significantly improve the filtering process. Thus, while higher-order filters can indeed enhance cancellation performance, this enhancement comes at the expense of increased computational complexity. Consequently, there exists a clear positive correlation between computational cost and the level of interference cancellation achieved which positions the reduced-order 2-D IIR filters as a favorable alternative to 2-D FIR filters in such applications.

In summary, the efficient design and implementation of reduced-order 2-D IIR filters provide a convincing method for optimizing 2-D signal processing tasks, especially in scenarios where computational resources are limited, and high performance is required. This makes them a preferred choice in many advanced digital signal processing applications, including beamforming and plane waves filtering.

Chapter 7

Conclusion and Future Work

7.1 Conclusion

This thesis presents innovative methods for designing nearly linear-phase digital filters, focusing on 1-D and 2-D recursive digital filters through balanced realization model reduction and optimization techniques. After presenting the required preliminaries and as we delved into the design of IIR filters. Chapter 3 explored the use of a constrained optimization approach for improving the performance of the obtained 1-D IIR filter. We presented the fundamentals of 1-D IIR filter design and highlighted the effectiveness of a constrained optimization technique for improving the performance of the designed filter, building the groundwork for our upcoming chapters in order to facilitate a smooth transition into the multidimensional world of 2-D IIR filters.

In Chapter 4, the design process initiated with the creation of a 2-D linear-phase FIR filter, which is then represented in state-space form as a 2-D system. By employing the structural controllability and observability gramians, which inherently satisfy a set of 2-D Lyapunov inequalities, a balanced realization method was used to obtain a reduced-order separable denominator 2-D IIR filters. These gramians were obtained by solving 2-D Lyapunov inequalities using a constrained optimization approach. The structural gramians ensure that the obtained filter complies with 2-D Lyapunov equations, thus guaranteeing its stability. The proposed method's effectiveness was demonstrated through numerical examples, which revealed that it is well-suited for designing reduced-order 2-D IIR filters with separable denominators and with nearly linear-phase in the passband. These filters exhibit performance comparable to, or better than, filters obtained using existing design techniques while

requiring less computational complexity than the original 2-D FIR filter.

Further, in Chapter 5 a nonlinear optimization design framework was proposed, addressing the design of 2-D IIR filters as a nonlinear constrained optimization problem where the group-delay deviation is minimized under soft and hard constraints. Soft constraints are not critical and do not result in filter rejection if unmet, while hard constraints must be satisfied for the filter to be acceptable. The designed filters are evaluated based on passband amplitude, group delay quality, and a newly introduced quality factor for stopband magnitude response. The obtained results show that these quality factors are all necessary to fully evaluate the optimality of the obtained filter. Comparative analyses with other 2-D IIR filters show that the proposed method enhances phase linearity in the passband and improves magnitude response with negligible degradation.

In Chapter 6, we focused specifically on the applications of 2-D FIR and IIR digital filters as a beamformer, benefiting from the knowledge of DOAs to isolate desired broadband PWs. We aimed to extract a broadband SOI signal from the interference and AWGN as the spectral nearness of interference to the SOI increased. We noted that increasing the number of filter coefficients was crucial in achieving significant interference cancellation and noise reduction. Therefore, it was of interest to evaluate the performance of 2-D FIR and IIR filters as a trade-off with the number of filter coefficients. However, the computational expense associated with increasing the filter order posed a substantial challenge. Thus, a careful balance arose between computational complexity and interference mitigation efficacy. For FIR filters, it is well known that they offer several advantages, such as guaranteed stability and phase linearity, but also that they may require a high filter order to fulfill the given specifications. Despite higher-order filters offering improved interference cancellation, they do so at increasingly higher computational cost, highlighting the clear trade-off between computational complexity and filtering performance. We have examined the efficacy of employing a 2-D FIR and IIR fan filters as beamformes in environments where the SOI signal was surrounded by closely-spaced interference and AWGN. Further investigation and comparison clarified the relationship between filter order, computational cost, and filtering performance.

The findings showed a reduction in the number of required coefficients of 2-D IIR compared to their FIR counterparts, thereby lowering computational complexity and enhancing efficiency in 2-D signal processing tasks. Overall, the results demonstrated that reduced-order 2-D IIR filters can maintain or even improve performance, making

them a favorable alternative to 2-D FIR filters in 2-D signal processing.

7.2 Future Work

The exploration of 2-D FIR and IIR digital filter design and applications in array signal processing, particularly in beamforming and plane wave filtering, opens several avenues for future research and technological advancements. This section outlines potential research directions and developments that could enhance the effectiveness of the application of these filters in complex signal processing environments.

- Multi-Objective Optimization: Using the multi-objective optimization method to improve the nonlinear optimization technique proposed in Chapter 5 by directly optimizing the quality factors instead of only the group delay deviation. The idea is to involve more than one objective function that could be minimized or maximized, and the answer will be a set of filters that include the best trade-off between competing objectives. This could also involve the exploration of alternative optimization techniques by investigating other optimization algorithms such as genetic algorithms to design 2-D IIR digital filters which could potentially improve the quality of the 2-D filter design and its broader applicability.

- Extension to M-dimensional Filters: It would be interesting to extend the current method to handle general multidimensional filters. Extending the concept of 2-D filtering to multidimensional filtering can open new research frontiers. This involves developing filters capable of processing signals in 3-D or higher dimensions, which is particularly relevant for applications in medical imaging and geophysics. This could broaden the applicability and effectiveness of the proposed design framework in more complex scenarios.

- Adaptive Filter Design: Develop adaptive methods that dynamically adjust filter order and parameters based on real-time signal characteristics. This could enhance performance in varying operational environments, especially in adaptive noise filtering and real-time image processing. By addressing these areas, future research can enhance the versatility, efficiency, and applicability of the proposed filter design methods, ensuring its relevance and utility in a wider range of 2-D signal processing applications.

- Extension to Non-Separable Denominator Filters and Stability Analysis: It would be interesting to extend the proposed design methods to handle non-separable filters. Additional research might be considered on the stability and performance analysis of 2-D IIR filters. This includes practical BIBO stability and possibly developing more comprehensive stability criteria, exploring the effects of non-linearities, and enhancing the understanding of filter behavior in various signal environments.

To conclude, the potential for future research and developments in the field of multi-dimensional FIR and IIR digital filters is wide and multifaceted. By addressing the outlined areas, researchers can significantly advance the state of the art, creating more robust, efficient, and flexible filtering solutions for a wide range of applications. The continuous evolution of signal processing technologies and methodologies promises exciting opportunities for innovation and discovery in this dynamic field.

List of Publications

- A. Omar, P. Agathoklis, and D. Shpak, "Nearly linear-phase 2-D recursive digital filters design using balanced realization model reduction," *Signals*, vol. 4, no. 4, pp. 800–815, 2023.
- A. Omar, D. Shpak, P. Agathoklis, and B. Moa, "A nonlinear optimization design algorithm for nearly linear-phase 2-D IIR digital filters," *Signals*, vol. 4, no. 3, pp. 575–590, 2023.
- A. Omar, D. Shpak, and P. Agathoklis, "Improved design method for nearly linear-phase IIR filters using constrained optimization," *Journal of Circuits, Systems and Computers*, vol. 30, no. 11, p. 2150207, 2021.
- A. Omar, D. Shpak, "Beamforming and Plane Wave Filtering using 2-D FIR Digital Fan Filters", will be submitted soon.

Appendix A

In this Appendix, two examples for obtaining the structured controllability and structured observability Gramians using LMI-based algorithm are presented. They include 2-D system matrices in the separable and non-separable characteristic polynomial.
Example 1: Consider a 2-D discrete system described by Roesser's model, $(m, n) = (2, 2)$, as follows

$$A = \begin{bmatrix} -0.5000 & 0.7500 & 0.3895 & 0.0389 \\ 0 & 0 & 0 & 0 \\ 0.1423 & 0 & -0.4000 & 0.0200 \\ -0.0342 & 0 & -0.6000 & 0.0300 \end{bmatrix}$$

where $x^h \in R^2$ and $x^v \in R^2$.

$$b = \begin{bmatrix} 1 & 0 & 1 & 0 \end{bmatrix}^T$$

$$c = \begin{bmatrix} 1 & 0 & 0 & 0 \end{bmatrix}$$

Applying the proposed algorithm to solve the Lyapunov inequalities, the controllability and observability gramians are found to be positive definite block diagonal matrices as given below.

$$P^s = \begin{bmatrix} 2.6744536 & 0.0000005 & 0 & 0 \\ 0.0000005 & 0.0000018 & 0 & 0 \\ 0 & 0 & 1.7237207 & 0.1361198 \\ 0 & 0 & 0.1361198 & 0.7926782 \end{bmatrix}$$

$$Q^s = \begin{bmatrix} 1.6523883 & -0.8820146 & 0 & 0 \\ -0.8820146 & 1.2662409 & 0 & 0 \\ 0 & 0 & 1.2060296 & 0.0671541 \\ 0 & 0 & 0.0671541 & 0.0173983 \end{bmatrix}$$

Example 2: We consider the following 2-D model $\Sigma = (A_{11}, A_{12}, A_{21}, A_{22}, b_1, b_2, c_1, c_2)$, also presented as illustrative example in Section 3.4 in [38]. The corresponding system matrices are given below

$$A_{11} = \begin{bmatrix} 0 & 1 & 0 & 0 \\ 0 & 0 & 1 & 0 \\ 0 & 0 & 0 & 1 \\ -0.282145 & 0.551205 & -0.875599 & 1.361780 \end{bmatrix},$$

$A_{12} = 0_{4\times 4}$,

$$A_{21} = \begin{bmatrix} -0.020056 & 0.114892 & -0.167819 & 0.227100 \\ 0.011559 & -0.054709 & 0.120890 & -0.150348 \\ 0.026037 & 0.035530 & -0.034800 & 0.047409 \\ 0.032347 & -0.055488 & 0.045669 & 0.077340 \end{bmatrix},$$

$$A_{22} = \begin{bmatrix} 0 & 0 & 0 & -0.090322 \\ 1 & 0 & 0 & 0.199219 \\ 0 & 1 & 0 & -0.390625 \\ 0 & 0 & 1 & 0.750000 \end{bmatrix},$$

$$b_1 = \begin{bmatrix} 0 & 0 & 0 & 1 \end{bmatrix}^T,$$

$$b_2 = \begin{bmatrix} 0.368103 & -0.315109 & 0.227313 & -0.073000 \end{bmatrix}^T,$$

$$c_1 = \begin{bmatrix} 0.261041 & -0.127614 & -0.033891 & 0.424881 \end{bmatrix},$$

$$c_2 = \begin{bmatrix} 0 & 0 & 0 & 1 \end{bmatrix},$$

$$d = 0.6520.$$

Here, $x^h \in R^4$ and $x^v \in R^4$. Note that, since A_{12} is a zero matrix, this is a separable-denominator system where the denominator of the corresponding transfer function can be factored as the product of a polynomial in z_1 by a polynomial in z_2. The controllability matrix P^s and the observability matrix Q^s are found to be symmetric positive-definite and block-diagonal matrices where $P^s = diag(p_1, p_2)$ and $Q^s = diag(q_1, q_2)$ and these sub-matrices p_i and q_i for i=1,2 are given as below.

$$p_1 = \begin{bmatrix} 8.1089 & 6.7562 & 4.6871 & 3.0064 \\ 6.7562 & 7.5461 & 6.2880 & 4.3242 \\ 4.6871 & 6.2880 & 7.0435 & 5.8058 \\ 3.0064 & 4.3242 & 5.8058 & 6.4723 \end{bmatrix},$$

$$p_2 = \begin{bmatrix} 2.5173 & -1.8049 & 1.0641 & 0.5113 \\ -1.8049 & 4.2626 & -2.7316 & 1.7339 \\ 1.0641 & -2.7316 & 4.2820 & -1.9780 \\ 0.5113 & 1.7339 & -1.9780 & 5.2563 \end{bmatrix},$$

$$q_1 = \begin{bmatrix} 0.6672 & -0.7158 & 0.7194 & -0.7046 \\ -0.7158 & 1.5485 & -1.5435 & 1.7515 \\ 0.7194 & -1.5435 & 2.3619 & -2.7027 \\ -0.7046 & 1.7515 & -2.7027 & 4.8899 \end{bmatrix},$$

$$q_2 = \begin{bmatrix} 3.0759 & 1.8324 & 0.6877 & 0.3077 \\ 1.8324 & 2.7993 & 1.6562 & 0.5947 \\ 0.6877 & 1.6562 & 2.5770 & 1.5290 \\ 0.3077 & 0.5947 & 1.5290 & 2.3714 \end{bmatrix},$$

For the same system presented in the above example, we consider now a non-separable denominator case where the matrix A_{12} is given by

$$A_{12} = \begin{bmatrix} -0.0050 & 0.0287 & -0.0420 & 0.0568 \\ 0.0029 & -0.0137 & 0.0302 & -0.0376 \\ 0.0065 & 0.0089 & -0.0087 & 0.0119 \\ 0.0081 & -0.0139 & 0.0114 & 0.0193 \end{bmatrix}$$

The results obtained for the block diagonal structured gramians $P^s = diag(p_1, p_2)$ and $Q^s = diag(q_1, q_2)$ are as follows:

$$p_1 = \begin{bmatrix} 8.7104 & 7.0353 & 5.0428 & 3.2759 \\ 7.0353 & 7.9591 & 6.6426 & 4.5683 \\ 5.0428 & 6.6426 & 7.3986 & 6.0962 \\ 3.2759 & 4.5683 & 6.0962 & 6.7877 \end{bmatrix},$$

$$p_2 = \begin{bmatrix} 2.4947 & -1.6721 & 0.7320 & 0.7283 \\ -1.6721 & 4.0632 & -2.3814 & 1.3424 \\ 0.7320 & -2.3814 & 4.4503 & -1.9242 \\ 0.7283 & 1.3424 & -1.9242 & 5.5830 \end{bmatrix},$$

$$q_1 = \begin{bmatrix} 0.7372 & -0.7142 & 0.7476 & -0.7911 \\ -0.7142 & 1.5399 & -1.5141 & 1.7804 \\ 0.7476 & -1.5141 & 2.4323 & -2.7913 \\ -0.7911 & 1.7804 & -2.7913 & 5.0316 \end{bmatrix},$$

$$q_2 = \begin{bmatrix} 3.4080 & 1.8370 & 0.6826 & 0.3415 \\ 1.8370 & 3.1150 & 1.6702 & 0.5627 \\ 0.6826 & 1.6702 & 2.8215 & 1.6037 \\ 0.3415 & 0.5627 & 1.6037 & 2.4459 \end{bmatrix},$$

Bibliography

[1] D. Goodman, "Some stability properties of two-dimensional linear shift-invariant digital filters," *IEEE Transactions on Circuits and Systems*, vol. 24, no. 4, pp. 201–208, 1977.

[2] R. C. Nongpiur, D. J. Shpak, and A. Antoniou, "Improved design method for nearly linear-phase IIR filters using constrained optimization," *IEEE Transactions on Signal Processing*, vol. 61, no. 4, pp. 895–906, 2013.

[3] X. Lai and Z. Lin, "Iterative reweighted minimax phase error designs of IIR digital filters with nearly linear phases," *IEEE Transactions on Signal Processing*, vol. 64, no. 9, pp. 2416–2428, 2016.

[4] C. Xiao and P. Agathoklis, "Design and implementation of approximately linear phase two-dimensional IIR filters," *IEEE Transactions on Circuits and Systems II: Analog and Digital Signal Processing*, vol. 45, no. 9, pp. 1279–1288, 1998.

[5] W.-K. Chen, *Passive, active, and digital filters*. Crc Press, 2009.

[6] A. Antoniou, *Digital Signal Processing: Signals, Systems, and Filters*. McGraw-Hill, 2005.

[7] A. V. Oppenheim and R. W. Schafer, *Discrete-time signal processing*. Pearson Education, 2014.

[8] A. Antoniou, *Digital Filters: Analysis, Design, and Signal Processing Applications*. McGraw-Hill, 2018.

[9] B. Anderson, P. Agathoklis, E. Jury, and M. Mansour, "Stability and the matrix lyapunov equation for discrete 2-dimensional systems," *IEEE Transactions on Circuits and Systems*, vol. 33, no. 3, pp. 261–267, 1986.

[10] J. Lodge and M. Fahmy, "Stability and overflow oscillations in 2-D state-space digital filters," *IEEE Transactions on Acoustics, Speech, and Signal Processing*, vol. 29, no. 6, pp. 1161–1171, 1981.

[11] W.-S. Lu and E. Lee, "Stability analysis for two-dimensional systems via a lyapunov approach," *IEEE Transactions on Circuits and Systems*, vol. 32, no. 1, pp. 61–68, 1985.

[12] D. E. Dudgeon and R. M. Mersereau, "Multidimensional digital signal processing," *Prentice-Hall Signal Processing Series, Englewood Cliffs: Prentice-Hall, 1984*, 1984.

[13] S. Yan, L. Sun, and L. Xu, "2-D zero-phase IIR notch filters design based on state-space representation of 2-D frequency transformation," in *2015 IEEE International Symposium on Circuits and Systems (ISCAS)*. IEEE, 2015, pp. 2369–2370.

[14] W. Wang, J. Doyle, C. Beck, and K. Glover, "Model reduction of lft systems," in *[1991] Proceedings of the 30th IEEE Conference on Decision and Control*. IEEE, 1991, pp. 1233–1238.

[15] K. Zhou, J. Aravena, G. Gu, and D. Xiong, "2-D model reduction by quasi-balanced truncation and singular perturbation," *IEEE Transactions on Circuits and Systems II: Analog and Digital Signal Processing*, vol. 41, no. 9, pp. 593–602, 1994.

[16] K. Premaratne, E. Jury, and M. Mansour, "An algorithm for model reduction of 2-D discrete time systems," *IEEE Transactions on Circuits and Systems*, vol. 37, no. 9, pp. 1116–1132, 1990.

[17] J. S. Lim, "Two-dimensional signal and image processing," *Englewood Cliffs, NJ, Prentice Hall, 1990, 710 p.*, 1990.

[18] T. Lin, M. Kawamata, and T. Higuchi, "Design of 2-D digital filters with an arbitrary response and no overflow oscillations based on a new stability condition," *IEEE Transactions on Circuits and Systems*, vol. 34, no. 2, pp. 113–126, 1987.

[19] V. Sreeram and P. Agathoklis, "Design of linear-phase IIR filters via impulse-response gramians," *IEEE Transactions on Signal Processing*, vol. 40, no. 2, pp. 389–394, 1992.

[20] A. Madanayake, C. Wijenayake, D. G. Dansereau, T. K. Gunaratne, L. T. Bruton, and S. B. Williams, "Multidimensional (MD) circuits and systems for emerging applications including cognitive radio, radio astronomy, robot vision and imaging," *IEEE Circuits and Systems Magazine*, vol. 13, no. 1, pp. 10–43, 2013.

[21] W.-S. Lu and A. Antoniou, *Two-dimensional digital filters*. CRC Press, 1992, vol. 80.

[22] R. T. Wijesekara, C. U. Edussooriya, L. T. Bruton, and P. Agathoklis, "A low-complexity 2-D spatially-interpolated FIR trapezoidal filter for enhancing broadband plane waves," in *2017 10th International Workshop on Multidimensional (nD) Systems (nDS)*. IEEE, 2017, pp. 1–6.

[23] J. Hua, W. Kuang, Z. Gao, L. Meng, and Z. Xu, "Image denoising using 2-D FIR filters designed with DEPSO," *Multimedia tools and applications*, vol. 69, no. 1, pp. 157–169, 2014.

[24] G. Gu and B. Shenoi, "A novel approach to the synthesis of recursive digital filters with linear phase," *IEEE Transactions on Circuits and Systems*, vol. 38, no. 6, pp. 602–612, 1991.

[25] D. Gorinevsky and S. Boyd, "Optimization-based design and implementation of multidimensional zero-phase IIR filters," *IEEE Transactions on Circuits and Systems I: Regular Papers*, vol. 53, no. 2, pp. 372–383, 2006.

[26] X. Lai, H. Meng, J. Cao, and Z. Lin, "A sequential partial optimization algorithm for minimax design of separable-denominator 2-D IIR filters," *IEEE Transactions on Signal Processing*, vol. 65, no. 4, pp. 876–887, 2017.

[27] N. E. Mastorakis, I. F. Gonos, and M. Swamy, "Design of two-dimensional recursive filters using genetic algorithms," *IEEE Transactions on Circuits and Systems I: Fundamental Theory and Applications*, vol. 50, no. 5, pp. 634–639, 2003.

[28] P. Ramamoorthy and L. Bruton, "Design of stable two-dimensional analogue and digital filters with applications in image processing," *International Journal of Circuit Theory and Applications*, vol. 7, no. 2, pp. 229–245, 1979.

[29] T. Hinamoto and S. Maekawa, "Design of two-dimensional recursive digital filters using mirror-image polynomials," *IEEE Transactions on Circuits and Systems*, vol. 33, no. 8, pp. 750–758, 1986.

[30] S. Aly and M. Fahmy, "Design of two-dimensional recursive digital filters with specified magnitude and group delay characteristics," *IEEE Transactions on Circuits and Systems*, vol. 25, no. 11, pp. 908–916, 1978.

[31] A. Chottera and G. Jullien, "A linear programming approach to recursive digital filter design with linear phase," *IEEE Transactions on Circuits and Systems*, vol. 29, no. 3, pp. 139–149, 1982.

[32] B. Dumitrescu, "Optimization of two-dimensional IIR filters with nonseparable and separable denominator," *IEEE Transactions on Signal Processing*, vol. 53, no. 5, pp. 1768–1777, 2005.

[33] T. Miyata, N. Aikawa, Y. Sugita, and T. Yoshikawa, "A design method for separable-denominator 2D IIR filters using a stability criterion based on the system matrix," in *2008 15th IEEE International Conference on Electronics, Circuits and Systems*. IEEE, 2008, pp. 826–829.

[34] F. Wysocka-Schillak, "Design of separable 2-D IIR filters with approximately linear phase in the passband using genetic algorithm," in *2008 Conference on Human System Interactions*. IEEE, 2008, pp. 66–70.

[35] S. Holford and P. Agathoklis, "The use of model reduction techniques for designing IIR filters with linear phase in the passband," *IEEE Transactions on Signal Processing*, vol. 44, no. 10, pp. 2396–2404, 1996.

[36] S. Lawson and M. Anderson, "The design of 2-D approximately linear phase filters using a direct approach," *Signal processing*, vol. 57, no. 3, pp. 205–221, 1997.

[37] A. B. H. A.-M. Lahcène Mitiche, "New procedure in designing 2D-IIR filters based on 2D-FIR filters approximation," *IEEE Transactions on Systems Signal Processing: Regular Papers*, vol. 57, no. 7, pp. 515–520, 2013.

[38] T.-Y. Guo, C. Hwang, L.-S. Shieh, and C.-H. Chen, "Reduced-order models of 2-d linear discrete separable-denominator system using bilinear routh approximations," *IEE Proceedings G (Circuits, Devices and Systems)*, vol. 139, no. 1, pp. 45–56, 1992.

[39] S. P. Boyd and L. Vandenberghe, *Convex optimization*. Cambridge university press, 2004.

[40] A. Chottera and G. Jullien, "Design of two-dimensional recursive digital filters using linear programming," *IEEE Transactions on Circuits and Systems*, vol. 29, no. 12, pp. 817–826, 1982.

[41] W.-S. Lu, "A unified approach for the design of 2-D digital filters via semidefinite programming," *IEEE Transactions on Circuits and Systems I: Fundamental Theory and Applications*, vol. 49, no. 6, pp. 814–826, 2002.

[42] W.-S. Lu, S.-C. Pei, and C.-C. Tseng, "A weighted least-squares method for the design of stable 1-D and 2-D IIR digital filters," *IEEE Transactions on Signal Processing*, vol. 46, no. 1, pp. 1–10, 1998.

[43] B. Dumitrescu and R. Niemistö, "An iterative reweighted least-squares algorithm for the design of 2D IIR filters," in *2004 12th European Signal Processing Conference*. IEEE, 2004, pp. 133–136.

[44] D. J. Shpak, "A weighted-least-squares matrix decomposition method with application to the design of two-dimensional digital filters," in *Proceedings of the 33rd Midwest Symposium on Circuits and Systems*. IEEE, 1990, pp. 1070–1073.

[45] P. Paraskevopoulos, P. Panagopoulos, G. Vaitsis, S. Varoufakis, and G. Antoniou, "Model reduction of 2-d systems via orthogonal series," *Multidimensional Systems and Signal Processing*, vol. 2, no. 1, pp. 69–83, 1991.

[46] H. Luo, W.-S. Lu, and A. Antoniou, "A weighted balanced approximation for 2-d discrete systems and its application to model reduction," *IEEE Transactions on Circuits and Systems I: Fundamental Theory and Applications*, vol. 42, no. 8, pp. 419–429, 1995.

[47] M. Diab, V. Sreeram, and W. Liu, "Model reduction of 2-d separable-denominator transfer functions via quasi-kalman decomposition," *IEE Proceedings-Circuits, Devices and Systems*, vol. 145, no. 1, pp. 13–18, 1998.

[48] E. Fornasini and G. Marchesini, "Doubly-indexed dynamical systems: State-space models and structural properties," *Mathematical systems theory*, vol. 12, no. 1, pp. 59–72, 1978.

[49] R. Roesser, "A discrete state-space model for linear image processing," *IEEE Transactions on Automatic Control*, vol. 20, no. 1, pp. 1–10, 1975.

[50] T. Hinamoto and W.-S. Lu, *Digital filter design and realization*. CRC Press, 2022.

[51] C.-T. Chen, "Linear system theory and design," Malla Reddy College of Engineering, 1999.

[52] B. Moore, "Principal component analysis in linear systems: Controllability, observability, and model reduction," *IEEE Transactions on Automatic Control*, vol. 26, no. 1, pp. 17–32, 1981.

[53] D. D. Givone and R. P. Roesser, "Multidimensional linear iterative circuits—general properties," *IEEE Transactions on Computers*, vol. 100, no. 10, pp. 1067–1073, 1972.

[54] E. Fornasini and G. Marchesini, "Algebraic realization theory of two-dimensional filters," in *Variable Structure Systems with Application to Economics and Biology: Proceedings of the Second US-Italy Seminar on Variable Structure Systems, May 1974*. Springer, 1975, pp. 64–82.

[55] E. Fornasini, "A note on output feedback stabilizability of multivariable 2D systems," *Systems & Control Letters*, vol. 10, no. 1, pp. 45–50, 1988.

[56] E. Fornasini and G. Marchesini, "State-space realization theory of two-dimensional filters," *IEEE Transactions on Automatic Control*, vol. 21, no. 4, pp. 484–492, 1976.

[57] A. Ahmed, "On the stability of two-dimensional discrete systems," *IEEE Transactions on Automatic Control*, vol. 25, no. 3, pp. 551–552, 1980.

[58] P.-A. Bliman, "Lyapunov equation for the stability of 2-D systems," *Multidimensional Systems and Signal Processing*, vol. 13, pp. 201–222, 2002.

[59] T. Ooba, "On stability analysis of 2-D systems based on 2-D lyapunov matrix inequalities," *IEEE Transactions on Circuits and Systems I: Fundamental Theory and Applications*, vol. 47, no. 8, pp. 1263–1265, 2000.

[60] T. Ooba and Y. Funahashi, "Stability analysis of two-dimensional systems by means of finitely constructed bilateral quadratic forms," *IEEE Transactions on Automatic Control*, vol. 49, no. 11, pp. 2068–2073, 2004.

[61] W.-S. Lu, "Stability robustness of two-dimensional discrete systems and its computation," *IEEE Transactions on Circuits and Systems*, vol. 36, no. 2, pp. 285–288, 1989.

[62] V. Singh, "On global asymptotic stability of 2-D discrete systems with state saturation," *Physics Letters A*, vol. 372, no. 32, pp. 5287–5289, 2008.

[63] V. Singh, "New approach to stability of 2-D discrete systems with state saturation," *Signal Processing*, vol. 92, no. 1, pp. 240–247, 2012.

[64] A. Bhaya, E. Kaszkurewicz, and Y. Su, "Stability of asynchronous two-dimensional fornasini–marchesini dynamical systems," *Linear Algebra and Its Applications*, vol. 332, pp. 257–263, 2001.

[65] D. Bouagada and P. V. Dooren, "On the stability of 2D state-space models," *Numerical Linear Algebra with Applications*, vol. 20, no. 2, pp. 198–207, 2013.

[66] P. Cook, "Stability of two-dimensional feedback systems," *International Journal of Control*, vol. 73, no. 4, pp. 343–348, 2000.

[67] H. Kar and V. Singh, "Robust stability of 2-D discrete systems described by the fornasini-marchesini second model employing quantization/overflow nonlinearities," *IEEE Transactions on Circuits and Systems II: Express Briefs*, vol. 51, no. 11, pp. 598–602, 2004.

[68] H. Kar and V. Singh, "Stability of 2-D systems described by the fornasini-marchesini first model," *IEEE Transactions on Signal Processing*, vol. 51, no. 6, pp. 1675–1676, 2003.

[69] H. Kar and V. Singh, "Stability analysis of 2-D digital filters described by the fornasini-marchesini second model using overflow nonlinearities," *IEEE*

Transactions on Circuits and Systems I: Fundamental Theory and Applications, vol. 48, no. 5, pp. 612–617, 2001.

[70] N. E. Mastorakis, "New necessary stability conditions for 2-D systems," *IEEE Transactions on Circuits and Systems I: Fundamental Theory and Applications*, vol. 47, no. 7, pp. 1103–1105, 2000.

[71] W.-S. Lu, "On robust stability of 2-D discrete systems," *IEEE Transactions on Automatic Control*, vol. 40, no. 3, pp. 502–506, 1995.

[72] H. Kar and V. Singh, "An improved criterion for the asymptotic stability of 2-D digital filters described by the fornasini-marchesini second model using saturation arithmetic," *IEEE Transactions on Circuits and Systems I: Fundamental Theory and Applications*, vol. 46, no. 11, pp. 1412–1413, 1999.

[73] G.-D. Hu and M. Liu, "Simple criteria for stability of two-dimensional linear systems," *IEEE Transactions on Signal Processing*, vol. 53, no. 12, pp. 4720–4723, 2005.

[74] T. Hinamoto, "Stability of 2-D discrete systems described by the fornasini-marchesini second model," *IEEE Transactions on Circuits and Systems I: Fundamental Theory and Applications*, vol. 44, no. 3, pp. 254–257, 1997.

[75] H. Fan and C. Wen, "A sufficient condition on the exponential stability of two-dimensional (2-D) shift-variant systems," *IEEE Transactions on Automatic Control*, vol. 47, no. 4, pp. 647–655, 2002.

[76] T. Ooba, "Asymptotic stability of two-dimensional discrete systems with saturation nonlinearities," *IEEE Transactions on Circuits and Systems I: Regular Papers*, vol. 60, no. 1, pp. 178–188, 2012.

[77] H. Trinh and T. Fernando, "Some new stability conditions for two-dimensional difference systems," *International Journal of Systems Science*, vol. 31, no. 2, pp. 203–211, 2000.

[78] Z. Wang and X. Liu, "Robust stability of two-dimensional uncertain discrete systems," *IEEE Signal processing letters*, vol. 10, no. 5, pp. 133–136, 2003.

[79] T. Huang, "Stability of two-dimensional recursive filters," *IEEE Transactions on Audio and Electroacoustics*, vol. 20, no. 2, pp. 158–163, 1972.

[80] J. Justice and J. Shanks, "Stability criterion for N-dimensional digital filters," *IEEE Transactions on Automatic Control*, vol. 18, no. 3, pp. 284–286, 1973.

[81] N. Bose, "A criterion to determine if two multivariable polynomials are relatively prime," *Proceedings of the IEEE*, vol. 60, no. 1, pp. 134–135, 1972.

[82] N. Bose, "An algorithm for GCF extraction from two multivariable polynomials," *Proceedings of the IEEE*, vol. 64, no. 1, pp. 185–186, 1976.

[83] W.-S. Lu, H. Luo, and A. Antoniou, "Recent results on model reduction methods for 2-D discrete systems," in *1996 IEEE International Symposium on Circuits and Systems. Circuits and Systems Connecting the World. ISCAS 96*, vol. 2. IEEE, 1996, pp. 348–351.

[84] K. Premaratne, E. Jury, and M. Mansour, "An algorithm for model reduction of 2-D discrete time systems," *IEEE Transactions on Circuits and Systems*, vol. 37, no. 9, pp. 1116–1132, 1990.

[85] V. Sreeram and P. Agathoklis, "Design of linear-phase IIR filters via impulse-response gramians," *IEEE Transactions on Signal Processing*, vol. 40, no. 2, pp. 389–394, Feb 1992.

[86] X. Lai and Z. Lin, "Minimax design of IIR digital filters using a sequential constrained least-squares method," *IEEE Transactions on Signal Processing*, vol. 58, no. 7, pp. 3901–3906, 2010.

[87] D. Guindon, D. J. Shpak, and A. Antoniou, "Design methodology for nearly linear-phase recursive digital filters by constrained optimization," *IEEE Transactions on Circuits and Systems I: Regular Papers*, vol. 57, no. 7, pp. 1719–1731, 2010.

[88] A. Jiang and H. K. Kwan, "Minimax design of IIR digital filters using iterative SOCP," *IEEE Transactions on Circuits and Systems I: Regular Papers*, vol. 57, no. 6, pp. 1326–1337, 2010.

[89] W.-S. Lu and T. Hinamoto, "Optimal design of IIR digital filters with robust stability using conic-quadratic-programming updates," *IEEE Transactions on Signal Processing*, vol. 51, no. 6, pp. 1581–1592, 2003.

[90] A. Deczky, "Synthesis of recursive digital filters using the minimum p-error criterion," *IEEE Transactions on Audio and Electroacoustics*, vol. 20, no. 4, pp. 257–263, 1972.

[91] L. Zhang, X. Lai, and H. Qiao, "Design of allpass IIR digital filters using a minimax frequency response error method," in *Proceedings of the 33rd Chinese Control Conference*. IEEE, 2014, pp. 7328–7332.

[92] A. Jiang and H. K. Kwan, "Minimax design of IIR digital filters using SDP relaxation technique," *IEEE Transactions on Circuits and Systems I: Regular Papers*, vol. 57, no. 2, pp. 378–390, 2009.

[93] X. Lai, Z. Lin, and H. K. Kwan, "A sequential minimization procedure for minimax design of IIR filters based on second-order factor updates," *IEEE Transactions on Circuits and Systems II: Express Briefs*, vol. 58, no. 1, pp. 51–55, 2011.

[94] W.-S. Lu, "Design of recursive digital filters with prescribed stability margin: A parameterization approach," *IEEE Transactions on Circuits and Systems II: Analog and Digital Signal Processing*, vol. 45, no. 9, pp. 1289–1298, 1998.

[95] R. Pal, "Comparison of the design of FIR and IIR filters for a given specification and removal of phase distortion from IIR filters," in *2017 International Conference on Advances in Computing, Communication and Control (ICAC3)*. IEEE, 2017, pp. 1–3.

[96] F. Serbet, T. Kaya, and M. Ozdemir, "Design of digital IIR filter using particle swarm optimization," in *2017 40th International Convention on Information and Communication Technology, Electronics and Microelectronics (MIPRO)*. IEEE, 2017, pp. 202–204.

[97] C. Zeintl and H. G. Brachtendorf, "Linear phase design of lattice wave digital filters," in *2018 28th International Conference Radioelektronika (RADIOELEKTRONIKA)*. IEEE, 2018, pp. 1–5.

[98] R. Singh and S. K. Arya, "Optimization of IIR digital filters using particle swarm optimization," in *2012 International Conference on Communication, Information & Computing Technology (ICCICT)*. IEEE, 2012, pp. 1–7.

[99] A. Ates, G. Kavuran, B. B. Alagoz, and C. Yeroglu, "Improvement of IIR filter discretization for fractional order filter by discrete stochastic optimization," in *2016 39th International Conference on Telecommunications and Signal Processing (TSP)*. IEEE, 2016, pp. 583–586.

[100] Y. Maghsoudi and M. Kamandar, "Low delay digital IIR filter design using metaheuristic algorithms," in *2017 2nd Conference on Swarm Intelligence and Evolutionary Computation (CSIEC)*. IEEE, 2017, pp. 95–99.

[101] N. Agrawal, A. Kumar, and V. Bajaj, "Digital IIR filter design with controlled ripple using cuckoo search algorithm," in *2016 International Conference on Signal and Information Processing (IConSIP)*. IEEE, 2016, pp. 1–5.

[102] R. Matei and D. Matei, "Circular IIR filter design and applications in biomedical image analysis," in *2018 10th International Conference on Electronics, Computers and Artificial Intelligence (ECAI)*. IEEE, 2018, pp. 1–6.

[103] T.-B. Deng, "Feasibility-check-based phase-filter design," in *2017 International Conference on Engineering Technology and Technopreneurship (ICE2T)*. IEEE, 2017, pp. 1–4.

[104] S. B. Nagaraj, R. Nongpiur, and A. Antoniou, "Design of nearly linear-phase recursive digital filters by using unconstrained least-pth minimax optimization," in *2010 4th International Symposium on Communications, Control and Signal Processing (ISCCSP)*. IEEE, 2010, pp. 1–6.

[105] C. Charalambous and A. Antoniou, "Equalisation of recursive digital fitters," in *IEE Proceedings G-Electronic Circuits and Systems*, vol. 127, no. 5. IET, 1980, pp. 219–225.

[106] M. C. Lang, "Least-squares design of IIR filters with prescribed magnitude and phase responses and a pole radius constraint," *IEEE Transactions on Signal Processing*, vol. 48, no. 11, pp. 3109–3121, 2000.

[107] X. Lai and Z. Lin, "Minimax phase error design of IIR digital filters with prescribed magnitude and phase responses," *IEEE Transactions on Signal Processing*, vol. 60, no. 2, pp. 980–986, 2012.

[108] C. Y.-F. Ho, B. W.-K. Ling, Z.-W. Chi, M. Shikh-Bahaei, Y.-Q. Liu, and K.-L. Teo, "Design of near-allpass strictly stable minimal-phase real-valued rational IIR filters," *IEEE Transactions on Circuits and Systems II: Express Briefs*, vol. 55, no. 8, pp. 781–785, 2008.

[109] G. Deng, J. Chen, J. Zhang, and C.-H. Chang, "Area-and power-efficient nearly-linear phase response IIR filter by iterative convex optimization," *IEEE Access*, vol. 7, pp. 22 952–22 965, 2019.

[110] D. Shpak and A. Antoniou, "A generalized remez method for the design of FIR digital filters," *IEEE Transactions on Circuits and Systems*, vol. 37, no. 2, pp. 161–174, 1990.

[111] W.-S. Lu, "An argument-principle based stability criterion and application to the design of IIR digital filters," in *Circuits and Systems, 2006. ISCAS 2006. Proceedings. 2006 IEEE International Symposium on.* IEEE, 2006, pp. 4–pp.

[112] M. Nakamoto and S. Ohno, "Closed-form approximation of linear phase IIR digital filters with guaranteed stability," in *2011 IEEE International Conference on Acoustics, Speech and Signal Processing (ICASSP).* IEEE, 2011, pp. 1645–1648.

[113] V. Lesnikov, T. Naumovich, and A. Chastikov, "The formulation of criteria of BIBO stability of 3rd-order IIR digital filters in space of coefficients of a denominator of transfer function," in *Proceedings of IEEE East-West Design & Test Symposium (EWDTS 2014).* IEEE, 2014, pp. 1–3.

[114] X. Lai, J. Cao, and Z. Lin, "Minimax magnitude response approximation of pole-radius constrained IIR digital filters," in *ICASSP 2019-2019 IEEE International Conference on Acoustics, Speech and Signal Processing (ICASSP).* IEEE, 2019, pp. 5491–5495.

[115] D. J. Shpak, "Improving IIR filter design by considering the allocation and locations of poles and zeros," in *2020 IEEE International Symposium on Circuits and Systems (ISCAS).* IEEE, 2020, pp. 1–5.

[116] J. Sun, W. Fang, and W. Xu, "A quantum-behaved particle swarm optimization with diversity-guided mutation for the design of two-dimensional IIR digital

filters," *IEEE Transactions on Circuits and Systems II: Express Briefs*, vol. 57, no. 2, pp. 141–145, 2010.

[117] B. Anderson, P. Agathoklis, E. Jury, and M. Mansour, "Stability and the matrix Lyapunov equation for discrete 2-dimensional systems," *IEEE Transactions on Circuits and Systems*, vol. 33, no. 3, pp. 261–267, 1986.

[118] B. Lashgari, L. Silverman, and J.-F. Abramatic, "Approximation of 2-D separable in denominator filters," *IEEE Transactions on Circuits and Systems*, vol. 30, no. 2, pp. 107–121, 1983.

[119] A. Kumar, F. Fairman, and J. Sveinsson, "Separately balanced realization and model reduction of 2-D separable-denominator transfer functions from input-output data," *IEEE Transactions on Circuits and Systems*, vol. 34, no. 3, pp. 233–239, 1987.

[120] B. Beliczynski, I. Kale, and G. D. Cain, "Approximation of FIR by IIR digital filters: An algorithm based on balanced model reduction," *IEEE Transactions on Signal Processing*, vol. 40, no. 3, pp. 532–542, 1992.

[121] W.-S. Lu, H.-P. Wang, and A. Antoniou, "Design of two-dimensional digital filters using singular-value decomposition and balanced approximation method," in *IEEE International Symposium on Circuits and Systems,*. IEEE, 1989, pp. 1656–1659.

[122] J. Willems, "Least squares stationary optimal control and the algebraic riccati equation," *IEEE Transactions on Automatic Control*, vol. 16, no. 6, pp. 621–634, 1971.

[123] S. Boyd, L. El Ghaoui, E. Feron, and V. Balakrishnan, *Linear matrix inequalities in system and control theory*. Siam, 1994, vol. 15.

[124] S. Knorn and R. H. Middleton, "Stability of two-dimensional linear systems with singularities on the stability boundary using LMIs," *IEEE Transactions on Automatic Control*, vol. 58, no. 10, pp. 2579–2590, 2013.

[125] D. Xue and Y. Chen, *Solving applied mathematical problems with MATLAB*. Chapman and Hall/CRC, 2008.

[126] L. Li and F. Paganini, "Structured coprime factor model reduction based on LMIs," *Automatica*, vol. 41, no. 1, pp. 145–151, 2005.

[127] A. Vandendorpe and P. Van Dooren, "On model reduction of interconnected systems," in *Proceedings International Symposium Math. Th. Netw. Syst., Belgium*, 2004.

[128] C. L. Beck, J. Doyle, and K. Glover, "Model reduction of multidimensional and uncertain systems," *IEEE Transactions on Automatic Control*, vol. 41, no. 10, pp. 1466–1477, 1996.

[129] Maryam,Haitham,Boyd, "A rank minimization heuristic with application to minimum order system approximation," *Proceedings of the American Control Conference*, pp. 4734–4739, 2001.

[130] J. W. Helton, S. McCullough, M. Putinar, and V. Vinnikov, "Convex matrix inequalities versus linear matrix inequalities," *IEEE Transactions on Automatic Control*, vol. 54, no. 5, pp. 952–964, 2009.

[131] T. Tran, "Linear matrix inequalities for dissipative constraints in stabilization with relaxed non-monotonic lyapunov function," in *2017 International Conference on Control, Automation and Information Sciences (ICCAIS)*. IEEE, 2017, pp. 61–66.

[132] R. E. Skelton, T. Iwasaki, and D. E. Grigoriadis, *A unified algebraic approach to control design*. CRC Press, 1997.

[133] M. Mesbahi, "On the rank minimization problem and its control applications," *Systems & Control Letters*, vol. 33, no. 1, pp. 31–36, 1998.

[134] M. Mesbahi and G. P. Papavassilopoulos, "On the rank minimization problem over a positive semidefinite linear matrix inequality," *IEEE Transactions on Automatic Control*, vol. 42, no. 2, pp. 239–243, 1997.

[135] A. Hmamed, M. Alfidi, A. Benzaouia, and F. Tadeo, "LMI conditions for robust stability of 2D linear discrete-time systems," *Mathematical Problems in Engineering*, vol. 2008, 2008.

[136] Mathworks. (2019, April) Minimize Linear Objectives under LMI Constraints . [Online]. Available: https://www.mathworks.com/help/robust/ug/minimizing-linear-objectives-under-lmi-constraints.html

[137] A. Ghafoor and V. Sreeram, "A survey/review of frequency-weighted balanced model reduction techniques," ASME. J. Dyn. Sys., Meas., Control, 2008.

[138] S. Kockanat and N. Karaboga, "The design approaches of two-dimensional digital filters based on metaheuristic optimization algorithms: a review of the literature," *Artificial Intelligence Review*, vol. 44, no. 2, pp. 265–287, 2015.

[139] L. Lessard, M. Hussein, and Y. Nooshabadi, "ME 7247: Advanced control systems, lecture 15: Balanced realization." Northeastern University, 2023, pp. 1–9.

[140] L. Mitiche and A. B. H. Adamou-Mitiche, "New procedure in designing 2D-IIR filters based on 2D-FIR filters approximation," in *2013 8th International Workshop on Systems, Signal Processing and their Applications (WoSSPA)*. IEEE, 2013, pp. 515–520.

[141] G. Gu, B. A. Shenoi, and C. Zhang, "Synthesis of 2-D linear phase digital filters," *IEEE Transactions on Circuits and Systems*, vol. 37, no. 12, pp. 1499–1508, Dec 1990.

[142] L. Bruton and N. Bartley, "A general-purpose computer program for the design of two-dimensional recursive filters—2DFil," *Circuits, Systems and Signal Processing*, vol. 3, no. 2, pp. 243–264, 1984.

[143] L. Bruton and N. Bartley, "Using nonessential singularities of the second kind in two-dimensional filter design," *IEEE Transactions on Circuits and Systems*, vol. 36, no. 1, pp. 113–116, 1989.

[144] R. Matei, "Design approach for a class of 2D recursive filters," in *2017 International Symposium on Signals, Circuits and Systems (ISSCS)*. IEEE, 2017, pp. 1–4.

[145] R. Matei, "Analytic design of directional and square-shaped 2D IIR filters based on digital prototypes," *Multidimensional Systems and Signal Processing*, pp. 1–23, 2019.

[146] T.-S. Chan and A. Kumar, "Reliable ear identification using 2-D quadrature filters," *Pattern Recognition Letters*, vol. 33, no. 14, pp. 1870–1881, 2012.

[147] C.-W. Wu, "Bit-level pipelined 2-D digital filters for real-time image processing," *IEEE Transactions on Circuits and Systems for Video Technology*, vol. 1, no. 1, pp. 22–34, 1991.

[148] W. Lertniphonphun and J. H. McClellan, "Unified design algorithm for complex FIR and IIR filters," in *IEEE International Conference on Acoustics, Speech, and Signal Processing. Proceedings (Cat. No. 01CH37221)*, vol. 6, 2001, pp. 3801–3804.

[149] B. O'connor and T. Huang, "Stability of general two-dimensional recursive digital filters," *IEEE Transactions on Acoustics, Speech, and Signal Processing*, vol. 26, no. 6, pp. 550–560, 1978.

[150] T. Katayama, *Subspace methods for system identification*. Springer Science & Business Media, 2006.

[151] A. Jiang and H. K. Kwan, "IIR digital filter design with new stability constraint based on argument principle," *IEEE Transactions on Circuits and Systems I: Regular Papers*, vol. 56, no. 3, pp. 583–593, 2009.

[152] H. Reddy and P. Rajan, "A comprehensive study of two-variable hurwitz polynomials," *IEEE Transactions on Education*, vol. 32, no. 3, pp. 198–209, 1989.

[153] V. M. Mladenov and N. E. Mastorakis, "Design of two-dimensional recursive filters by using neural networks," *IEEE Transactions on Neural Networks*, vol. 12, no. 3, pp. 585–590, 2001.

[154] J.-T. Tsai, W.-H. Ho, and J.-H. Chou, "Design of two-dimensional IIR digital structure-specified filters by using an improved genetic algorithm," *Expert Systems with Applications*, vol. 36, no. 3, pp. 6928–6934, 2009.

[155] L. Liang, M. Ahmadi, and M. Sid-Ahmed, "Design of 2D IIR filters with canonical signed-digit coefficients using genetic algorithm," in *2003 46th Midwest Symposium on Circuits and Systems*, vol. 2. IEEE, 2003, pp. 633–635.

[156] M. Kawamata, J. Imakubo, and T. Higuchi, "Optimal design method of 2-D IIR digital filters based on a simple genetic algorithm," in *Proceedings of 1st*

International Conference on Image Processing, vol. 1. IEEE, 1994, pp. 780–784.

[157] C. Lv, S. Yan, G. Cheng, L. Xu, and X. Tian, "Design of two-dimensional IIR digital filters by using a novel hybrid optimization algorithm," *Multidimensional Systems and Signal Processing*, vol. 28, no. 4, pp. 1267–1281, 2017.

[158] C. Charalambous, "Design of 2-dimensional circularly-symmetric digital filters," in *IEE Proceedings G (Electronic Circuits and Systems)*, vol. 129, no. 2. IET, 1982, pp. 47–54.

[159] T. Miyata, N. Aikawa, Y. Sugita, and T. Yoshikawa, "A design method for separable-denominator 2D IIR filters with a necessary and sufficient stability check," *IEICE transactions on fundamentals of electronics, communications and computer sciences*, vol. 92, no. 1, pp. 307–310, 2009.

[160] A. Omar, D. Shpak, and P. Agathoklis, "Improved design method for nearly linear-phase IIR filters using constrained optimization," *Journal of Circuits, Systems and Computers*, vol. 30, no. 11, p. 2150207, 2021.

[161] A. Omar, P. Agathoklis, and D. Shpak, "Nearly linear-phase 2-D recursive digital filters design using balanced realization model reduction," *Signals*, vol. 4, no. 4, pp. 800–815, 2023.

[162] K. Kim, J. Kim, and S. Nam, "Design of computationally efficient 2D FIR filters using sampling-kernel-based interpolation and frequency transformation," *Electronics Letters*, vol. 51, no. 17, pp. 1326–1328, 2015.

[163] A. Antoniou and W.-S. Lu, "Design of two-dimensional digital filters by using the singular value decomposition," *IEEE Transactions on Circuits and Systems*, vol. 34, no. 10, pp. 1191–1198, 1987.

[164] M. Ahmadi, M. Boraie, V. Ramachandran, and C. Gargour, "Design of 2-D recursive digital filters with constant group delay characteristics using separable denominator transfer function and a new stability test," *IEEE transactions on acoustics, speech, and signal processing*, vol. 33, no. 5, pp. 1316–1318, 1985.

[165] E. D. Andersen, J. Gondzio, C. Mészáros, X. Xu *et al.*, *Implementation of interior point methods for large scale linear programming.* HEC/Université de Geneve, 1996.

[166] L. Liu and L. Fan, "The complexity analysis of an efficient interior-point algorithm for linear optimization," in *2010 Third International Joint Conference on Computational Science and Optimization*, vol. 2. IEEE, 2010, pp. 21–24.

[167] R. Wirski, "Synthesis and realization of two-dimensional separable denominator orthogonal systems via decomposition into 1-D systems," *IEEE Transactions on Circuits and Systems I: Regular Papers*, vol. 66, no. 11, pp. 4309–4322, 2019.

[168] H. C. Reddy, I.-H. Khoo, and P. Rajan, "2-D symmetry: Theory and filter design applications," *IEEE Circuits and Systems Magazine*, vol. 3, no. 3, pp. 4–33, 2003.

[169] H. L. Van Trees, *Optimum array processing: Part IV of detection, estimation, and modulation theory*. John Wiley & Sons, 2002.

[170] T. K. Gunaratne and L. T. Bruton, "Beamforming of broad-band bandpass plane waves using polyphase 2-D FIR trapezoidal filters," *IEEE Transactions on Circuits and Systems I: Regular Papers*, vol. 55, no. 3, pp. 838–850, 2008.

[171] J. G. Ryan, "Criterion for the minimum source distance at which plane-wave beamforming can be applied," *The Journal of the Acoustical Society of America*, vol. 104, no. 1, pp. 595–598, 1998.

[172] I. Moazzen, S. Harrison, P. Agathoklis, and P. Driessen, "A nested microphone array for broadband audio signal processing," in *2013 IEEE Pacific Rim Conference on Communications, Computers and Signal Processing (PACRIM)*. IEEE, 2013, pp. 377–382.

[173] I. Moazzen, "Array signal processing for beamforming and blind source separation," Ph.D. dissertation, 2013, University of Victoria - UVicSpace.